

# OPTIMAL CONTROL ON ROCK WINDER HOIST SCHEDULING

by

**Werner Badenhorst**

Submitted in partial fulfilment of the requirements for the degree

Master of Engineering (Electrical Engineering)

in the

Faculty of Engineering, the Built Environment and Information Technology

UNIVERSITY OF PRETORIA

November 2009

## Summary

Title: Optimal control on rock winder hoist scheduling  
By: Werner Badenhorst  
Supervisor: Professor X. Xia  
Co-supervisor: Dr. J. Zhang  
Degree: Master of Engineering (Electrical Engineering)

This dissertation addresses the problem of optimally scheduling the hoists of a twin rock winder system in a demand side management context. The objective is to schedule the hoists at minimum energy cost taking into account various physical and operational constraints and production requirements as well as unplanned system delays.

The problem is solved by first developing a static linear programming model of the rock winder system. The model is built on a discrete dynamic winder model and consists of physical and operational winder system constraints and an energy cost based objective function.

Secondly a model predictive control based scheduling algorithm is applied to the model to provide closed-loop feedback control. The scheduling algorithm first solves the linear programming problem before applying an adapted branch and bound integer solution methodology to obtain a near optimal integer schedule solution. The scheduling algorithm also compensates for situations resulting in infeasible linear programming solutions.

The simulation results show the model predictive control based scheduling algorithm to be able to successfully generate hoist schedules that result in steady state solutions in all scenarios studied, including where delays are enforced. The energy cost objective function is proven to be very effective in ensuring minimal hoisting during expensive peak periods and maximum hoisting during low energy cost off-peak periods. The algorithm also ensures that the hoist target is achieved while controlling all system states within or around their boundaries for a sustainable and continuous hoist schedule.

**Keywords:** Rock Winders, Load Modelling, Optimal Load Scheduling, Constrained Linear Programming, Model Predictive Control.

## Opsomming

Titel:	Optimale beheer op rotshyserskedulering
Deur:	Werner Badenhorst
Studieleier:	Professor X. Xia
Mede-studieleier:	Dr. J. Zhang
Graad:	Meesters in Ingenieurswese (Elektriese Ingenieurswese)

Hierdie verhandeling spreek die probleem insake die optimale skedulering van 'n dubbele rotshysingstelsel aan in die konteks van aanvraagkant bestuur. Die doel is om die hysers teen 'n minimum energiekoste te skeduleer inaggenome verskeie fisiese en operasionele beperkinge en produksie vereistes sowel as onbeplande stelsel vertragsings.

Die probleem word opgelos deur eerstens 'n statiese lineêre programmeringsmodel van die rotshysingstelsel te ontwikkel. Die model is gebou op 'n diskreet dinamiese hysersmodel en bestaan uit fisiese en operasionele hysingstelsel beperkinge asook 'n energiekoste gebaseerde doelfunksie.

Tweedens word 'n model voorspellende beheer gebaseerde skeduleringsalgoritme op die model toegepas vir geslote lus terugvoer beheer. Die skeduleringsalgoritme los eerstens die lineêre programmeringsprobleem op alvorens 'n aangepaste vertak-en-beperk heelgetal oplossingsmetodologie toegepas word om 'n bykans-optimale heelgetal skedule oplossing te verkry. Die skeduleringsalgoritme kompenseer ook vir gevalle waarin die resultaat 'n onuitvoerbare lineêre programmerings-oplossing is.

Die simulasiereultate toon dat die model skeduleringsalgoritme in staat is om suksesvol hyserskedules te genereer wat bestendige toestand oplossings tot gevolg het vir alle gevalle wat bestudeer is, insluitende waar vertragsings afgedwing word. Dit word getoon dat die energiekoste doelfunksie baie effektief die minimum hysings gedurende die duur piek periodes en maksimum hysings gedurende die lae energiekoste af-piek periodes verseker. Die algoritme verseker ook dat die hysteiken behaal word terwyl alle stelseltoestande binne of rondom die beperkinge beheer word ter wille van 'n volhoubare en kontinue hyserskedule.

**Sleutelwoorde:** Rotshysers, Lasmodellering, Optimale Lasskedulering, Beperkte Lineêre Programmering, Model Voorspellende Beheer

## Acknowledgements

“To the King of ages, immortal, invisible, the only God, be honour and glory forever and ever. Amen.” 1 Timothy 1:17.

“To Him belong glory and dominion forever and ever. Amen” 1 Peter 4:11.

“Now to him who is able to keep you from stumbling and to present you blameless before the presence of his glory with great joy, to the only God, our Saviour through Jesus Christ our Lord, be glory, majesty dominion and authority, before all time and now and forever. Amen.” Jude 1:24,25.

Therefore unto Jesus the glory and praise for:

- The support and love of my wife Elouie, especially over the two months of writing up this dissertation.
- Health, endurance and clarity of mind.
- Prof. Leuschner’s patience and guidance.
- Prof. Xia who as my fourth study leader in my second topic’s third version finally provided the structure and direction to complete this dissertation within 2 years.
- Finally being able to complete an endeavour that originally started in 2001 as a course masters.

“Of making many books there is no end, and much study is wariness of the flesh. The end of the matter, all has been heard. Fear God and keep his commandments, for this is the whole duty of man. For God will bring every deed into judgement, with every secret thing, whether good or evil.” Eccl. 12:12 – 14.

# CONTENTS

<b>CHAPTER 1: INTRODUCTION AND BACKGROUND .....</b>	<b>1</b>
1.1 PROBLEM STATEMENT .....	1
1.2 DEMAND SIDE MANAGEMENT BACKGROUND AND TECHNIQUES.....	2
1.3 DSM IN SOUTH AFRICA AND TOU TARIFFS .....	5
1.4 DEEP LEVEL MINING AND ROCK WINDER OPERATION.....	7
1.5 NEED FOR FEEDBACK CONTROL.....	10
1.6 OBJECTIVES AND CONTRIBUTION.....	11
1.7 ORGANISATION.....	12
<b>CHAPTER 2: MODELLING OF A TWIN ROCK WINDER SYSTEM.....</b>	<b>13</b>
2.1 LOAD MODELLING AND CONTROL.....	13
2.2 SINGLE ROCK WINDER MODEL PARAMETERS.....	15
2.3 DISCRETE DYNAMIC TWIN ROCK WINDER SYSTEM MODEL .....	18
2.3.1 <i>Twin rock winder system layout</i> .....	18
2.3.2 <i>Discrete dynamic modelling</i> .....	19
2.4 ROCK WINDER SYSTEM CONSTRAINTS .....	20
2.4.1 <i>Tariff constraint</i> .....	21
2.4.2 <i>Hoist constraints</i> .....	21
2.4.3 <i>Level constraints</i> .....	22
2.4.4 <i>Hoist target constraint</i> .....	23
2.4.5 <i>Winder maintenance and testing</i> .....	24
2.5 COST OR OBJECTIVE FUNCTION DEVELOPMENT.....	24
2.6 STATIC LINEAR PROGRAMMING MODEL (SLPM) DEVELOPMENT .....	25
2.6.1 <i>General SLPM statement</i> .....	25
2.6.2 <i>Objective function</i> .....	26
2.6.3 <i>Lower and upper boundary constraints</i> .....	27
2.6.4 <i>Inequality constraints</i> .....	27
2.6.5 <i>Equality constraints</i> .....	32
2.7 SUMMARY OF THE TWIN ROCK WINDER SYSTEM MODEL .....	35
<b>CHAPTER 3: ROCK WINDER MODEL PREDICTIVE CONTROL.....</b>	<b>37</b>
3.1 MODEL PREDICTIVE CONTROL BACKGROUND.....	37
3.1.1 <i>Applications and advantages of MPC</i> .....	37
3.1.2 <i>Defining MPC</i> .....	38

3.2	APPLICATION OF THE DMC MPC ALGORITHM FORMULATION TO THE SLPM OF THE TWIN ROCK WINDER SYSTEM.....	41
3.2.1	<i>Reformulating the discrete dynamic state functions.....</i>	42
3.2.2	<i>Reformulating the objective function at sampling instant k.....</i>	44
3.2.3	<i>Reformulating the level inequality constraints.....</i>	45
3.2.4	<i>Reformulating the winder maintenance and testing equality constraints ...</i>	46
3.2.5	<i>Reformulating the hoist target inequality constraint.....</i>	49
3.3	MPC ALGORITHM FOR HOIST CONTROL AND SCHEDULING .....	53
3.3.1	<i>Branch and bound .....</i>	53
3.3.2	<i>Step 1: Initialise variables.....</i>	55
3.3.3	<i>Step 2: Construct and define vectors and matrices .....</i>	56
3.3.4	<i>Step 3: Minimise for a real solution.....</i>	56
3.3.5	<i>Step 4: Branch and add equality constraints .....</i>	57
3.3.6	<i>Step 5: Re-minimise for a mixed integer solution.....</i>	57
3.3.7	<i>Step 6: Select, set and implement only <math>u_s^k</math> and <math>u_g^k</math>.....</i>	58
3.3.8	<i>Step 7: Update system state.....</i>	58
3.4	ROCK WINDER MODEL PREDICTIVE CONTROL SUMMARY .....	59

## **CHAPTER 4: IMPACT SIMULATION RESULTS AND DISCUSSIONS**

<b>EXCLUDING DELAYS .....</b>	<b>61</b>	
4.1	INITIALISATION AND ASSUMPTIONS.....	61
4.1.1	<i>Calculation of <math>E_s</math> and <math>E_g</math>.....</i>	61
4.1.2	<i>Feed-in rate into orepass system.....</i>	62
4.1.3	<i>Megaflex TOU energy rates .....</i>	62
4.1.4	<i>Initial system and control variable values.....</i>	63
4.1.5	<i>Obtaining values for <math>m_1^0</math>, <math>m_2^0</math> and <math>u_{sm}</math>.....</i>	64
4.2	IMPACT OF MPC, HISTORICAL INFORMATION AND BnB .....	65
4.2.1	<i>Impact of not applying MPC and not having historical hoist information .</i>	66
4.2.2	<i>Impact of not applying MPC but taking historical hoist information into account .....</i>	67
4.2.3	<i>Impact of applying MPC whilst not having historical hoist information....</i>	69
4.2.4	<i>Impact of applying MPC and taking historical hoist information into account .....</i>	71
4.2.5	<i>Impact of applying BnB.....</i>	72
4.2.6	<i>MPC, historical information and BnB impact summary.....</i>	73

4.3	TARIFF IMPACT ON WINDER SCHEDULES .....	74
4.3.1	<i>TOU versus flat rate</i> .....	74
4.3.2	<i>Effect of a high <math>M_{blast}</math> on the hoisting schedule</i> .....	76
4.3.3	<i>Effect of a high <math>M_{min}</math> and <math>M_{blast}</math> on the hoisting schedule</i> .....	78
4.3.4	<i>Tariff impact summary</i> .....	79
4.4	IMPACT OF $M_{BLAST}$ RATIO TO $M_{MIN}$ .....	80
4.4.1	<i>Motivation for ratio impact study</i> .....	80
4.4.2	<i><math>M_{blast}</math> equal to <math>M_{min}</math> at 8 013.5 tons</i> .....	81
4.4.3	<i><math>M_{min}</math> equal to 7 700 tons and <math>M_{blast}</math> equal to 8 200 tons</i> .....	83
4.4.4	<i><math>M_{min}</math> equal to 7 200 tons and <math>M_{blast}</math> equal to 8 200 tons</i> .....	84
4.4.5	<i><math>M_{min}</math> to <math>M_{blast}</math> difference impact summary</i> .....	85
<b>CHAPTER 5: DELAY IMPACT SIMULATION RESULTS AND DISCUSSIONS</b>		<b>86</b>
5.1	ELEMENTARY DELAY IMPACT ILLUSTRATION .....	86
5.2	HOW AND HOW MUCH DELAY CAN BE INTRODUCED .....	88
5.3	$M_{BLAST}$ EQUAL TO 8 200 TONS AND $M_{MIN}$ EQUAL TO 8 013.5 TONS.....	89
5.4	$M_{BLAST}$ EQUAL TO 8 200 TONS AND $M_{MIN}$ EQUAL TO 7 200 TONS.....	92
5.5	CAUSE AND EFFECT OF LEVEL BOUNDARY CONSTRAINT VIOLATIONS .....	94
5.6	LEVEL AND ENERGY COST COMPARISON FOR VARIOUS IMPACT FACTORS .....	97
5.7	SUMMARY OF THE DELAY IMPACT STUDY .....	100
<b>CHAPTER 6: CONCLUSIONS AND RECOMMENDATIONS</b>		<b>103</b>
6.1	CONCLUSIONS .....	103
6.2	RECOMMENDATIONS FOR FURTHER STUDY .....	105
<b>REFERENCES</b> .....		<b>106</b>
<b>ADDENDUM A: ESKOM MEGAFLEX CHARGES</b> .....		<b>111</b>
<b>ADDENDUM B: DAILY HOIST REPORT</b> .....		<b>113</b>
<b>ADDENDUM C: ROCK WINDER DUTY CYCLE MODEL</b> .....		<b>114</b>
<b>ADDENDUM D: PERIODS AND NUMBER OF HOISTS DELAYED</b> .....		<b>116</b>
<b>ADDENDUM E: HIGH NUMBER OF HOISTS DELAYED OVER 5 DAYS</b> .....		<b>117</b>

## List of Abbreviations

BnB	Branch and Bound
DMC	Dynamic Matrix Control
DSM	Demand Side Management
EE	Energy Efficiency
ESCo	Energy Services Company
HWC	Hot Water Cylinders
IP	Integer Programming
LM	Load Management
LR	Linear Relaxation Programming
MILP	Mixed Integer Linear Programming
MPC	Model Predictive Control
NAC	Network Access Charge
NDC	Network Demand Charge
NMD	Notified Maximum Demand
REMS	Real-time Energy Management System
SCADA	Supervisory Control And Data Acquisition
SLPM	Static Linear Programming Model
TOU	Time-Of-Use

## List of Figures

Figure 1.1: Six load management techniques for modifying demand curves. ....	3
Figure 1.2: Megaflex TOU periods taken from [20].....	6
Figure 1.3: Schematic layout of a typical deep level ore transport system .....	8
Figure 2.1: Measured active load profile for two hoist cycles of a rock winder. ....	15
Figure 2.2: Modelled active load profile for a single hoist cycle of rock winder. ....	16
Figure 2.3: Schematic diagram of a twin rock winder system containing a surface winder in the main shaft and an underground winder in the sub-shaft.....	19
Figure 3.1: Graphical illustration of the MPC receding horizon approach. ....	39
Figure 3.2: Basic concept for model predictive control [51].....	40
Figure 3.3: Illustration of the position of $u$ within $N$ required for $\hat{y}$ at each step $j$ ...	41
Figure 3.4: Graphical illustration of (3.24) for $h = 5 = H = P$ and $N = 2H = 10$ .....	50
Figure 3.5: Current and future control actions for $u_s$ at $k = 0$ . ....	51
Figure 3.6: Illustration of the increase in step ahead predictions for $0 < k < 4$ . ....	52
Figure 3.7: Illustration of $u_s$ values required in hoist target constraint for $4 \leq k < 9$ .	53
Figure 3.8: Branching of the solution at period $k$ into four subproblems.....	Error!
Bookmark not defined.	
Figure 3.9: MPC algorithm flow diagram for rock winder feedback control. ....	60
Figure 4.1: Percentage function for feed-in rate of rock from stopes into orepass system.....	62
Figure 4.2: Ore levels $m_1$ and $m_2$ showing a transient behaviour along with $m_N$ approaching steady state after $N = 4$ days.....	64
Figure 4.3: An optimal 2-day hoisting schedule without applying MPC and not having historical hoist information. ....	66
Figure 4.4: An optimal 2-day hoisting schedule without applying MPC but taking into account historical hoist information. ....	68
Figure 4.5: An optimal 2-day hoisting schedule with MPC applied and not having historical hoist information. ....	69
Figure 4.6: An optimal 2-day hoisting schedule with MPC applied and taking into account historical hoist information. ....	71
Figure 4.7: A near optimal 2-day hoisting schedule with MPC and BnB applied while taking into account historical hoist information.....	72
Figure 4.8: A near optimal hoist schedule based on a weighted average flat rate tariff with both MPC and BnB applied and $u_{sm}$ taken into account.....	75

**Figure 4.9: A near optimal solution with  $M_{min} = 8013.5$  tons and  $M_{blast} = 9000$  tons... 77**

**Figure 4.10: A near optimal solution with  $M_{min} = 9\ 611.5$  tons and  $M_{blast} = 10\ 000$  tons. .... 79**

**Figure 4.11: Ore level transient analysis for  $M_{blast}$  and  $M_{min}$  equal to 8 013.5 tons over 60 days. .... 81**

**Figure 4.12: Indication of some of the causes for infeasible solutions on the last two days. .... 82**

**Figure 4.13: Ore level transient analysis for  $M_{blast} = 8\ 200$  tons and  $M_{min} = 7\ 700$  tons over 90 days..... 83**

**Figure 4.14: Ore level transient analysis over 40 days for  $M_{blast} = 8\ 200$  tons and  $M_{min} = 7\ 200$  tons..... 84**

**Figure 5.1: Elementary illustration of the effect that delays have on the hoist schedules when using MPC..... 87**

**Figure 5.2: Recorded rock winder system delays..... 88**

**Figure 5.3: Box plot of winder system delays within the 138 available working days of data..... 89**

**Figure 5.4: Simulated historical winder schedules and ore levels with delays introduced at  $M_{blast} = 8\ 200$  tons and  $M_{min} = 8\ 013.5$  tons. .... 90**

**Figure 5.5: Repeated simulation of Fig. 5.4 where  $M_{blast} = 8\ 200$  tons and  $M_{min} = 8\ 013.5$  tons but with hoist boundaries enforced. .... 91**

**Figure 5.6: Indication of the times at which  $m_N$  from Fig. 5.4 is less than the target constraint of 8 013.5 tons. .... 92**

**Figure 5.7: Simulated historical winder schedules and ore levels with delays introduced at  $M_{blast} = 8\ 200$  tons and  $M_{min} = 7\ 214.5$  tons. .... 93**

**Figure 5.8: Cause and effect of level boundary constraint violations with  $M_{min} = 8\ 013.5$  tons and  $M_{blast} = 8\ 200$  tons with  $H = h$ . .... 94**

**Figure 5.9: Effect of level boundary constraint violations for  $M_{min} = 4\ 000$  tons and  $M_{blast} = 4\ 400$  tons with  $H = h$ ..... 95**

**Figure 5.10: Effect of level boundary constraint violations for  $M_{min} = 7\ 200$  tons and  $M_{blast} = 7\ 600$  tons with  $H = 2h$ ..... 96**

**Figure 5.11: Six day ore level result for the case 6 operating on the bases of hoisting ‘what you can when you can’. .... 99**

**Figure 5.12: Six day ore level result for the case 6 with no hoisting during peak periods unless the ore levels exceeded their upper boundaries. .... 100**

## List of Tables

<b>Table 2.1: Rock winding cycle state description.....</b>	<b>16</b>
<b>Table 2.2. Assigned values for the elements of the discrete cost function <math>C</math>. .....</b>	<b>25</b>
<b>Table 3.1: List of variables to be initialised at <math>k = 0</math>.....</b>	<b>55</b>
<b>Table 4.1: System and control variables to be initialised at <math>k = 0</math>.....</b>	<b>63</b>
<b>Table 4.2: Numerical results for Fig. 4.3.....</b>	<b>67</b>
<b>Table 4.3: Numerical results for Fig. 4.4.....</b>	<b>69</b>
<b>Table 4.4: Numerical results for Fig. 4.5.....</b>	<b>70</b>
<b>Table 4.5: Numerical results for Fig. 4.6.....</b>	<b>71</b>
<b>Table 4.6: Numerical results for Fig. 4.7.....</b>	<b>73</b>
<b>Table 4.7: Numerical results for Fig. 4.8.....</b>	<b>76</b>
<b>Table 4.9: Numerical results for Fig. 4.10.....</b>	<b>79</b>
<b>Table 5.1: Comparative results for the various impact factors on the ore levels and energy costs. ....</b>	<b>97</b>

# CHAPTER 1

## INTRODUCTION AND BACKGROUND

### 1.1 Problem statement

Global electricity demand is projected to increase by 45% between 2006 and 2030 according to the International Energy Agency's 2008 World Energy Outlook report [1]. In order for future supply to meet demand, supply capacity needs to be increased and the rate of demand increase needs to be reduced through effective demand side management (DSM) of the electricity market. By reducing demand the need for additional future generation capacity is reduced [2, 3]. A simple economic rationale for DSM activities is stated in [2]: "an extra kWh required in the energy system can be obtained either by building new power capacity or by reducing demand. The choice should be made according to which is the cheaper solution of the two."

In light of the aforementioned Africa's largest electricity supplier, Eskom, has made DSM a priority with respect to the efficient use of electricity [4]. Eskom's objectives include maintaining an acceptable national load factor to ensure more efficient use of power stations and minimising stress on the network through various DSM techniques and the use of more energy efficient systems [5, 6, 7]. Eskom also aims at reducing peak demand by 3 000 MW between April 2007 and April 2011 and by a further 5 000 MW by March 2026 [4].

Industry in South Africa consumes approximately 65% of all electrical energy of which the mining sector is the largest representing approximately 24% of industry consumption and 16% of total electrical energy consumption in South Africa [8]. DSM projects have successfully been implemented in various industries consuming significant amounts of electrical energy. This includes deep level gold mines where DSM has primarily been implemented on the underground pumping and cooling systems [9, 10]. The first significant contribution towards DSM in deep level mines was made in [11] in which an integrated electricity end-use planning methodology in deep level mines is proposed. More recently a Real-time Energy Management System (REMS) was developed by HVAC

International (Pty) Ltd that enabled the real-time simulation, optimisation and control of the actual on-site situation on deep level mines in South Africa [10].

Another significant consumer of electrical energy on deep level mines which has been identified for DSM applications are the rock winder systems responsible for hoisting ore and rock from underground to the surface where the gold is extracted. Rock winders consume approximately 15% of the electrical energy on deep level mines [11, 12]. Currently only two developments and implementations of DSM control strategies for rock winders are known to exist [12, 13]. The study in this dissertation proposes and presents a model predictive control (MPC) approach for rock winder hoist control and scheduling to further contribute to the effectiveness and robustness of rock winder control.

## 1.2 Demand side management background and techniques

Demand side management programmes were first implemented as load management programmes in Europe and New Zealand in the 1960's and 1970's then later in United States with the initial objective of reducing the need for future generation capacity [3,14]. Various definitions exist for demand side management, though all has the general underlying principle of: "...the need to modify customer end-use of electricity (and other utility supplies) to shape demand in some beneficial manner," [3]. Eskom defines DSM in [15] as: "... the process whereby an electricity supplier influences the way electricity is used by customers." Another definition by the Electric Power Research Institute (EPRI) and favoured in this particular study reads: "DSM is the deliberate influence of customer appliance selection and energy use patterns to achieve a desired impact or load shape consistent with company goals" [15].

The objective of any DSM or load management (LM) program is to maintain a constant load level or load factor approaching unity as best possible [16]. Benefits of DSM and LM discussed in [16] and [17] include:

- Reducing the generation margin.
- Improving transmission and distribution investment and operation efficiency.
- Assisting in managing demand-supply balance in networks having intermittent renewable and distributed sources.

Traditionally DSM entailed six techniques also referred to as LM techniques: peak clipping; valley filling; load shifting; strategic conservation; strategic load growth [2, 5, 6, 14]. Each technique has a unique approach to changing or modifying the shape of demand or power load profiles as illustrated in Fig. 1.1 and briefly described below as discussed in [5].

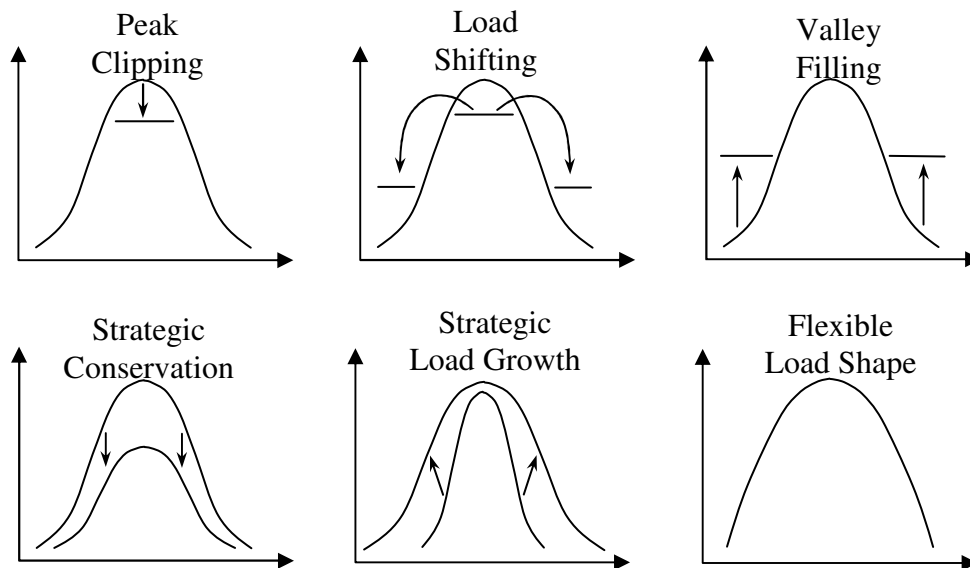


**Figure 1.1: Six load management techniques for modifying demand curves.**

*Peak clipping:* Also referred to as load shedding through direct load control. Loads are not deferred, rescheduled or shifted but simply switched off for a short period due to a lack of supply or to ensure that total load does not exceed a predetermined peak demand. Peak clipping has also been referred to as demand response programmes [18].

*Load shifting:* Shifting load from peak to off-peak periods. Applicable to loads having a storage capability, such as hot water cylinders (HWC). Enough water can be heated prior to a peak demand period ensuring sufficient hot water during the peak period whilst the HWC's elements are switched off. Important to note is that load shifting does not necessarily reduce the amount of energy consumed but only changes the time at which it is consumed [17].

*Valley filling:* Building load during off-peak periods thereby increasing the utilisation of the installed capacity.

*Strategic load conservation:* Reduction in demand due to energy efficiency programmes driven by utilities.

*Strategic load growth:* Increase in energy consumption and sales outside of the valley filling periods.

*Flexible load shape:* Reliability of supply to individual customers is tailored by reducing or postponing demand for selected customers.

In [5] these six demand curve-altering techniques are grouped into one of five DSM techniques called modifying power curves. The remaining four DSM techniques popular at the time and still being used today include:

- Reducing the lighting loads.
- Replacing old motors with more energy efficient motors and drives.
- Improving HVAC.
- Smart home automation systems.

Other major techniques practised today and briefly reviewed in [18] include:

- Night-time heating with load switching.
- Domestic-load control.
- Limiting the power to individual consumers.
- Frequency regulation using large interruptible industrial consumer loads.
- Time-of-use (TOU) energy pricing where energy costs are significantly higher during high demand peak periods compared to low demand off-peak periods to more closely reflect the cost structure of production and investment of energy sources.
- Demand bidding where customers are willing to reduce or even relinquish their energy consumption at a certain predetermined price.

DSM can effectively be divided into LM programmes and energy efficiency (EE) programmes [15, 19]. LM programmes are defined as programmes targeting reductions in energy demand (kW) and EE programmes as programmes targeting reductions in energy use (kWh) [19]. In [15] it is stated that DSM has two aspects: efficient use of electricity and the flattening of the load curve. The latter implies both demand reduction and an improvement of load factor. Both definitions in [15] and [19] are inline with Eskom's DSM programme that differentiates between demand and energy efficiency projects [7] and shall hence be used as such within the South African context of this study.

### 1.3 DSM in South Africa and TOU tariffs

The first step towards DSM in South Africa was taken in 1991 with the launch of a local efficient lighting initiative BONESA with the aim to lower the price of compact florescent lights. In 2002 the National DSM fund was approved and in 2003 the DSM business model was set up along with the establishment of Energy Services Companies (ESCOs). In 2004 and 2005 the first clients and projects were being registered and implemented in all sectors of the market. The primary focus at this time was the realisation of savings within the evening peak period between 18:00 and 20:00 with specific focus in the industrial, mining and commercial economy sectors. As from 2007 the focus has however shifted towards energy efficiency projects. The primary reason for this can be attributed to the success of DSM projects where a 1 082 MW reduction in evening peak demand was achieved from 2004 to 2008 of which 650 MW was in 2008 alone [4].

Even though the focus has been shifted towards energy efficiency projects, one of the four objectives of the Accelerated DSM Plan launched by Eskom in the middle of 2007 is: “to achieve and sustain 3 000 MW of electricity reduction during the evening peak by March 2011 and a further 5 000 MW by March 2026, through short, medium and long-term initiatives,” [4]. Twelve key elements are stated in order to achieve these objectives of which the 6<sup>th</sup> and 7<sup>th</sup> are of extreme relevance to this study. The 6<sup>th</sup> key element states: “Focus on the implementation of a limited number of large scale energy efficiency projects. In the Industrial, Mining and Agricultural sectors examples of technologies that can be undertaken in this fashion are: processing, pumping, material handling and compressed air.” Rock winders on deep level mines naturally fall under the category of mining and material handling. The 7<sup>th</sup> key element states: “Develop and implement tariffs for all end consumers, including households, that will encourage energy efficiency, including Time-of-Use (TOU) tariffs.” TOU tariffs are specifically aimed at encouraging load shifting from high demand periods during which energy and demand costs are high, into lower demand periods during which the costs are low. It is shown in [17] that through load shifting generation fuel cost can be reduced and the investment utilisation improved.

Currently most mines operate on a TOU tariff package known as Megaflex. The Megaflex TOU electricity tariff was developed for urban customers with a notified maximum

demand (NMD) of greater than 1 MVA and that are able to do load shifting [20]. The tariff has the following characteristics stated in [20]:

- Seasonally and TOU differentiated c/kWh active energy charges.
- Three TOU periods, namely, peak, standard, and off-peak as illustrated in Fig. 1.2.
- Energy rates differentiated by transmission and distribution loss factors.
- A R/kVA network access charge (NAC) applicable to all time periods, differentiated by voltage and transmission zone.
- A R/kVA network demand charge (NDC) applicable during peak and standard periods.
- A R/day service and administration charge based on the size of supply.
- A c/kWh contribution to cross-subsidies to rural and Homelight tariffs.

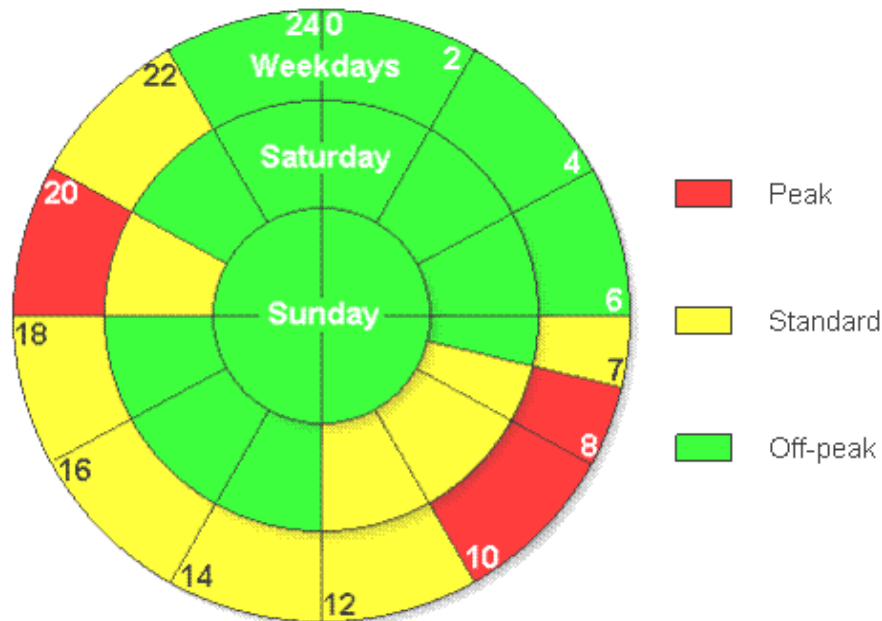


**Figure 1.2: Megaflex TOU periods taken from [20].**

Most noticeable in the Megaflex TOU energy charges provided in Addendum A is the high c/kWh cost of active energy during peak periods when compared to standard and off-peak periods, in particular during the high-demand season from June to August. This is purely aimed at encouraging and almost forcing customers on the Megaflex tariff to minimise energy consumption during both morning and evening peak periods and also to shift as much load as possible outside these peak periods.

## 1.4 Deep level mining and rock winder operation

Each workday is divided into a morning (06:00 – 14:00), afternoon (14:00 – 22:00) and night (22:00 – 06:00) shift with specific tasks that needs to be completed during each shift [11]. The mining process starts by drilling of holes in the stopes into the gold-bearing reef. The holes are filled with explosives that are detonated according to a predetermined sequence of blasts [21]. Operations in all sections underground are suspended during and for a number of hours after a blast has occurred in accordance to safety regulations [11]. The blasted ore-bearing rock is then scraped away from the stopes into box holes from where it is drawn off onto conveyer belts or into small railway cars known as hoppers hauled by locomotives and transported to the shaft area. The rock is dropped down orepasses to the lowest level of the mine where it is crushed into smaller segments. The crushed rock is fed through boxes onto conveyer belts feeding flasks that weigh off a set payload to be loaded into the skips in which the rock is hoisted to surface by the rock winder [21]. A schematic layout of a deep level gold mine and its ore transport system is shown in Fig. 1.3 of which the most critical component is the rock winder.

The ore transport system consists primarily of three energy consuming components namely the rock winder motors and it's associated peripheral equipment, the conveyer belts and the crushers.

- Rock winder motor and peripheral components

Older mines have DC motors whilst newer mines have induction motors responsible for hoisting the skip containing the payload of ore and lowering the empty skip. Peripheral equipment associated with the winder motor includes all equipment between the winder motor and the point of supply such as transformers, drives, rectifiers, field circuits and cables. Winders that are electrically coupled can be operated independently should a problem occur on either of the winders. It is however more efficient and productive to operate the winders as a coupled system. A detailed description of the various winder types is provided in [12].

- Conveyers

Conveyers are responsible for transporting the ore underground between orepasses and from the orepasses to the flasks at the rock winder. On surface conveyers are used to

transport the ore from the rock winder to the stockpile. In the case where the transport system is automated, the underground conveyers only operate whilst filling the flasks and will therefore have a distinct on/off profile in correlation with the rock winder operation. The surface conveyers however runs continuously with load increasing as the skip is emptied onto the conveyer and decreasing as the ore is dropped onto the stockpile whilst the next loaded skip is hoisted to surface.

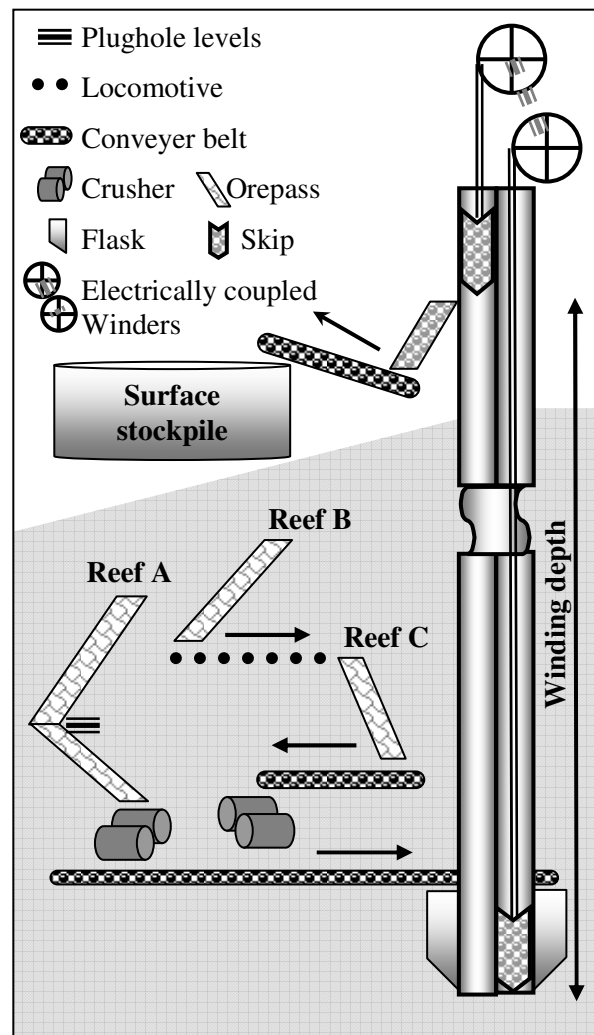


**Figure 1.3: Schematic layout of a typical deep level ore transport system**

- Crushers

Before the ore can be transported to surface, large rocks must be crushed in order to fit through the system channels and on the conveyer belts. The crushers also run continuously and similarly to the surface conveyers, the load increases as rock is dropped into the crusher once the underground conveyers starts moving.

An example of the sequence of events within an automated rock winder system is explained where time 0 ( $t_0$ ) is at the moment that the empty skip has reached the bottom of the shaft and the full skip has reached the surface. Both flasks are filled with the preset payload in tons at  $t_0$ .

- $t_0$ : The ore in one of the flasks is emptied into the empty skip. The loaded skip on surface is emptied onto the surface conveyer belts.
- $t_1$ : The loaded skip is hoisted to surface and the empty skip is lowered simultaneously.
- $t_2$ : The underground conveyers are switched on to fill the empty flask leading to an increase of the crusher load as the rocks fall through the crushers.
- $t_3$ : The flask is filled to capacity. Underground conveyers are stopped and the load on the crushers inherently reduced.
- $t_4$ : The empty skip reaches shaft bottom and the loaded skip reaches surface.

Delays within the rock winder system are logged in daily hoist reports and grouped into winder and operational delays. The delays indicate the total time in minutes that each type of delay caused the winder not to hoist for that day. A brief description of each type of delay is provided below whilst an example of a hoist report can be found in Addendum B.

Winder delays include:

- Winder legals: Tests and inspections required by law, carried out daily and/or weekly.
- Maintenance: Planned and unplanned maintenance on the rock winder.
- Breakdowns: Any breakdowns in the winder resulting in hoisting being stopped.
- Conveyers: Breakdown of conveyers resulting in no ore being fed to flasks.
- Other: Other winder related delays.

Operational delays include:

- Tip Full: Tip in which ore is emptied into on surface is full and hence the skip cannot be emptied.
- Waiting / No Reef / System empty: No ore available to be hoisted
- Barring: Large rocks stuck in the box at the end of an orepass feeding the conveyers need to be blasted into smaller pieces to unblock the system.

- Big Rock/Hang up/Blasting: Large rocks stuck in the orepass need to be blasted into smaller pieces in order to unblock the system.
- Other: Other operational related delays.

## 1.5 Need for feedback control

Determining the costs and benefits of a DSM opportunity is usually not straight forward, but requires both prediction and speculation [3]. Eight factors are listed in [3] that might be relevant in assessing the effects of DSM programmes, but predicting these effects requires statistical techniques based on past observations. Predictions based on past observations are however only sensible if the underlying conditions affecting future behaviour will not change [22]. Although the mining and ore transport systems are operated according to planned schedules and within certain constraints with historical records kept on supervisory control and data acquisition (SCADA) system databases, the mining environment remains dynamic due to various unpredictable and uncontrollable factors influencing operations. Included therein are the unplanned and unpredictable delays within the system causing the daily targets set for blasting and hoisting of rock often not to be met. Both the time and duration of these delays are unknown and unpredictable.

It is possible to create probability models of the total daily delays or even sub divisions thereof such as operational and winder delays with very good levels of confidence using the daily hoist reports. Going a step further into reliability engineering it is possible to develop reliability or availability models of the rock winders based on historical data. These models will however only supply the controller with an estimation of the amount of time available per day for hoisting at a certain level of confidence without information as to what times of the day it will be available. This approach can therefore not be used where real-time control is required as in the case of rock winders.

Implementing a sustainable load shift program therefore requires the control system to simulate, optimise and control the actual on-site situation in real-time [10]. Load control programs also require controlled devices to be able to reschedule operation or continue operating by drawing from some form of storage [17]. In order to achieve real-time control, the controller must receive continuous feedback of what is happening on-site so as to take unplanned delays or changes in operations into account. Due to these unpredictable

and dynamic circumstances within a mine it is therefore not possible to have a fixed daily hoisting schedule based on past observations [12].

As meeting production targets are of utmost importance, the control system must be able to take into account unforeseen delays in the system and compensate by altering the rock winder hoist schedule whilst taking into account constraints and minimising costs. To this extent this dissertation proposes a model predictive control strategy for the rock winder system.

## 1.6 Objectives and contribution

The primary objective of this dissertation is the development of a near optimal half hourly hoist control scheduling program for a deep level mine twin rock winder system to achieve a set hoist target at minimum energy cost based on a TOU tariff whilst operating within various physical and operational constraints.

In achieving the primary objective the following is to be developed or formulated:

- A discrete dynamic model of the rock winder system.
- A set of winder system constraints.
- An energy cost or objective function to be minimised.
- A static linear programming problem for the winder system.
- A closed-loop MPC algorithm taking into account on-site measurements.
- An algorithm that will provide an integer schedule solution.

This dissertation contributes the following:

- A near optimal hoist control scheduling program based on a discrete dynamic constrained mixed integer linear programming (MILP) rock winder model using measured system states and delays as feedback every 30 minutes in applying closed-loop MPC.
- A program that simulates and plots a hoist schedule for the winders during weekday operating hours indicating the number of hoists and predicted system state levels for each half hour period over the simulated weekday period.
- An algorithm that combines MILP, MPC and branch and bound (BnB) principles to achieve closed-loop control providing an integer scheduling solution.

- An energy cost and objective function to be minimised based on the physical parameters of the winder system and a TOU tariff.

## 1.7 Organisation

Chapter 2 provides a brief literature study on load modelling and control within the context of this study. The chapter continues in developing and formulating a discrete dynamic winder model, winder system constraints, an energy cost function and finally a static linear programming model of the rock winder system.

Chapter 3 focuses on MPC background and applying MPC on the static linear programming model developed in Chapter 2. An MPC and integer solution algorithm is then developed and presented.

Chapter 4 provides simulated results and discussions indicating the near optimality of the integer control algorithm solution by comparing associated energy costs. A number of impact studies are conducted that include the impact of applying or not applying MPC, having or not having historical hoist information and applying or not applying the BnB methodology, the impact of applying a TOU tariff instead of a flat rate tariff on costs and schedules and finally the impact of the ratio between required hoist target per day and what is blasted in the stopes each day. Graphical results of these impact studies provide hoist schedules and ore levels against time and tabled results provides a numerical comparison between tons hoisted and energy costs.

Chapter 5 is dedicated to the study of the impact that the introduction of delays into the system has on the MPC algorithm, the constrained linear programming problem and the resulting energy costs, hoist schedules and ore levels.

Chapter 6 concludes with a summary of the dissertation highlighting the most significant observations and results. Recommendations for future study are also made with reference to this particular study.

## CHAPTER 2

### MODELLING OF A TWIN ROCK WINDER SYSTEM

#### 2.1 Load modelling and control

Various types of load modelling methods exist for various applications such as power system load analysis [23], energy models for planning, supply-demand, forecasting, optimisation and energy models based on neural networks [24, 25] and dynamic load modelling [26, 27]. With the arrival of DSM numerous models for DSM applications and evaluation have also been introduced [10, 11, 12, 13, 28, 29, 30, 31].

Assessing DSM opportunities or programmes on either power system level or in the aggregation of individual loads involves two steps [11, 28, 29, 30, 31, 32, 33, 34]. The first step is the development of accurate and adequate models of individual loads for aggregation or load groups. The second step involves applying the developed load models in methods and strategies of evaluating and selecting between different DSM or LM control strategies. Load models to be used in DSM evaluation must fulfil two objectives [30]. First the model must provide enough information to evaluate the benefits obtained through DSM and secondly the model must allow evaluation of numerous control strategies implemented by the end-user.

The deep level mine model presented in [11] reflects both objectives in [30] by developing end-user group models through a building block concept consisting of inputs, a storage buffer, a process and outputs. End-user groups for which models were developed include the mineral processing plant, mine winding system, underground mining system, compressed air system, underground water pumping system, fridge plant and the ventilation system. The end-user groups are then integrated such that the interaction and exchanging of information between end-user groups are taken into account when analysing and making load management and energy cost decisions.

Another physically based model presented in [28] aims to achieve the two objectives in [30] by including storage, process, flow and production constraints as well as the time dependent utilisation and efficiency parameters of the loads. This physically based model

is incorporated into an integer linear programming technique used to schedule the loads for a flour mill in order to minimise electricity costs [28].

An optimal load management strategy for an air conditioning plant utilising load shifting is presented in [35]. First a model of the plant and all its energy consuming components are developed to obtain a non-linear energy cost or objective function. Taking into account both energy cost savings and the costs for providing cool storage, the model minimises the total operating cost of the air conditioning plant.

In [36] a model is presented for peak-load management in steel plants coupled with an optimisation formulation utilising binary integer programming for minimising the total electricity costs while satisfying various system constraints for different tariff structures including TOU tariffs. Again process and storage constraints are taken into account and a mathematical formulation of equipment is developed to construct an operating cost or objective function that includes both energy and demand cost. The minimisation of the objective function within the constraints provides an optimal scheduling of equipment to batch processes.

An optimal control model for load shifting of a colliery conveyer transport system is presented in [37]. Taking into account silo storage constraints, conveyer belt feed rates and transport schedules an optimal control model is developed by minimising a linear energy cost objective function. As in [36] this problem is solved using binary integer programming.

Two studies directly related to the control of rock winders on deep level mines are presented in [12] and [13]. The study conducted in [13] focuses primarily on developing a system that keeps a mine's maximum demand below a certain level by controlling the rock winders in conjunction with other DSM activities on the mine. In [12] a linear energy cost model very similar to the model to be developed in this study is presented for controlling and underground rock winder system taking into account various operational and system constraints. This optimisation model is then simulated using an existing Real-time Energy Management System (REMS) [10] to provide an hourly operating schedule for the rock winders. The type of feedback control implemented in the REMS is however not made known.

A summary of the initial work done on what is presented in this chapter is contained in [38]. The paper highlights the basic dynamic programming model for a twin rock winder system and its conversion into a static linear programming problem for a near optimal hoist schedule.

## 2.2 Single rock winder model parameters

In order to minimise the energy cost of a rock winder system it is necessary to define a single rock winder model from which the amount and rate of energy consumption can be determined based on the winder's physical parameters. A typical active power load profile of two hoist cycles for a double drum rock winder is shown in Fig. 2.1 as provided by ABB South Africa.

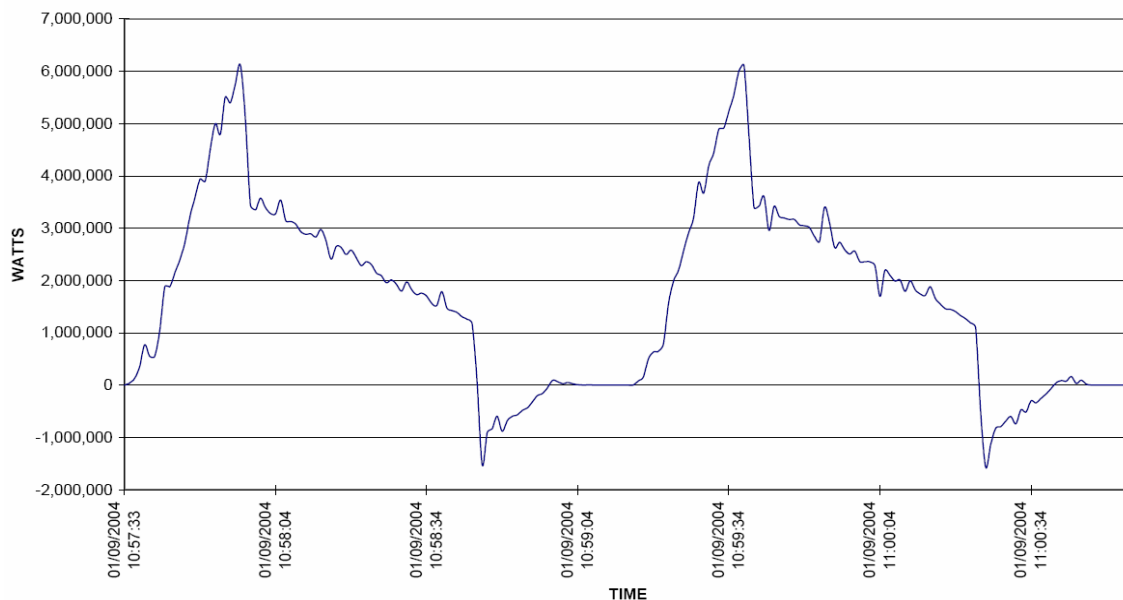


**Figure 2.1: Measured active load profile for two hoist cycles of a rock winder.**

A model to determine the active power load profile was developed in Microsoft Excel for a winder using the information provided by ALSTOM SA (Pty)Ltd. in Addendum C. The result is displayed in Fig. 2.2 from which eight states within a rock winding cycle can be observed as described in Table 2.1.

In essence four of these states (1, 3, 5, 7) are constant speed or zero acceleration states and the other four (0, 2, 4, 6) are constant positive or negative acceleration states. Integrating the power load profile in Fig. 2.2 over the whole hoist cycle period provides the energy consumed for a single hoist cycle.

**Table 2.1: Rock winding cycle state description.**

State	Time (s)	State description
0	0 - 0.7	Constant acceleration from $v = 0$ m/s to creep out speed ( $v_{co}$ ). The loaded cage starts its ascent and the empty cage starts its descent.
1	0.7 - 5.7	Constant speed at creep out speed ( $v_{co}$ ). Cages move out of the stations.
2	5.7- 26.8	Constant acceleration from $v_{co}$ to rated mean rope speed ( $v_{rmr}$ ). Cages accelerate for journey up and journey down.
3	26.8 - 112.6	Constant speed at rated mean rope speed $v_{rmr}$ . Cage now travelling in shaft at constant speeds.
4	112.6 - 133.7	Constant retardation from $v_{rmr}$ to creep in speed ( $v_{ci}$ ). Cages decelerate as they approach stations through regenerative braking causing power to be generated back into the grid.
5	133.7 - 138.7	Constant speed at creep in speed ( $v_{ci}$ ). Cages creep into stations.
6	138.7 - 139.4	Constant retardation from $v_{ci}$ to $v = 0$ m/s. Cages decelerate to standstill.
7	139.4 - 151.4	Decking / loading time. Loaded cage is emptied and vice versa.


**Figure 2.2: Modelled active load profile for a single hoist cycle of rock winder.**

In order to calculate the approximate energy consumption based on the physical parameters of the winding system the following simplifying assumptions for the winder system can be made [11]:



- The extra load because of winder skip friction is constant per winder but not included in the efficiency of the winder system.
- The payload per hoist is constant for every cycle and measured in ton.
- The influence of the weight of the skips can be neglected for a balanced system.
- The influence of the weight of the rope can be neglected for a balanced winder.

These simplifications result in the physical parameters of the winding system contained in (2.1) to be taken into account as stated in [11] for a single winder:

$$P_{input} = \frac{(tons_{payload} / skip + tons_{friction} / skip) \times g \times h}{\eta \times \left[ \frac{h}{v} + T_{unload\_time} \right]} \quad (2.1)$$

where:

- h*: Vertical winding depth or height in meters.
- tons<sub>payload</sub>/skip*: Payload per hoist in ton.
- tons<sub>friction</sub>/skip*: Friction load per hoist in ton.
- v*: Vertical speed in m/s.
- η*: Efficiency measured as the ratio of shaft output power required over total electrical input power required.
- T<sub>unload\_time</sub>*: Time to unload skip in seconds.
- g*: Gravitational acceleration as 9.81 m/s<sup>2</sup>.

The following simplifications can be made to (2.1):

- To shorten notation *tons<sub>payload</sub>/skip* is replaced with *R*.
- As indicated in the simulation data of Addendum C the friction load can be accounted for by adding a percentage of the payload to the payload. This shall be defined as the friction factor (*ff*) such that  $0 \leq ff < 0.3$ , normally taken to be approximately 0.18.
- The vertical speed in (2.1) is assumed to be constant in calculating *h/v*, but it has been seen in Table 2.1 that the speed differs from state to state. It is however possible to determine an average cycle time in seconds, *T<sub>cycle</sub>*, from measured data. This has been done using the daily hoist report data within (2.2).

$$T_{cycle} = \frac{60}{D} \sum_{d=1}^D \frac{(1440 - T_{delay}^d)}{ST^d / R} \quad (2.2)$$

where:

$D$ : Number of days used in data set.

$T_{delay}^d$ : Total delay in minutes for day  $d$ .

$ST^d$ : Screened tons hoisted on day  $d$ .

$R$ : Payload per hoist or skip in ton.

After the three simplifications above the power required for a single hoist  $P_{hoist}$  in (2.1) can be reformulated as stated in (2.3) from which the amount of energy required per hoist  $E_{hoist}$  can be calculated using (2.4):

$$P_{hoist} = \frac{(1 + ff)R \times g \times h}{\eta \times T_{cycle}} \quad [kW] \quad (2.3)$$

$$E_{hoist} = \frac{(1 + ff)R \times g \times h}{\eta} \quad [kJ] = \frac{(1 + ff)R \times g \times h}{\eta \times 3600} \quad [kWh] \quad (2.4)$$

## 2.3 Discrete dynamic twin rock winder system model

### 2.3.1 Twin rock winder system layout

Apart from the physical parameters stated above there are also other physical winder system related parameters that imposes storage, process, flow and production constraints as referred to in [28]. A schematic of the twin rock winder system to be modelled in this study is provided in Fig. 2.3.

A certain amount of tons of ore-bearing rock,  $m_{in}$ , is transported from the stopes and stored in the underground orepass system each day. The amount of rock stored in the orepass system,  $m_2$ , must remain within a minimum and maximum level. The minimum level, also referred to as plugholes, is set to prevent scaling from within the orepasses. From the orepasses the rock is conveyed into a flask where the rock is weighed to a set payload for the underground winder,  $R_g$ , before being emptied into the underground winder's skip. The loaded skip is then hoisted by the underground winder in the sub-shaft and emptied into a change-over storage. The amount of rock stored in the change-over,  $m_1$ , must also

remain within set minimum and maximum levels. Again the rock is conveyed into a flask where the rock is now weighed to a set payload for the surface winder,  $R_s$ , before being emptied into the surface winder's skip. The loaded skip is then hoisted to surface where it is in turn emptied onto a conveyance transporting the rock to a surface stockpile having a level of  $m_0$  tons. From the stockpile the rock is transported to the gold plant where the gold is extracted from the ore-bearing rock. For the purposes of this study the surface stockpile capacity and flow rate to the gold plant is deemed sufficient and will not be considered in the modelling process.

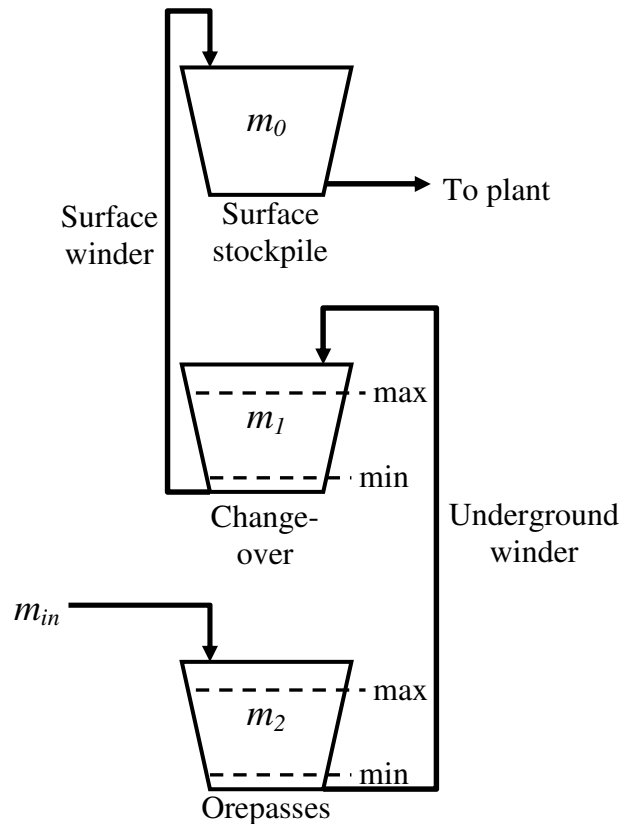


**Figure 2.3: Schematic diagram of a twin rock winder system containing a surface winder in the main shaft and an underground winder in the sub-shaft.**

### 2.3.2 Discrete dynamic modelling

The initial modelling of the rock winder system is based on the basic dynamic programming model defined in [39] as given in (2.5):

$$x_{k+1} = f_k(x_k, u_k, w_k), \quad k = 0, 1, \dots, H - 1 \quad (2.5)$$

where:

$k$ : Indexes discrete time, period number.

$H$ : Horizon, number of times control is applied or the number of control periods.



- $x_k$ : State of the system and summary of past information relevant for future optimisation.
- $u_k$ : Control or decision variable to be selected at time  $k$ .
- $w_k$ : Disturbance or noise parameter depending on the context.
- $f_k$ : Function that describes the system and in particular the mechanism by which the state is updated.

From Fig. 2.3 the following two state variables are defined:

$m_1^k$ : Tons stored in the change over at the start of period  $k$ .

$m_2^k$ : Tons stored in the underground orepass system at the start of period  $k$ .

Applying the basic dynamic programming model in (2.5) to the rock winder system results in two discrete dynamic functions:

$$\begin{aligned} m_1^{k+1} &= m_1^k + R_g u_g^k - R_s u_s^k \\ m_2^{k+1} &= m_2^k - R_g u_g^k + m_{in}^k \end{aligned} \quad \text{for } k = 0, 1, 2, \dots, H-1 \quad (2.6)$$

where:

$R_s, R_g$ : Payload per skip for the surface and underground winder respectively.

$u_s^k, u_g^k$ : Number of hoists scheduled for period  $k$  for the surface and underground winder respectively.

$R_s u_s^k, R_g u_g^k$ : Amount of tons hoisted during period  $k$  by the surface and underground winder respectively.

$m_{in}^k$ : Tons transported from the stopes into the orepass system during period  $k$ .

The dynamic functions in (2.6) are similar to the rock flow formulas developed in [12]. The disturbance or noise parameter shall in this study be incorporated as the delays that occur and will be fed back into (2.6) using MPC feedback control which will be explained in Chapter 3.

## 2.4 Rock winder system constraints

Four sets of constraints can be defined for the rock winder system of Fig. 2.3 of which three are based on physical parameters.

### 2.4.1 Tariff constraint

As stated in section 1.3 most mines operate on the Megaflex tariff with the TOU intervals as indicated in Fig. 1.2. It was also mentioned in section 1.6 that only energy costs will be considered in this study. The reason for this is explained later in this section. Mathematically the energy cost in cents per kWh at any time  $t$ ,  $c(t)$ , based on the TOU intervals can be stated as in (2.7) similar to that in [37]:

$$c(t) = \begin{cases} c_p & t \in [7,10) \cup [18,20) \\ c_s & t \in [6,7) \cup [10,18) \cup [20,22) \\ c_o & t \in [0,6) \cup [22,24) \end{cases} \quad (2.7)$$

where:

$c_p$ : Cost during peak periods;

$c_s$ : Cost during standard periods;

$c_o$ : Cost during off-peak periods;

and  $c_p > c_s > c_o$ .

The minimum period duration in (2.7) is one hour thereby putting an upper limit on the duration of a single control period  $k$ . For the purposes of this study the duration of a single control period shall be set at half an hour based on the fact that Eskom operates on half hourly integration periods to calculate maximum demand. By minimising the energy cost in half hourly control periods, the NDC cost is inherently also minimised during peak and standard periods because the average demand is directly proportional to the energy consumed. Smaller control periods will unnecessarily increase the number of variables required in a discrete solution.

### 2.4.2 Hoist constraints

Both surface and underground winders have a maximum number of hoists it can achieve within a single control period of half an hour based on the particular winder's hoist cycle period in (2.2). Before determining the upper bound for each of the winders' number of hoists however, recall that a primary part of the objective is to determine a hoist schedule for each winder stating the number of hoists to complete within each 30-minute period. This requires each scheduled value to be an integer value because the number of hoists can only be controlled as integer values. It is not possible to control or complete for example

8.67 hoists per half hour because the exact position of the skip within the shaft at the end of a 30-minute period cannot be controlled.

Using (2.2) the average cycle period for the surface winder was calculated at 158.6 seconds and that of the underground winder at 105.3 seconds. Dividing the number of seconds within half an hour by the respective cycle periods resulted in the upper bounds to be 11.35 hoists per half an hour for the surface winder and 17.09 hoists for the underground winder. The hoist constraints can therefore be stated in (2.8) as a lower and upper boundary constraint:

$$\begin{aligned} 0 \leq u_s^k \leq 11 \\ 0 \leq u_g^k \leq 17 \end{aligned} \quad \text{for all } k = 0, 1, 2, \dots, H - 1 \quad (2.8)$$

Therefore in contrast to the binary integer problems presented in [36] and [37] where a machine is either on or off during a certain period, the winders can be scheduled to complete any number of integer valued hoists within a 30-minute period within the boundaries stated in (2.8).

#### 2.4.3 Level constraints

Similar to the storage constraints taken into account in [28, 35, 36], the underground storage capacity available for ore also needs to be taken into account. The minimum and maximum rock level or state variable constraints for both the change-over and orepass system can be stated in the general form given in (2.9):

$$\begin{aligned} m_{1\min} \leq m_1^k \leq m_{1\max} \\ m_{2\min} \leq m_2^k \leq m_{2\max} \end{aligned} \quad \text{for all } k = 0, 1, 2, \dots, H - 1 \quad (2.9)$$

The minimum levels are determined by specified plughole levels that aim to prevent excessive scaling from within the orepass system and change-over. The maximum levels are determined by the sizes of the orepass system and change-over. The difference between the minimum and maximum represents the storage capacity of the orepass system and change-over. For this study all the individual orepasses are grouped together as a single storage entity or orepass system. Hence  $m_2$  represents the sum of the levels in all the underground orepasses.

#### 2.4.4 Hoist target constraint

The mine has a set production target of tons to be blasted and set hoist target of tons to be hoisted each production day and shall be defined as follows:

$M_{blast}$ : Tons of ore bearing rock to be blasted in the stopes each day.

$M_{min}$ : Minimum amount of tons to be hoisted to surface each day.

The definition of the hoist target constraint is based on the production constraints presented in [28, 35, 36, 37]. The hoist target constraint can be defined as either a daily target constraint or a horizon target constraint. If a daily target constraint is set it will be expected that the target of  $M_{min}$  be achieved each and every day. The daily target constraint takes the form of (2.10) which will result in  $d$  inequality constraints:

$$\sum_{k=h(d-1)}^{dh-1} u_s^k R_s \geq M_{min} \quad \text{for } d = 1, 2, \dots, D \quad (2.10)$$

where:

$h$ : Number of periods per day equalling 48 half hours per day.

$D$ : Number of days in the control horizon  $H$ .

Should a horizon constraint be set it will be required that the sum of the daily targets is met at the end of the horizon. The horizon target takes the form of (2.11) and will result in a single inequality constraint:

$$\sum_{k=0}^{Dh-1} u_s^k R_s \geq D \times M_{min} \quad (2.11)$$

From (2.11) it becomes clear that the number of control periods in the control horizon  $H$ , is a function of the number of days to be scheduled and can hence be calculated using (2.12).

$$H = D \times h = D \times 48 \quad (2.12)$$

If  $M_{blast} < M_{min}$  over a prolonged period of time it is obvious that winders will not be able to meet either the daily or the horizon constraints even after the minimum orepass level has been breached. If  $M_{blast} > M_{min}$  for a prolonged period of time the tons hoisted will have to exceed  $M_{min}$  to prevent the orepass level from exceeding its upper limit or boundary. For



the above reasons  $M_{blast}$  and  $M_{min}$  are usually very close in value with  $M_{blast}$  slightly exceeding  $M_{min}$ .

#### 2.4.5 Winder maintenance and testing

Law requires that routine daily winder maintenance or tests be carried out on all winders and hence no hoisting of rock is allowed during this period. For the purposes of this study the duration and starting time of these routines can be specified and shall be defined as:

$T_m$ : Number of half hourly periods required for either planned maintenance or testing.

$T_{start}$ : Time at which planned maintenance or testing is to start, either top or bottom of the hour.

In most scenarios  $T_{start}$  will be selected to be 7am or 7 since that is the start of the morning peak period. Therefore doing the required maintenance and testing during the high cost peak periods inherently reduces the energy costs. The winder maintenance and testing constraints can be classified as process constraints as in [28, 36].

## 2.5 Cost or objective function development

As the primary objective is to minimise the energy cost of the winders based on the given tariff structure within the various constraints, the objective function  $J$  will take the form of an energy cost function. The objective function will take a form similar to that developed in [28, 35, 36, 37]. It has been shown that the energy consumption per hoist can be calculated using (2.4) for both the surface and underground winders. Since the payloads, heights and efficiencies can safely be assumed to be constant, the energy consumption per hoist can also be assumed constant. Therefore the energy consumption of a winder during period  $k$  can be calculated as the product of the number of hoists during the  $k^{th}$  period,  $u^k$ , and the energy consumption per hoist  $E$  as defined below:

$E_s$ : Surface rock winder energy consumption per hoist.

$E_g$ : Underground rock winder energy consumption per hoist.

$u_s^k E_s$ : Surface rock winder energy consumption during period  $k$ .

$u_g^k E_g$ : Underground rock winder energy consumption during period  $k$ .

The time intervals for the TOU tariff defined in (2.7) are continuous and cannot be implemented for a discrete system. Hence a discrete cost function defined as a cost vector over the entire control horizon  $H$  is required and hence defined in (2.13).

$$C = [c_0 \quad c_1 \quad c_2 \quad \dots \quad c_{H-1}]^T \quad (2.13)$$

As an example Table 2.2 indicates which values in (2.7) are assigned to the elements in (2.13) for the case of  $H = 48$  periods. The cost of the energy consumed by each winder during any period  $k$  can now be calculated as the product of the energy consumed and the cost of energy as stated in Table 2.2. Hence the energy cost in period  $k$  for the surface and underground winder equates to  $c_k u_s^k E_s$  and  $c_k u_g^k E_g$  respectively.

**Table 2.2. Assigned values for the elements of the discrete cost function  $C$ .**

$t \in$	$k$	$c_k$
[0,6)	0,...,11	$c_0, \dots, c_{11} = c_o$
[6,7)	12, 13	$c_{12}, c_{13} = c_s$
[7,10)	14,...,19	$c_{14}, \dots, c_{19} = c_p$
[10,18)	20,...,35	$c_{20}, \dots, c_{35} = c_s$
[18,20)	36,...,39	$c_{36}, \dots, c_{39} = c_p$
[20,22)	40,...,43	$c_{40}, \dots, c_{43} = c_s$
[22,24)	44,...,47	$c_{44}, \dots, c_{47} = c_o$

Finally the summation of the surface and underground winder energy costs over the whole control horizon  $H$  results in the energy cost and linear objective function set in (2.14) that is to be minimised:

$$\min J = \min \left[ \sum_{k=0}^{H-1} c_k (u_s^k E_s + u_g^k E_g) \right] \quad (2.14)$$

## 2.6 Static linear programming model (SLPM) development

### 2.6.1 General SLPM statement

The constrained linear minimisation problem defined in sections 2.4 and 2.5 can be solved using static linear programming. This will however require that the objective function and

all constraints be explicitly stated for each control period within the control horizon  $H$ . The static problem can be written in the form of (2.15) for the objective function, (2.16) for lower and upper boundary constraints, (2.17) for inequality constraints and in the form of (2.18) for equality constraints. This is similar to the form presented in [37].

$$\min_u f^T \cdot u \quad (2.15)$$

$$lb \leq u \leq ub \quad (2.16)$$

$$A \cdot u \leq b \quad (2.17)$$

$$Aeq \cdot u = beq \quad (2.18)$$

$A$  and  $Aeq$  are matrices and  $f$ ,  $u$ ,  $lb$ ,  $ub$ ,  $b$  and  $beq$  are column vectors where the optimal real solution  $u$  represents the number of scheduled hoists for both rock winders for each period in  $H$ .

### 2.6.2 Objective function

The objective function  $J$  in (2.14) is divided into two vectors  $f$  and  $u$ . The first vector  $f$  contains the product between  $C$  in (2.13) and the energy per hoist for each winder. This results in a  $2H$ -element vector containing the energy cost per hoist during each period over  $H$  for each winder as stated in (2.19).

$$f = [c_0 E_s \quad c_0 E_g \quad c_1 E_s \quad c_1 E_g \quad \cdots \quad c_{H-1} E_s \quad c_{H-1} E_g]^T \quad (2.19)$$

The second vector  $u$  will, after minimisation, contain the optimal real solution of the number of scheduled hoists for both winders for each period in  $H$  and is defined in (2.20).

$$\begin{aligned} u &= [u_1 \quad u_2 \quad u_3 \quad u_4 \quad \cdots \quad u_{(2H-1)} \quad u_{2H}]^T \\ &= [u_s^0 \quad u_g^0 \quad u_s^1 \quad u_g^1 \quad \cdots \quad u_s^{(H-1)} \quad u_g^{(H-1)}]^T \end{aligned} \quad (2.20)$$

Clearly  $u$  is also a  $2H$ -element vector where uneven numbered elements represents the surface winder hoists and even numbered elements the underground winder hoists. The product of the two vectors  $f^T \cdot u$ , equals the objective function defined in (2.14).



### 2.6.3 Lower and upper boundary constraints

The hoist constraints in (2.8) stating the lower and upper boundaries for the number of hoists achievable within a half an hour period for both winders, can be written in the form of  $lb \leq u \leq ub$  as stated in (2.16). The definition of  $u$  in (2.20) must however be kept in mind and hence the uneven and even numbered elements of  $lb$  and  $ub$  must correspond to the surface and underground winder respectively. Both  $lb$  and  $ub$  will also be  $2H$ -element column vectors and is defined in (2.21) and (2.22).

$$\begin{aligned} lb &= [lb_1 \quad lb_2 \quad lb_3 \quad lb_4 \quad \cdots \quad lb_{(2H-1)} \quad lb_{2H}]^T \\ &= [lb_s \quad lb_g \quad lb_s \quad lb_g \quad \cdots \quad lb_s \quad lb_g]^T \\ &= [0 \quad 0 \quad 0 \quad 0 \quad \cdots \quad 0 \quad 0]^T \end{aligned} \quad (2.21)$$

$$\begin{aligned} ub &= [ub_1 \quad ub_2 \quad ub_3 \quad ub_4 \quad \cdots \quad ub_{(2H-1)} \quad ub_{2H}]^T \\ &= [ub_s \quad ub_g \quad ub_s \quad ub_g \quad \cdots \quad ub_s \quad ub_g]^T \\ &= [11 \quad 17 \quad 11 \quad 17 \quad \cdots \quad 11 \quad 17]^T \end{aligned} \quad (2.22)$$

The above definitions result in (2.16) being stated as in (2.23).

$$\begin{bmatrix} 0 \\ 0 \\ 0 \\ 0 \\ \vdots \\ 0 \\ 0 \end{bmatrix} \leq \begin{bmatrix} u_s^0 \\ u_g^0 \\ u_s^1 \\ u_g^1 \\ \vdots \\ u_s^{H-1} \\ u_g^{H-1} \end{bmatrix} \leq \begin{bmatrix} 11 \\ 17 \\ 11 \\ 17 \\ \vdots \\ 11 \\ 17 \end{bmatrix} \quad (2.23)$$

### 2.6.4 Inequality constraints

Both hoist target and level constraints are to be incorporated into the inequality constraint equation of (2.17):  $A \cdot u \leq b$ . The dimensions of the  $A$ -matrix will depend on  $H$  for the number of columns while the number of inequalities will determine the number of rows. From (2.17) it is clear that the number of columns of  $A$  must equal the number of rows of  $u$ , namely  $2H$ . This section will start with defining the hoist target constraint as part of  $A$  and  $b$  and then continue with the level constraints.

As discussed previously the hoist target can be stated as either a daily target constraint as defined in (2.10) or a horizon target constraint as defined in (2.11). Both (2.10) and (2.11)

are however written as “greater than” inequalities whereas (2.17) requires inequalities to be written in the form of “less than” inequalities. Converting (2.10) and (2.11) in matrix form as required by (2.17) results in (2.24) and (2.25) respectively for  $D = 2$  and hence  $H = 96$  according to (2.12).

$$\begin{bmatrix} -R_s & 0 & \dots & -R_s & 0 & 0 & 0 & \dots & 0 & 0 \\ 0 & 0 & \dots & 0 & 0 & -R_s & 0 & \dots & -R_s & 0 \end{bmatrix} \cdot \begin{bmatrix} u_s^0 & u_g^0 & \dots & u_s^{47} & u_g^{47} & u_s^{48} & u_g^{48} & \dots & u_s^{95} & u_g^{95} \end{bmatrix}^T \leq \begin{bmatrix} -M_{\min} \\ -M_{\min} \end{bmatrix} \quad (2.24)$$

$$\begin{bmatrix} -R_s & 0 & \dots & -R_s & 0 & -R_s & 0 & \dots & -R_s & 0 \end{bmatrix} \cdot \begin{bmatrix} u_s^0 & u_g^0 & \dots & u_s^{47} & u_g^{47} & u_s^{48} & u_g^{48} & \dots & u_s^{95} & u_g^{95} \end{bmatrix}^T \leq [-(D \times M_{\min})] \quad (2.25)$$

From the two inequalities above it is noted that enforcing a daily target constraint results in  $D$  inequality constraints whilst a horizon constraint results in a single inequality constraint. Formulating the discrete inequality level constraints in the required form of (2.17) requires some manipulation of (2.9) in combination with (2.6), both of which are provided again below for ease of reference.

$$\begin{aligned} m_1^{k+1} &= m_1^k + R_g u_g^k - R_s u_s^k \\ m_2^{k+1} &= m_2^k - R_g u_g^k + m_{in}^k \end{aligned} \quad \text{for } k = 0, 1, 2, \dots, H-1 \quad (2.6)$$

$$\begin{aligned} m_{1\min} &\leq m_1^k \leq m_{1\max} \\ m_{2\min} &\leq m_2^k \leq m_{2\max} \end{aligned} \quad \text{for all } k = 0, 1, 2, \dots, H-1 \quad (2.9)$$

The discrete inequality constraints (2.6a) for  $m_l$  in the change-over shall be formulated first.

Step 1: Divide (2.9a) into two “less than” inequalities as required by (2.17).

$$\begin{aligned} m_1^k &\leq m_{1\max} \\ -m_1^k &\leq -m_{1\min} \end{aligned} \quad (2.26)$$

Step 2: Substitute (2.6a) in (2.26):

$$\begin{aligned} m_1^k + R_g u_g^k - R_s u_s^k &\leq m_{1\max} \\ -(m_1^k + R_g u_g^k - R_s u_s^k) &\leq -m_{1\min} \end{aligned} \quad (2.27)$$



Step 3: Write down the discrete inequalities for (2.27a) in the form of  $A \cdot u \leq b$ :

$$\begin{aligned}
 k=0: \quad & m_1^0 + R_g u_g^0 - R_s u_s^0 \leq m_{1\max} \\
 k=1: \quad & m_1^1 + R_g u_g^1 - R_s u_s^1 \leq m_{1\max} \\
 k=1: \quad & m_1^0 + R_g u_g^0 + R_g u_g^1 - R_s u_s^0 - R_s u_s^1 \leq m_{1\max} \\
 k=1: \quad & R_g (u_2 + u_4) - R_s (u_1 + u_3) \leq m_{1\max} - m_1^0 \\
 & \vdots \\
 k=H-1: \quad & m_1^0 + R_g (u_g^0 + u_g^1 + \dots + u_g^{H-1}) - R_s (u_s^0 + u_s^1 + \dots + u_s^{H-1}) \leq m_{1\max} \\
 k=H-1: \quad & R_g (u_2 + u_4 + \dots + u_{2H}) - R_s (u_1 + u_3 + \dots + u_{2H-1}) \leq m_{1\max} - m_1^0
 \end{aligned} \tag{2.28}$$

where  $m_1^0$  is the amount of rock stored in the change-over at the beginning of the control horizon.

Step 4: Repeat step 3 for (2.27b):

$$\begin{aligned}
 k=0: \quad & -m_1^0 - R_g u_g^0 + R_s u_s^0 \leq -m_{1\min} \\
 k=1: \quad & -m_1^1 - R_g u_g^1 + R_s u_s^1 \leq -m_{1\min} \\
 k=1: \quad & -m_1^0 - R_g u_g^0 - R_g u_g^1 + R_s u_s^0 + R_s u_s^1 \leq -m_{1\min} \\
 k=1: \quad & -R_g (u_2 + u_4) + R_s (u_1 + u_3) \leq -m_{1\min} + m_1^0 \\
 & \vdots \\
 k=H-1: \quad & -m_1^0 - R_g (u_g^0 + u_g^1 + \dots + u_g^{H-1}) + R_s (u_s^0 + u_s^1 + \dots + u_s^{H-1}) \leq -m_{1\min} \\
 k=H-1: \quad & -R_g (u_2 + u_4 + \dots + u_{2H}) + R_s (u_1 + u_3 + \dots + u_{2H-1}) \leq -m_{1\min} + m_1^0
 \end{aligned} \tag{2.29}$$

Step 5: Write (2.28) and (2.29) in general form:

$$\begin{aligned}
 \sum_{j=0}^k (R_g u_g^j - R_s u_s^j) &\leq (m_{1\max} - m_1^0) \\
 \sum_{j=0}^k (R_g u_{2j+2} - R_s u_{2j+1}) &\leq (m_{1\max} - m_1^0)
 \end{aligned} \quad \text{for } k = 0, 1, 2, \dots, H-1 \tag{2.30}$$

$$\begin{aligned}
 \sum_{j=0}^k (-R_g u_g^j + R_s u_s^j) &\leq (-m_{1\min} + m_1^0) \\
 \sum_{j=0}^k (-R_g u_{2j+2} + R_s u_{2j+1}) &\leq (-m_{1\min} + m_1^0)
 \end{aligned} \quad \text{for } k = 0, 1, 2, \dots, H-1 \tag{2.31}$$

Step 6: Visualise (2.30) and (2.31) in matrix form  $A \cdot u \leq b$ :

$$\begin{bmatrix}
 -R_s & R_g & 0 & 0 & 0 & 0 & \cdots & 0 & 0 & 0 & 0 \\
 -R_s & R_g & -R_s & R_g & 0 & 0 & \cdots & 0 & 0 & 0 & 0 \\
 \vdots & \vdots & \vdots & \vdots & \vdots & \vdots & \ddots & \vdots & \vdots & \vdots & \vdots \\
 -R_s & R_g & -R_s & R_g & -R_s & R_g & \cdots & -R_s & R_g & 0 & 0 \\
 -R_s & R_g & -R_s & R_g & -R_s & R_g & \cdots & -R_s & R_g & -R_s & R_g \\
 R_s & -R_g & 0 & 0 & 0 & 0 & \cdots & 0 & 0 & 0 & 0 \\
 R_s & -R_g & R_s & -R_g & 0 & 0 & \cdots & 0 & 0 & 0 & 0 \\
 \vdots & \vdots & \vdots & \vdots & \vdots & \vdots & \ddots & \vdots & \vdots & \vdots & \vdots \\
 R_s & -R_g & R_s & -R_g & R_s & -R_g & \cdots & R_s & -R_g & 0 & 0 \\
 R_s & -R_g & R_s & -R_g & R_s & -R_g & \cdots & R_s & -R_g & R_s & -R_g
 \end{bmatrix} \cdot \begin{bmatrix}
 u_s^0 \\
 u_g^0 \\
 u_s^1 \\
 u_g^1 \\
 u_s^2 \\
 u_g^2 \\
 \vdots \\
 u_s^{H-2} \\
 u_g^{H-2} \\
 u_s^{H-1} \\
 u_g^{H-1}
 \end{bmatrix} \leq \begin{bmatrix}
 m_{1\max} - m_1^0 \\
 m_{1\max} - m_1^0 \\
 \vdots \\
 m_{1\max} - m_1^0 \\
 m_{1\max} - m_1^0 \\
 -m_{1\min} + m_1^0 \\
 -m_{1\min} + m_1^0 \\
 \vdots \\
 -m_{1\min} + m_1^0 \\
 -m_{1\min} + m_1^0
 \end{bmatrix}$$

In essence (2.30) states that the net inflow of rock into the change-over must be less than or equal to the available storage capacity at the end of any period  $k$ . Similarly (2.31) states that the net outflow must be less than or equal to the available reserve rock inside the change-over at the end of any period  $k$ .

The discrete inequality constraints for  $m_2$  in the orepass system are developed next in a similar manner as that of  $m_1$  above.

Step 1: Divide (2.9b) into two “less than” inequalities:

$$\begin{aligned}
 m_2^k &\leq m_{2\max} \\
 -m_2^k &\leq -m_{2\min}
 \end{aligned} \tag{2.32}$$

Step 2: Substitute (2.6b) into (2.32):

$$\begin{aligned}
 m_2^k - R_g u_g^k + m_{in}^k &\leq m_{2\max} \\
 -\left(m_2^k - R_g u_g^k + m_{in}^k\right) &\leq -m_{2\min}
 \end{aligned} \tag{2.33}$$

Step 3: Write down the discrete inequalities for (2.33a) in the form of  $A \cdot u \leq b$ :



$$\begin{aligned}
k = 0: & \quad m_2^0 - R_g u_g^0 + m_{in}^0 \leq m_{2\max} \\
k = 1: & \quad m_2^1 - R_g u_g^1 + m_{in}^1 \leq m_{2\max} \\
k = 1: & \quad m_2^0 - R_g u_g^0 - R_g u_g^1 + m_{in}^0 + m_{in}^1 \leq m_{2\max} \\
k = 1: & \quad -R_g (u_2 + u_4) \leq m_{2\max} - m_2^0 - (m_{in}^0 + m_{in}^1) \\
& \quad \vdots \\
k = H - 1: & \quad m_2^0 - R_g (u_g^0 + u_g^1 + \dots + u_g^{H-1}) + (m_{in}^0 + m_{in}^1 + \dots + m_{in}^{H-1}) \leq m_{2\max} \\
k = H - 1: & \quad -R_g (u_2 + u_4 + \dots + u_{2H}) \leq m_{2\max} - m_2^0 - (m_{in}^0 + m_{in}^1 + \dots + m_{in}^{H-1})
\end{aligned} \tag{2.34}$$

where  $m_2^0$  is the amount of rock stored in the orepass system at the beginning of the control horizon.

Step 4: Repeat step 3 for (2.33b):

$$\begin{aligned}
k = 0: & \quad -m_2^0 + R_g u_g^0 - m_{in}^0 \leq -m_{2\min} \\
k = 1: & \quad -m_2^1 + R_g u_g^1 - m_{in}^1 \leq -m_{2\min} \\
k = 1: & \quad -m_2^0 + R_g u_g^0 + R_g u_g^1 - m_{in}^0 - m_{in}^1 \leq -m_{2\min} \\
k = 1: & \quad R_g (u_2 + u_4) \leq -m_{2\min} + m_2^0 + (m_{in}^0 + m_{in}^1) \\
& \quad \vdots \\
k = H - 1: & \quad -m_2^0 + R_g (u_g^0 + u_g^1 + \dots + u_g^{H-1}) - (m_{in}^0 + m_{in}^1 + \dots + m_{in}^{H-1}) \leq -m_{2\min} \\
k = H - 1: & \quad R_g (u_2 + u_4 + \dots + u_{2H}) \leq -m_{2\min} + m_2^0 + (m_{in}^0 + m_{in}^1 + \dots + m_{in}^{H-1})
\end{aligned} \tag{2.35}$$

Step 5: Write (2.34) and (2.35) in general form:

$$-\sum_{j=0}^k R_g u_g^j \leq m_{2\max} - m_2^0 - \sum_{j=0}^k m_{in}^j \quad \text{for } k = 0, 1, 2, \dots, H - 1 \tag{2.36}$$

$$-\sum_{j=0}^k R_g u_{2j+2} \leq m_{2\max} - m_2^0 - \sum_{j=0}^k m_{in}^j$$

$$\sum_{j=0}^k R_g u_g^j \leq -m_{2\min} + m_2^0 + \sum_{j=0}^k m_{in}^j \quad \text{for } k = 0, 1, 2, \dots, H - 1 \tag{2.37}$$

$$\sum_{j=0}^k R_g u_{2j+2} \leq -m_{2\min} + m_2^0 + \sum_{j=0}^k m_{in}^j$$

Step 6: Visualise (2.36) and (2.37) in matrix form  $A \cdot u \leq b$ :

$$\begin{bmatrix}
 0 & -R_g & 0 & 0 & 0 & 0 & \cdots & 0 & 0 & 0 & 0 \\
 0 & -R_g & 0 & -R_g & 0 & 0 & \cdots & 0 & 0 & 0 & 0 \\
 \vdots & \vdots & \vdots & \vdots & \vdots & \vdots & \ddots & \vdots & \vdots & \vdots & \vdots \\
 0 & -R_g & 0 & -R_g & 0 & -R_g & \cdots & 0 & -R_g & 0 & 0 \\
 0 & -R_g & 0 & -R_g & 0 & -R_g & \cdots & 0 & -R_g & 0 & -R_g \\
 0 & R_g & 0 & 0 & 0 & 0 & \cdots & 0 & 0 & 0 & 0 \\
 0 & R_g & 0 & R_g & 0 & 0 & \cdots & 0 & 0 & 0 & 0 \\
 \vdots & \vdots & \vdots & \vdots & \vdots & \vdots & \ddots & \vdots & \vdots & \vdots & \vdots \\
 0 & R_g & 0 & R_g & 0 & R_g & \cdots & 0 & R_g & 0 & 0 \\
 0 & R_g & 0 & R_g & 0 & R_g & \cdots & 0 & R_g & 0 & R_g
 \end{bmatrix}
 \cdot
 \begin{bmatrix}
 u_s^0 \\
 u_g^0 \\
 u_s^1 \\
 u_g^1 \\
 u_s^2 \\
 u_g^2 \\
 \vdots \\
 u_s^{H-2} \\
 u_g^{H-2} \\
 u_s^{H-1} \\
 u_g^{H-1}
 \end{bmatrix}
 \leq
 \begin{bmatrix}
 m_{2\max} - m_2^0 - \sum_{j=0}^0 m_{in}^j \\
 m_{2\max} - m_2^0 - \sum_{j=0}^1 m_{in}^j \\
 \vdots \\
 m_{2\max} - m_2^0 - \sum_{j=0}^{H-2} m_{in}^j \\
 m_{2\max} - m_2^0 - \sum_{j=0}^{H-1} m_{in}^j \\
 -m_{2\min} + m_2^0 + \sum_{j=0}^0 m_{in}^j \\
 -m_{2\min} + m_2^0 + \sum_{j=0}^1 m_{in}^j \\
 \vdots \\
 -m_{2\min} + m_2^0 + \sum_{j=0}^{H-2} m_{in}^j \\
 -m_{2\min} + m_2^0 + \sum_{j=0}^{H-1} m_{in}^j
 \end{bmatrix}$$

Similar to the case in (2.30), (2.36) states that the net inflow of rock into the orepass system must be less than or equal to the available storage capacity at the end of any period  $k$ . So to does (2.31) state that the net outflow from the orepass system must be less than or equal to the available reserve rock inside the orepass system at the end of any period  $k$ .

### 2.6.5 Equality constraints

The equality constraint definition,  $A_{eq} \cdot u = b_{eq}$ , in (2.18) is used to incorporate the planned winder maintenance and testing constraints where as previously stated:

$T_m$ : The number of half hourly periods required for either maintenance or testing.

$T_{start}$ : Time at which planned maintenance or testing is to start where for example 07:30 is stated as the real decimal value 7.5.

The maintenance and testing constraint requires each winder to stop hoisting rock from a certain time  $T_{start}$  for a set number of periods  $T_m$ . These values can however differ for the two winders. Since the program operates using period numbers instead of time, it is necessary to convert  $T_{start}$  from an hour-based value into a period based value  $T_s$ . This is done using (2.38):

$$T_s = 2 \times T_{start} \quad (2.38)$$



In order to distinguish between the surface and underground winders'  $T_m$  and  $T_s$  values the following definitions are made by again using subscripts  $s$  for the surface winder and  $g$  for the underground winder:

$T_{ms}$ :  $T_m$  for the surface winder.

$T_{ss}$ :  $T_s$  for the surface winder.

$T_{mg}$ :  $T_m$  for the underground winder.

$T_{sg}$ :  $T_s$  for the underground winder.

In deriving the general equation for stating the equality constraint as a function of  $T_s$  and  $T_m$ ,  $T_m$  will be set to 8 periods and  $T_s$  to 14 for both winders and  $D = 1$  day resulting in  $H = 48$  periods. The above assigned values result in the following definitions for the matrix and vectors in  $Aeq \cdot u = beq$ .

The  $u$  vector can be stated from (2.20) as:

$$u = [u_1 \quad u_2 \quad \dots \quad u_{27} \quad u_{28} \quad u_{29} \quad u_{30} \quad u_{31} \quad u_{32} \quad \dots \quad u_{43} \quad u_{44} \quad u_{45} \quad u_{46} \quad \dots \quad u_{95} \quad u_{96}]^T$$

$$u = [u_s^0 \quad u_g^0 \quad \dots \quad u_s^{13} \quad u_g^{13} \quad u_s^{14} \quad u_g^{14} \quad u_s^{15} \quad u_g^{15} \quad \dots \quad u_s^{21} \quad u_g^{21} \quad u_s^{22} \quad u_g^{22} \quad \dots \quad u_s^{47} \quad u_g^{47}]^T$$

The  $Aeq$  matrix and  $beq$  vector is to be written as follows in accordance with  $u$ :

$$Aeq = \begin{bmatrix} 0 & 0 & \dots & 0 & 0 & 1 & 0 & 1 & 0 & \dots & 1 & 0 & 0 & 0 & \dots & 0 & 0 \\ 0 & 0 & \dots & 0 & 0 & 0 & 1 & 0 & 1 & \dots & 0 & 1 & 0 & 0 & \dots & 0 & 0 \end{bmatrix} \quad beq = \begin{bmatrix} 0 \\ 0 \end{bmatrix}$$

Writing the above in the form of  $Aeq \cdot u = beq$  results in:

$$\begin{bmatrix} 0 & 0 & \dots & 0 & 0 & 1 & 0 & 1 & 0 & \dots & 1 & 0 & 0 & 0 & \dots & 0 & 0 \\ 0 & 0 & \dots & 0 & 0 & 0 & 1 & 0 & 1 & \dots & 0 & 1 & 0 & 0 & \dots & 0 & 0 \end{bmatrix} \cdot$$

$$[u_s^0 \quad u_g^0 \quad \dots \quad u_s^{13} \quad u_g^{13} \quad u_s^{14} \quad u_g^{14} \quad u_s^{15} \quad u_g^{15} \quad \dots \quad u_s^{21} \quad u_g^{21} \quad u_s^{22} \quad u_g^{22} \quad \dots \quad u_s^{47} \quad u_g^{47}]^T = \begin{bmatrix} 0 \\ 0 \end{bmatrix}$$

From the above multiplication the following two equations are obtained:

$$u_s^{14} + u_s^{15} + u_s^{16} + u_s^{17} + u_s^{18} + u_s^{19} + u_s^{20} + u_s^{21} = 0 \quad (2.39)$$

$$u_g^{14} + u_g^{15} + u_g^{16} + u_g^{17} + u_g^{18} + u_g^{19} + u_g^{20} + u_g^{21} = 0 \quad (2.40)$$



Equations (2.39) and (2.40) can also be respectively written as (2.41) and (2.42):

$$u_{29} + u_{31} + u_{33} + u_{35} + u_{37} + u_{39} + u_{41} + u_{43} = 0 \quad (2.41)$$

$$u_{30} + u_{32} + u_{34} + u_{36} + u_{38} + u_{40} + u_{42} + u_{44} = 0 \quad (2.42)$$

The  $u$ -vector element numbers in (2.41) and (2.42) corresponds to the element numbers in  $Aeq$  row 1 and 2 respectively that must have values of 1. Writing (2.41) and (2.42) as functions of  $T_s$  and  $T_m$  results in (2.43) and (2.44) respectively:

$$\sum_{j=T_{ss}+1}^{T_{ss}+T_{ms}} u_{2j-1} = 0 \quad (2.43)$$

$$\sum_{j=T_{sg}+1}^{T_{sg}+T_{mg}} u_{2j} = 0 \quad (2.44)$$

Equations (2.43) and (2.44) are however only valid if  $D = 1$  resulting in  $H = 48$  and needs to be reformulated for values of  $D > 1$  as follows:

$$\sum_{d=0}^{D-1} \sum_{j=T_{ss}+1}^{T_{ss}+T_{ms}} u_{2(j+dh)-1} = 0 \quad (2.45)$$

$$\sum_{d=0}^{D-1} \sum_{j=T_{sg}+1}^{T_{sg}+T_{mg}} u_{2(j+dh)} = 0 \quad (2.46)$$

If we denote  $Aeq[r,c]$  to refer to matrix  $Aeq$  row  $r$  and column  $c$ , and using (2.43) and (2.44) we can write two equations that can be used to construct  $Aeq$ :

$$Aeq[1, (2(j+dh)-1)] = 1 \quad \text{for } j = T_{ss} + 1, \dots, T_{ss} + T_{ms}; \quad d = 0, 1, \dots, D-1 \quad (2.47)$$

$$Aeq[1, (2(j+dh))] = 1 \quad \text{for } j = T_{sg} + 1, \dots, T_{sg} + T_{mg}; \quad d = 0, 1, \dots, D-1 \quad (2.48)$$

The importance of writing the equality constraints  $u$  and not  $u_s$  and  $u_g$  will become apparent in the context of applying MPC in Chapter 3.



## 2.7 Summary of the twin rock winder system model

In Chapter 2 a static linear programming model has been developed for a twin rock winder system. The model was built on discrete dynamic state functions and an energy cost objective function with various constraints explicitly stated for each control period within the control horizon  $H$ . The most important functions developed in this chapter are presented below.

The two discrete dynamic state functions are:

$$\begin{aligned} m_1^{k+1} &= m_1^k + R_g u_g^k - R_s u_s^k \\ m_2^{k+1} &= m_2^k - R_g u_g^k + m_{in}^k \end{aligned} \quad \text{for } k = 0, 1, 2, \dots, H-1 \quad (2.6)$$

The energy cost objective function vectors in the form of  $\min_u f^T \cdot u$  are:

$$f = [c_0 E_s \quad c_0 E_g \quad c_1 E_s \quad c_1 E_g \quad \dots \quad c_{H-1} E_s \quad c_{H-1} E_g]^T \quad (2.19)$$

$$\begin{aligned} u &= [u_1 \quad u_2 \quad u_3 \quad u_4 \quad \dots \quad u_{(2H-1)} \quad u_{2H}]^T \\ &= [u_s^0 \quad u_g^0 \quad u_s^1 \quad u_g^1 \quad \dots \quad u_s^{(H-1)} \quad u_g^{(H-1)}]^T \end{aligned} \quad (2.20)$$

with the values assigned to the cost vector elements in (2.13) given in Table 2.2.

The hoist constraints are written in the form of  $lb \leq u \leq ub$ , where both  $lb$  and  $ub$  vectors contain  $2H$  elements:

$$lb = [0 \quad 0 \quad 0 \quad 0 \quad \dots \quad 0 \quad 0]^T \quad (2.21)$$

$$ub = [11 \quad 17 \quad 11 \quad 17 \quad \dots \quad 11 \quad 17]^T \quad (2.22)$$

The hoist target constraint can be written as either a daily target (2.10), or horizon target (2.11) inequality constraint. Converting (2.10) and (2.11) in the form of  $A \cdot u \leq b$  resulted in (2.24) and (2.25) respectively.

$$\sum_{k=h(d-1)}^{dh-1} u_s^k R_s \geq M_{\min} \quad \text{for } d = 1, \dots, D \quad (2.10)$$

$$\sum_{k=0}^{Dh-1} u_s^k R_s \geq D \times M_{\min} \quad (2.11)$$

The rock or ore level inequality constraints are written in the form of  $A \cdot u \leq b$  for  $k = 0, 1, 2, \dots, H - 1$

$$\sum_{j=0}^k (R_g u_g^j - R_s u_s^j) \leq (m_{1\max} - m_1^0) \quad (2.30a)$$

$$\sum_{j=0}^k (-R_g u_g^j + R_s u_s^j) \leq (-m_{1\min} + m_1^0) \quad (2.31a)$$

$$-\sum_{j=0}^k R_g u_g^j \leq m_{2\max} - m_2^0 - \sum_{j=0}^k m_{in}^j \quad (2.36a)$$

$$\sum_{j=0}^k R_g u_g^j \leq -m_{2\min} + m_2^0 + \sum_{j=0}^k m_{in}^j \quad (2.37a)$$

Finally the two mandatory winder maintenance and testing equality constraints in the form of  $Aeq \cdot u = beq$ , takes into account the time or periods required by the surface (2.45) and underground (2.46) winder for maintenance and testing:

$$\sum_{d=0}^{D-1} \sum_{j=T_{ss}+1}^{T_{ss}+T_{ms}} u_{2(j+dh)-1} = 0 \quad (2.45)$$

$$\sum_{d=0}^{D-1} \sum_{j=T_{sg}+1}^{T_{sg}+T_{mg}} u_{2(j+dh)} = 0 \quad (2.46)$$

## CHAPTER 3

### ROCK WINDER MODEL PREDICTIVE CONTROL

The need for feedback control of the rock winder system has been discussed in section 1.5 where model predictive control was proposed as the feedback control strategy for the rock winder system. The first section of Chapter 3 will give only a brief background on MPC as the focus of this dissertation is not on MPC control theories. The MPC principles presented will then be applied to the static linear programming model developed in Chapter 2 after which the MPC algorithm and associated flow diagram will be presented. The MPC algorithm includes a methodology for obtaining an integer scheduling solution by using principles from the branch and bound methodology.

#### 3.1 Model predictive control background

##### 3.1.1 Applications and advantages of MPC

An extensive historical background on MPC is given in [40] and [41]. MPC's ability to handle constraints and simple models along with its robustness and closed-loop stability, has made MPC one of the most widely used multivariable control algorithms in many industry applications [40, 42, 43] including power systems. A few examples are mentioned hereafter. An optimisation of a power plant's economic performance efficiency is presented in [44] using a short-term operating strategy via a decision support system based on MPC. MPC is also applied in [45] for optimal voltage and reactive power control. In [46] an MPC approach is proposed to alleviate thermal overloads by bringing line currents below their limits within the remaining protection time interval while at each step accounting for control change constraints. In [47] the economic operation of combined cycle power plants is optimised using MPC in order to take into account time variability of system variables. Some of these variables were integer variables, which required the MPC scheme to be formulated as a mixed integer linear programming (MILP) problem. In [48] MPC is applied for load shifting of a water pumping scheme using binary integer programming optimisation taking into account both TOU and maximum demand charges. As a final example of industry application [49] presents an MPC approach to the dynamic economic dispatch problem of generators with ramp rate constraints.

Advantages of using MPC include [40, 41]:

- High performance control systems capable of operating without expert intervention for long periods of time.
- Flexible constraint handling capabilities which are very sought after in practical applications.
- Though not inherently more or less robust than classical feedback, MPC can be adjusted more easily for robustness.
- The ability to handle or cope with hard constraints on states and controls.

### 3.1.2 Defining MPC

At the heart of all MPC algorithms lies the moving or receding horizon approach proposed in [50] back in 1963 [41]. MPC is defined in [40] as: “a form of control in which the current control action is obtained by solving on-line, at each sampling instant, a finite horizon open-loop optimal control problem, using the current state of the plant as the initial state; the optimisation yields an optimal control sequence and the first control in this sequence is applied to the plant.” The term “on-line” refers to the optimisation being repeated at each sampling instant based on real-time or updated measurements or information of the plant’s processes, outputs or state variables [41].

To explain the concept of the receding horizon approach Fig. 3.1 illustrates a single input controlled plant for which an optimal sequence of control moves is determined over a control horizon of 5 periods at each sampling instant  $k$ . At  $k = 0$ , the start of period 0, the first optimisation is completed resulting in an input sequence of 5 control moves to the plant for periods 0 through 4 as illustrated in Fig. 3.1a. However only the first move is implemented at the start of period 0.

At the beginning of period 1 or the next sampling instant  $k = 1$ , updated measurements or information of the plant state is obtained and taken as the new initial state of the plant. A new optimised solution is determined over the control horizon resulting in a new input sequence of 5 control moves to the plant for periods 1 through 5 as illustrated in Fig. 3.1b. Again only the first move is implemented at the start of period 1. Notice that the move implemented for period 1 at  $k = 1$  differs from the second move scheduled for period 1 at  $k = 0$ .

This process continues for all sampling instants  $k$  for which two more illustrations are provided in Fig. 3.1c and d. At every sampling instant  $k$  an optimal sequence of 5 control moves, which equals the horizon length of 5 periods, is determined by taking the system's state at the beginning of period  $k$  as the new initial state of the system. Every time only the first of the control moves is implemented which in most cases will differ from the move that was scheduled previously. Determining the new initial system state is based on updated measurements and information obtained on-line or in real-time from within the system or plant.

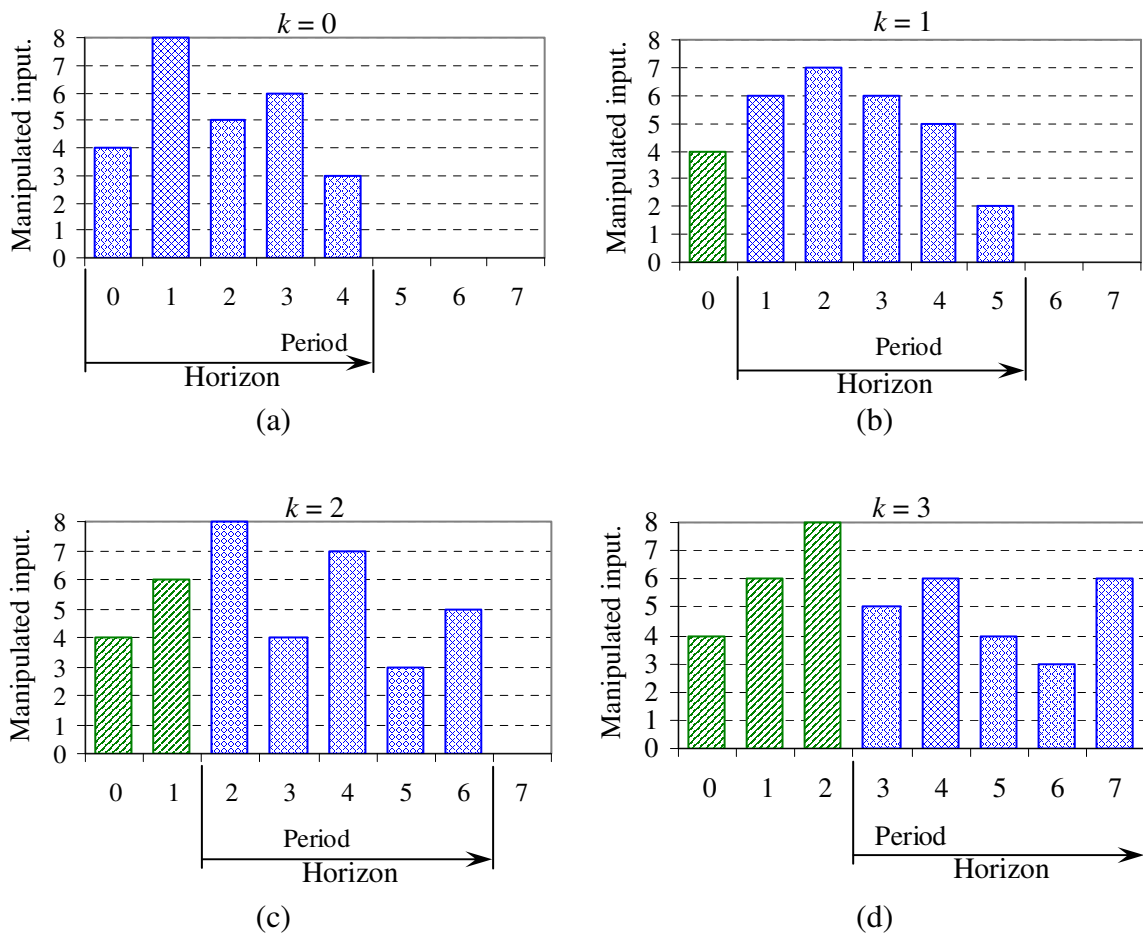


**Figure 3.1: Graphical illustration of the MPC receding horizon approach.**

Figure 3.2 shows another illustration of the basic concept for model predictive control as provided by [51]. The objective of the MPC control calculations over a control horizon  $H$  is to determine a sequence of manipulated inputs  $u$ ,  $\{u(k+j-1), j=1, 2, \dots, H\}$ , such that a set of predicted outputs over a prediction horizon  $P$ ,  $\{\hat{y}(k+j), j=1, 2, \dots, P\}$ , reaches a target in an optimal manner [51]. An explicit dynamic system model is required

to predict the future response of plant outputs or state variables over a finite prediction horizon  $P$  based on the manipulated input variables [41, 51].

The illustration in Fig. 3.2 and the objective stated above are applicable to a single step ahead prediction. Control calculations are however usually based on multiple  $j$ -step ahead predictions of future outputs  $\hat{y}(k+j)$ , current measurements including actual outputs  $y$ , and on optimizing an objective function.

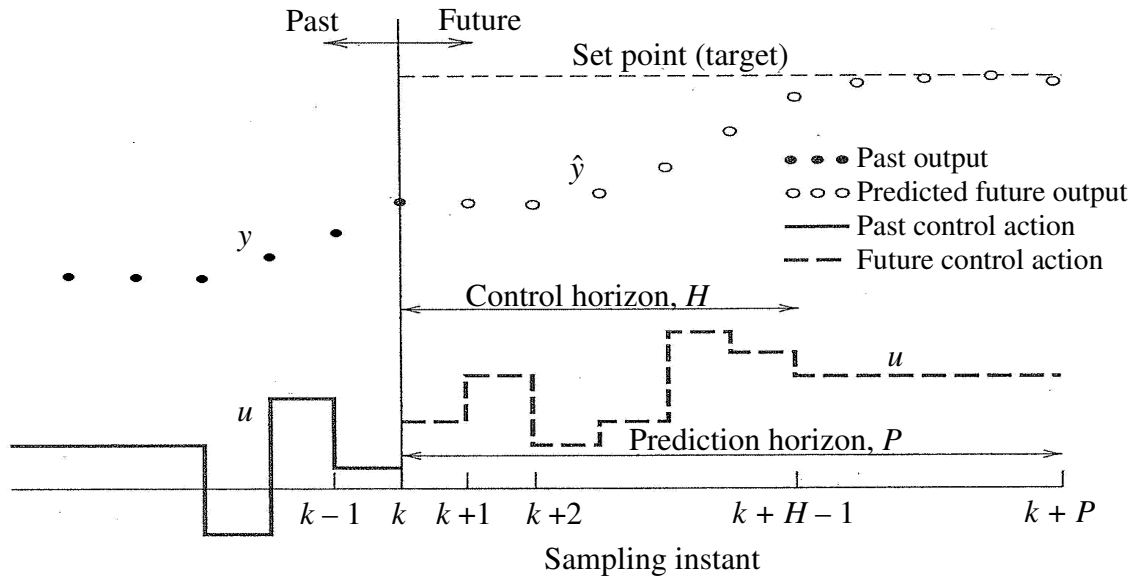


**Figure 3.2: Basic concept for model predictive control [51].**

The expression in (3.1) from [51] for a  $j$ -step ahead prediction is applicable to the step-response model of a stable, single input single output system. This MPC algorithm formulation is also presented in [41] and referred to as Dynamic Matrix Control (DMC). The first summation term represents the effect of current and future control actions while the combination of the second summation and third term represents the effect of past control actions.

$$\hat{y}(k+j) = \underbrace{\sum_{i=1}^j S_i \Delta u(k+j-i)}_{\text{Effect of current and future control actions}} + \underbrace{\sum_{i=j+1}^{N-1} S_i \Delta u(k+j-i) + S_N u(k+j-N)}_{\text{Effect of past control actions}} \quad (3.1)$$

$j = 1, 2, \dots, P \quad k = 0, 1, 2, \dots$

where:

$\hat{y}(k+j)$ : Predicted future output  $j$ -steps ahead of period  $k$ .

- $S_i$ : Model parameters.
- $N$ : Model horizon such that  $2H \leq N \leq 3H$  as recommended in [51].
- $H$ : Control horizon which if increased causes the MPC controller's aggressiveness and computational effort to increase and vice versa.
- $\Delta u$ : Change in manipulated input:  $u(k-j+1) - u(k-j)$ .

A graphical illustration of (3.1) is provided in Fig. 3.3 indicating the time location of the manipulated inputs  $u$ ,  $\{u(k+j-1), j=1, 2, \dots, H\}$ , represented by the black dots, within the model horizon  $N$  required for calculating the predicted future output  $\{\hat{y}(k+j), j=1, 2, \dots, P\}$ .

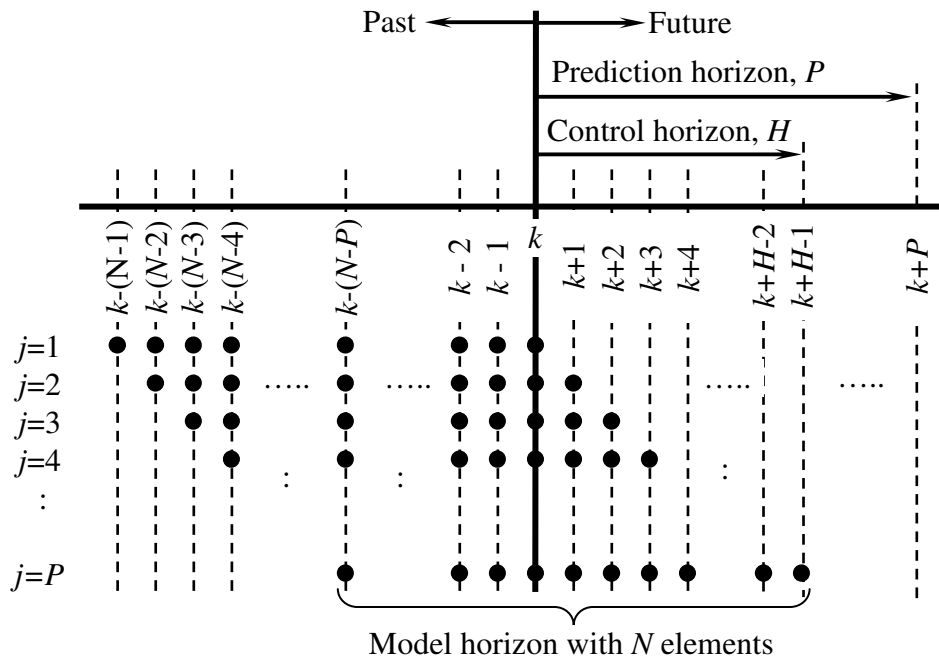


**Figure 3.3:** Illustration of the position of  $u$  within  $N$  required for  $\hat{y}$  at each step  $j$ .

### 3.2 Application of the DMC MPC algorithm formulation to the SLPM of the twin rock winder system

In this dissertation the optimisation is to be done on the predefined cost objective function subject to the constraints on the system state variables and manipulated input variables as defined and discussed in Chapter 2 and summarised in section 2.7. Applying the MPC algorithm of (3.1) to the winder system requires:

- Equation (3.1) to be reformulated so as to be a function of manipulated inputs  $u$  instead of manipulated input changes  $\Delta u$  so that the actual inputs,  $u_s$  and  $u_g$ , are manipulated as illustrated in Fig. 3.2 and not the change in inputs as is in (3.1).
- The two discrete dynamic state functions of (2.6) to be reformulated in the form of the  $j$ -step ahead DMC algorithm in (3.1).
- The objective function to be reformulated at every sampling instant  $k$  over the new control horizon  $H$ .
- The constraints on the two state variables  $m_1$  and  $m_2$  to be reformulated for  $j$ -step ahead predictions.
- The constraints that are functions of the manipulated inputs,  $u_s$  and  $u_g$ , to be reformulated for  $j$ -step ahead predictions. This excludes only the lower and upper boundary hoist constraint of (2.23).
- The prediction horizon to be set equal to the control horizon, hence  $P = H$ , due to the highly dynamic nature of the rock winder problem and for (3.1) to be written in terms of  $u$  instead of  $\Delta u$ .
- The past  $N-1$  control moves of  $u_s$  to be recorded or known as seen in Fig. 3.3. Only  $u_s$  will be required since  $u_g$  does not form part of the hoist target constraint. In the case of the absence of historical data, the algorithm is to be adjusted until  $k \geq N-1$  and sufficient historical data for  $u_s$  has been recorded or generated.

### 3.2.1 Reformulating the discrete dynamic state functions

As a first step (3.1) presented in [41] and [51] is reformulated in (3.2) so as to be a function of manipulated inputs  $u$  instead of manipulated input changes  $\Delta u$ . This results in the effect of past control actions becoming a single summation term.

$$\hat{y}(k+j) = \underbrace{\sum_{i=1}^j S_i u(k+j-i)}_{\text{Effect of current and future control actions}} + \underbrace{\sum_{i=j+1}^N S_i u(k+j-i)}_{\text{Effect of past control actions}} \quad \begin{matrix} j = 1, 2, \dots, P \\ k = 0, 1, 2, \dots \end{matrix} \quad (3.2)$$

For ease of reference the two discrete dynamic state functions are stated again below:

$$\begin{aligned} m_1^{k+1} &= m_1^k + R_g u_g^k - R_s u_s^k \\ m_2^{k+1} &= m_2^k - R_g u_g^k + m_{in}^k \end{aligned} \quad \text{for } k = 0, 1, 2, \dots, H-1 \quad (2.6)$$



The predicted output  $\hat{y}$  in (3.2) will be replaced by the two state variables  $m_1$  and  $m_2$  in (2.6). The model parameters  $S_i$  will be replaced by either of the two payload weights  $R_s$  or  $R_g$ . First the reformulation of the change-over level state function in (2.6a) into the form of (3.2) is presented by writing out (2.6a) for two steps:

$$\begin{aligned}\hat{m}_1^{k+1} &= m_1^k + R_g u_g^k - R_s u_s^k \\ \hat{m}_1^{k+2} &= \hat{m}_1^{k+1} + R_g u_g^{k+1} - R_s u_s^{k+1} \\ \hat{m}_1^{k+2} &= m_1^k + (R_g u_g^k - R_s u_s^k) + (R_g u_g^{k+1} - R_s u_s^{k+1})\end{aligned}$$

This leads to the generalised  $j$ -step ahead prediction formulation of (3.3):

$$\hat{m}_1^{k+j} = m_1^k + \overbrace{\sum_{i=1}^j (R_g u_g^{k+j-i} - R_s u_s^{k+j-i})}^{\text{Effect of current and future control actions}} \text{ for } j = 1, 2, 3, \dots, P \quad (3.3)$$

It might initially seem that only the effect of current and future control actions are contained within (3.3), but the information regarding past actions are contained in  $m_1^k$ .

Secondly the reformulation of the orepass level state function in (2.6b) into the form of (3.2) is presented by similarly writing out (2.6b) for two steps:

$$\begin{aligned}\hat{m}_2^{k+1} &= m_2^k - R_g u_g^k + m_{in}^k \\ \hat{m}_2^{k+2} &= \hat{m}_2^{k+1} - R_g u_g^{k+1} + m_{in}^{k+1} \\ \hat{m}_2^{k+2} &= m_2^k - R_g u_g^k + m_{in}^k - R_g u_g^{k+1} + m_{in}^{k+1} \\ \hat{m}_2^{k+2} &= m_2^k - (R_g u_g^k + R_g u_g^{k+1}) + (m_{in}^k + m_{in}^{k+1})\end{aligned}$$

This leads to the generalised  $j$ -step ahead prediction formulation of (3.4):

$$\hat{m}_2^{k+j} = m_2^k - \overbrace{\sum_{i=1}^j R_g u_g^{k+j-i}}^{\text{Effect of current and future control actions}} + \overbrace{\sum_{i=1}^j m_{in}^{k+j-i}}^{\text{Effect of current and future uncontrolled actions}} \text{ for } j = 1, 2, 3, \dots, P \quad (3.4)$$

Similar to the case in (3.3) the information regarding past actions are contained in  $m_2^k$ . Apart from the effect of current and future control actions, a third term is introduced representing the future anticipated inflow of rock into the orepass system, which cannot be controlled automatically. This term is therefore defined as the effect of current and future uncontrolled actions.

### 3.2.2 Reformulating the objective function at sampling instant $k$

First a new variable  $k'$  is defined as part of a truncation function:

$$k' = k - h \left\lfloor \frac{k}{h} \right\rfloor = k - hk_{tr} \quad (3.5)$$

where  $h$  was stated in (2.10) to always have a value 48 since there are 48 half hours in a day. The above definition will hence result in  $k'$  to be an element of  $[0, 1, 2, \dots, 47]$ .

Next the energy cost objective function vectors in (2.19) and (2.20) required for  $\min_u f^T \cdot u$  can be reformulated using (3.5) at sampling instant  $k$  for application in a  $j$ -step ahead prediction MPC formulation of which the result is given in (3.6) and (3.7):

$$f = \begin{bmatrix} c_{k'+j-1} E_s \\ c_{k'+j-1} E_g \\ c_{k'+j} E_s \\ c_{k'+j} E_g \\ c_{k'+j+1} E_s \\ c_{k'+j+1} E_g \\ \vdots \\ c_{k'+j+H-1} E_s \\ c_{k'+j+H-1} E_g \end{bmatrix} \quad (3.6) \quad u = \begin{bmatrix} u_1 \\ u_2 \\ u_3 \\ u_4 \\ u_5 \\ u_5 \\ \vdots \\ u_{(2H-1)} \\ u_{2H} \end{bmatrix} = \begin{bmatrix} u_s^k \\ u_g^k \\ u_s^{k+1} \\ u_g^{k+1} \\ u_s^{k+2} \\ u_g^{k+2} \\ \vdots \\ u_s^{k+H-1} \\ u_g^{k+H-1} \end{bmatrix} \quad (3.7)$$

Note the use of  $k'$  in (3.6) and of  $k$  in (3.7). It can also be seen from (3.6) that the cost vector  $C$  now needs to contain  $(P + H - 1)$  elements for the case of  $j = P$  whereas  $C$  only required  $(H - 1)$  elements in its original definition of (2.13). And since  $P = H$  for this particular problem  $C$  ends being an  $(2H - 1)$  element vector. The added elements are required because the model horizon  $N$  stretches  $(H - 1)$  elements into the future as can be seen in Fig. 3.3. The cost vector  $C$  therefore has to be reformulated.

First a 48-element cost vector  $c'$  is defined having the values given in Table 2.2 based on the TOU tariff.

$$c' = [c_0 \quad c_1 \quad c_2 \quad \cdots \quad c_{47}]^T \quad (3.8)$$

Next the cost vector  $C$  is reformulated to contain  $2D$  vector elements of  $c'$  resulting in a total of  $2Dh$  single value elements.  $D$  has previously been defined in (2.10) as the number of days in the control horizon  $H$ .

$$C = [c'_1 \quad c'_2 \quad c'_3 \quad \cdots \quad c'_{2D}]^T \quad (3.9)$$

$$C = \left[ [c_0 \quad \cdots \quad c_{47}]_1 \quad [c_0 \quad \cdots \quad c_{47}]_2 \quad [c_0 \quad \cdots \quad c_{47}]_3 \quad \cdots \quad [c_0 \quad \cdots \quad c_{47}]_{2D} \right]^T \quad (3.10)$$

### 3.2.3 Reformulating the level inequality constraints

For ease of reference the level inequalities are again stated below as defined in (2.26) and (2.32).

$$\begin{aligned} m_1^k &\leq m_{1\max} \\ -m_1^k &\leq -m_{1\min} \end{aligned} \quad (2.26)$$

$$\begin{aligned} m_2^k &\leq m_{2\max} \\ -m_2^k &\leq -m_{2\min} \end{aligned} \quad (2.32)$$

Substituting the newly formulated state functions of (3.3) and (3.4) into (2.26) and (2.32) respectively results in four newly formulated level constraints below all for  $j = 1, 2, 3, \dots, P$ :

$$\sum_{i=1}^j (R_g u_g^{k+j-i} - R_s u_s^{k+j-i}) \leq (m_{1\max} - m_1^k) \quad (3.11)$$

$$\sum_{i=1}^j (R_s u_s^{k+j-i} - R_g u_g^{k+j-i}) \leq (m_1^k - m_{1\min}) \quad (3.12)$$

$$-\sum_{i=1}^j R_g u_g^{k+j-i} \leq \left( m_{2\max} - m_2^k - \sum_{i=1}^j m_{in}^{k+j-i} \right) \quad (3.13)$$

$$\sum_{i=1}^j R_g u_g^{k+j-i} \leq \left( m_2^k + \sum_{i=1}^j m_{in}^{k+j-i} - m_{2\min} \right) \quad (3.14)$$

The four level inequality constraints in (3.11) through (3.14) respectively correspond to the four level inequality constraints in (2.30a), (2.31a), (2.36a) and (2.37a).

### 3.2.4 Reformulating the winder maintenance and testing equality constraints

The challenge faced with the two equality constraints and the reason for writing them in terms of  $u$  and not  $u_s$  and  $u_g$ , is best explained by going back and starting at the results obtained in (2.39) and (2.40) corresponding to respectively (2.41) and (2.42) shown below for ease of reference. These four equations were obtained for the SLPM case of  $T_m = 8$  periods and  $T_s = 14$  for both winders and  $D = 1$  day resulting in  $H = 48$  periods.

$$u_s^{14} + u_s^{15} + u_s^{16} + u_s^{17} + u_s^{18} + u_s^{19} + u_s^{20} + u_s^{21} = 0 \quad (2.39)$$

$$u_{29} + u_{31} + u_{33} + u_{35} + u_{37} + u_{39} + u_{41} + u_{43} = 0 \quad (2.41)$$

$$u_g^{14} + u_g^{15} + u_g^{16} + u_g^{17} + u_g^{18} + u_g^{19} + u_g^{20} + u_g^{21} = 0 \quad (2.40)$$

$$u_{30} + u_{32} + u_{34} + u_{36} + u_{38} + u_{40} + u_{42} + u_{44} = 0 \quad (2.42)$$

When applying the receding horizon formulation, the above will hold true only at sampling instant  $k = 0$ . As the model horizon recedes one period at a time (2.39) and (2.40) remains unchanged, but they no longer correspond to (2.41) and (2.42). For the case of  $k = 1$  the two equalities of (2.41) and (2.42) will be as stated below:

$$u_{27} + u_{29} + u_{31} + u_{33} + u_{35} + u_{37} + u_{39} + u_{41} = 0 \quad (3.15)$$

$$u_{28} + u_{30} + u_{32} + u_{34} + u_{36} + u_{38} + u_{40} + u_{42} = 0 \quad (3.16)$$

For ease of deriving the definition of the equality constraints in the MPC formulation, only (3.15) corresponding to the surface winder equality constraint shall be developed further, since that of the underground winder in (3.16) will follow the same process.

If the process followed from (2.41) to (3.15) is continued the following series of equalities result:

$$\text{Phase 1} \left\{ \begin{array}{l}
 k=0: u_{29} + u_{31} + u_{33} + u_{35} + u_{37} + u_{39} + u_{41} + u_{43} = 0 \\
 k=1: u_{27} + u_{29} + u_{31} + u_{33} + u_{35} + u_{37} + u_{39} + u_{41} = 0 \\
 \vdots \\
 k=13: u_3 + u_5 + u_7 + u_9 + u_{11} + u_{13} + u_{15} + u_{17} = 0 \\
 k=14: u_1 + u_3 + u_5 + u_7 + u_9 + u_{11} + u_{13} + u_{15} = 0
 \end{array} \right.$$

$$\text{Phase 2} \left\{ \begin{array}{l}
 k=15: u_1 + u_3 + u_5 + u_7 + u_9 + u_{11} + u_{13} + u_{95} = 0 \\
 k=16: u_1 + u_3 + u_5 + u_7 + u_9 + u_{11} + u_{93} + u_{95} = 0 \\
 k=17: u_1 + u_3 + u_5 + u_7 + u_9 + u_{91} + u_{93} + u_{95} = 0 \\
 k=18: u_1 + u_3 + u_5 + u_7 + u_{89} + u_{91} + u_{93} + u_{95} = 0 \\
 k=19: u_1 + u_3 + u_5 + u_{87} + u_{89} + u_{91} + u_{93} + u_{95} = 0 \\
 k=20: u_1 + u_3 + u_{85} + u_{87} + u_{89} + u_{91} + u_{93} + u_{95} = 0 \\
 k=21: u_1 + u_{83} + u_{85} + u_{87} + u_{89} + u_{91} + u_{93} + u_{95} = 0
 \end{array} \right.$$

$$\text{Phase 3} \left\{ \begin{array}{l}
 k=22: u_{81} + u_{83} + u_{85} + u_{87} + u_{89} + u_{91} + u_{93} + u_{95} = 0 \\
 k=23: u_{79} + u_{81} + u_{83} + u_{85} + u_{87} + u_{89} + u_{91} + u_{93} = 0 \\
 \vdots \\
 k=46: u_{33} + u_{35} + u_{37} + u_{39} + u_{41} + u_{43} + u_{45} + u_{47} = 0 \\
 k=47: u_{31} + u_{33} + u_{35} + u_{37} + u_{39} + u_{41} + u_{43} + u_{45} = 0
 \end{array} \right.$$

The  $u$ -element numbers correspond to the element numbers within the  $A_{eq}$  matrix's first row that must have a value of 1. The above sequence can be divided into three distinct phases as indicated above and defined below:

*Phase 1*,  $0 \leq k \leq T_{ss}$ : The element numbers are in chronological order.

*Phase 2*,  $T_{ss} < k < T_{ss} + T_{ms}$ : A break occurs in the chronological order due to a wrap around effect dividing the order into two parts.

*Phase 3*,  $T_{ss} + T_{ms} \leq k < h$ : The wrap around phase is complete and again there is an unbroken chronological order.

It is now possible to reformulate the equality constraint for  $u_s$  in (2.43) for each of the three phases:



Phase 1,  $0 \leq k \leq T_{ss}$  :

$$\sum_{i=T_{ss}}^{T_{ss}+T_{ms}} u_{2(i-k)+1} = 0 \quad (3.17)$$

Phase 2,  $T_{ss} < k < T_{ss} + T_{ms}$  :

$$\sum_{i=1}^{T_{ms}+T_{ss}-k} u_{2i-1} + \sum_{j=h+T_{ss}-k}^{h-1} u_{2i+1} = 0 \quad (3.18)$$

Phase 3,  $T_{ss} + T_{ms} \leq k < h$  :

$$\sum_{i=T_{ss}}^{T_{ss}+T_{ms}} u_{2(h+i-k)+1} = 0 \quad (3.19)$$

In order to state the equality constraints at each sampling point  $k$  over a control horizon of more than one day,  $k'$  as defined in (3.5) needs to be implemented again. This is because the definition of the equality constraints not only depends on the value of  $k$ , but also the phase in which  $k'$  is in. Following the same derivation approach for the underground winder equality constraint, replacing  $k$  with  $k'$  and defining it for  $D > 1$  will lead to the following equality constraints for each of the three phases in terms of  $u$ ,  $u_s$  and  $u_g$ . Note that from the definition in (3.5) we have  $k_{tr} = \lfloor k/h \rfloor$ .

Phase 1,  $0 \leq k' \leq T_{ss}$  :

$$\sum_{d=0}^{D-1} \left( \sum_{i=T_{ss}}^{T_{ss}+T_{ms}-1} u_{2(i-k'+dh)+1} \right) = \sum_{d=0}^{D-1} \left( \sum_{i=T_{ss}}^{T_{ss}+T_{ms}-1+(d+k_{tr})h} u_s^{i+(d+k_{tr})h} \right) = 0 \quad (3.20a)$$

$$\sum_{d=0}^{D-1} \left( \sum_{i=T_{sg}}^{T_{sg}+T_{mg}-1} u_{2(i-k'+dh)+2} \right) = \sum_{d=0}^{D-1} \left( \sum_{i=T_{sg}}^{T_{sg}+T_{mg}-1+(d+k_{tr})h} u_g^{i+(d+k_{tr})h} \right) = 0 \quad (3.20b)$$

Phase 2,  $T_{ss} < k' < T_{ss} + T_{ms}$  :

$$\sum_{d=0}^{D-1} \left( \sum_{i=1}^{T_{ms}+T_{ss}-k'} u_{2(i+dh)-1} + \sum_{i=h+T_{ss}-k'}^{h-1} u_{2(i+dh)+1} \right) = \sum_{d=0}^{D-1} \left( \sum_{i=k'}^{T_{ms}+T_{ss}-1+(d+k_{tr})h} u_s^{i+(d+k_{tr})h} + \sum_{i=T_{ss}}^{k'-1} u_s^{i+(d+k_{tr}+1)h} \right) = 0 \quad (3.21a)$$

$$\sum_{d=0}^{D-1} \left( \sum_{i=1}^{T_{mg}+T_{sg}-k'} u_{2(i+dh)+2} + \sum_{i=h+T_{sg}-k'}^{h-1} u_{2(i+dh)+2} \right) = \sum_{d=0}^{D-1} \left( \sum_{i=k'}^{T_{mg}+T_{sg}-1+(d+k_{tr})h} u_g^{i+(d+k_{tr})h} + \sum_{i=T_{sg}}^{k'-1} u_g^{i+(d+k_{tr}+1)h} \right) = 0 \quad (3.21b)$$



Phase 3,  $T_{ss} + T_{ms} \leq k' < h$ :

$$\sum_{d=0}^{D-1} \left( \sum_{i=T_{ss}}^{T_{ss}+T_{ms}-1} u_{2(h+i-k'+dh)+1} \right) = \sum_{d=0}^{D-1} \left( \sum_{i=T_{ss}}^{T_{ss}+T_{ms}-1} u_s^{i+(d+k_{tr}+1)h} \right) = 0 \quad (3.22a)$$

$$\sum_{d=0}^{D-1} \left( \sum_{i=T_{sg}}^{T_{sg}+T_{mg}-1} u_{2(h+i-k'+dh)+2} \right) = \sum_{d=0}^{D-1} \left( \sum_{i=T_{sg}}^{T_{sg}+T_{mg}-1} u_g^{i+(d+k_{tr}+1)h} \right) = 0 \quad (3.22b)$$

### 3.2.5 Reformulating the hoist target inequality constraint

Due to the receding horizon formulation of the problem the daily hoist target constraint as first defined in (2.10) cannot be applied because it is defined for a fixed time frame. On the other hand the horizon constraint defined in (2.11) is ideally suited for application in this MPC formulation and is stated again below for ease of reference.

$$\sum_{k=0}^{Dh-1} u_s^k R_s \geq D \times M_{\min} \quad (2.11)$$

Formulating the hoist target constraint of (2.11) in the form of (3.2) over the model horizon  $N$  results in (3.23) as stated below:

$$\underbrace{\sum_{i=1}^j R_s u_s^{k+j-i}}_{\text{Effect of current and future control actions}} + \underbrace{\sum_{i=j+1}^N R_s u_s^{k+j-i}}_{\text{Effect of past control actions}} \geq \frac{N}{h} M_{\min} \quad \text{for } j = 1, 2, \dots, P \quad (3.23)$$

The formulation in (3.23) can be read as follows: “The sum of the tons to be hoisted during the next  $j$  period(s) and the actual tons already hoisted to surface during the past  $(N - j)$  periods, must be greater than or equal to the product between the number of days within the model horizon  $N$  equal to  $(N/h)$ , and the daily minimum target  $M_{\min}$ .” Rewriting (3.23) in the form of  $A \cdot u \leq b$  gives:

$$-\sum_{i=1}^j R_s u_s^{k+j-i} \leq \left( \sum_{i=j+1}^N R_s u_s^{k+j-i} - \frac{N}{h} M_{\min} \right) \quad \text{for } j = 1, 2, \dots, P \quad (3.24)$$

The formulation in (3.24) can now be read as follows: “The tons to be hoisted during the next  $j$  period(s) must be equal to or greater than the difference between the actual tons

already hoisted to surface during the past  $(N - j)$  periods and the product between the number of days within the model horizon  $N$ ,  $(N/h)$ , and the daily minimum target  $M_{min}$ .”

A graphical illustration following the example of Fig. 3.3 is given for (3.24) for the case of  $h = 5 = H = P$  and  $N = 2H = 10$ . Fig. 3.4 illustrates the required past known  $u_s$  values and current and future  $u_s$  values within the target window or model horizon of  $N$  elements at each step  $j$ .

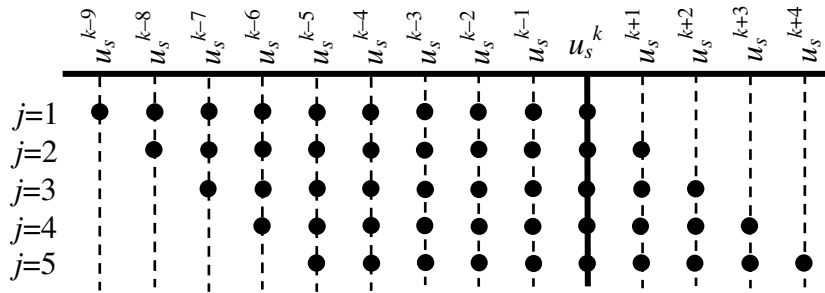


**Figure 3.4:** Graphical illustration of (3.24) for  $h = 5 = H = P$  and  $N = 2H = 10$ .

A few observations can be made from (3.24) and Fig. 3.4.

- The hoist target inequality basically states that a minimum target of  $NM_{min}/h$  tons is required over any window of  $N$  periods.
- The hoist target inequality constraint will no longer only consist of a single inequality, but of  $P$  inequalities.
- The hoist target constraint requires a minimum of  $N-1$  known or actual past control actions at  $j = 1$  as can clearly be seen from Fig. 3.4. This poses a challenge if control is to be started without having historical data of past control action. This problem is addressed as follows.

If no historical data of  $u_s^{k-1}$  to  $u_s^{N-1}$  is available at the start of the control or scheduling process, a record of the data needs to be built as time passes and the target constraint of (3.24) needs to be adapted to include what historical data is available until  $k \geq N - 1$ . This requires the time of  $0 \leq k < N - 1$  to be divided into four phases each having its own hoist target inequality formulation. The derivation of the inequalities shall be done using the example used to construct Fig. 3.4 where  $h = 5 = H = P$  and  $N = 2H = 10$ .

*Phase 1:  $k = 0$*

The first phase occurs only once at the time when there is no historical data available and hence no step ahead predictions can be made. Hence only a single target inequality constraint can be stated. The size of the available window is also not  $N$  periods or  $N/h$  days as in the case of (3.24). The available window shall be defined as being  $W$  days wide in (3.25) which equals the number of days  $D$  within the control horizon as defined in (2.12).

$$W = \frac{H}{h} \quad (3.25)$$

Graphically phase 1 can be illustrated as in Fig. 3.5 indicating that only a single inequality constraint will be written that only takes into account current and future control actions.

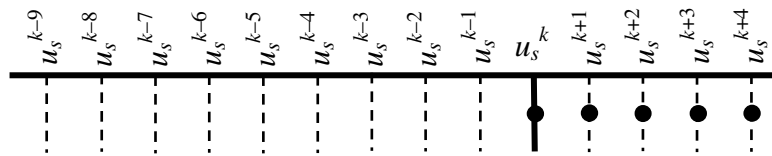


**Figure 3.5: Current and future control actions for  $u_s$  at  $k = 0$ .**

The complete inequality in (3.24) is hence reduced to include only the current and future control actions as formulated in (3.26):

$$-\sum_{i=1}^j R_s u_s^{k+j-i} \leq (-WM_{\min}) \quad \text{for } \begin{matrix} j = P \\ k = 0 \end{matrix} \quad (3.26)$$

After the first optimisation  $u_s^0$  will become  $u_s^{-1}$  at the start of the 2<sup>nd</sup> sampling instant  $k = 1$ .

*Phase 2:  $0 < k < P - 1$*

After each period's optimisation, one more historical data point for  $u_s$  becomes available, but not enough is yet available such that a full  $j$ -step ahead prediction for  $j = 1, 2, \dots, P$  can be made. As  $k$  increases after each optimisation,  $u_s^k$  becomes  $u_s^{-1}$ ,  $u_s^{-1}$  becomes  $u_s^{-2}$ ,  $u_s^{-2}$  becomes  $u_s^{-3}$ , and so forth. It will therefore be possible to make  $(k + 1)$  step ahead predictions at sampling instant  $k$  though the window size remains the same as in phase 1, namely  $W = H/h$ . A graphical illustration of this process at  $k = 1, k = 2$  and  $k = 3$  is provided in Fig. 3.6.

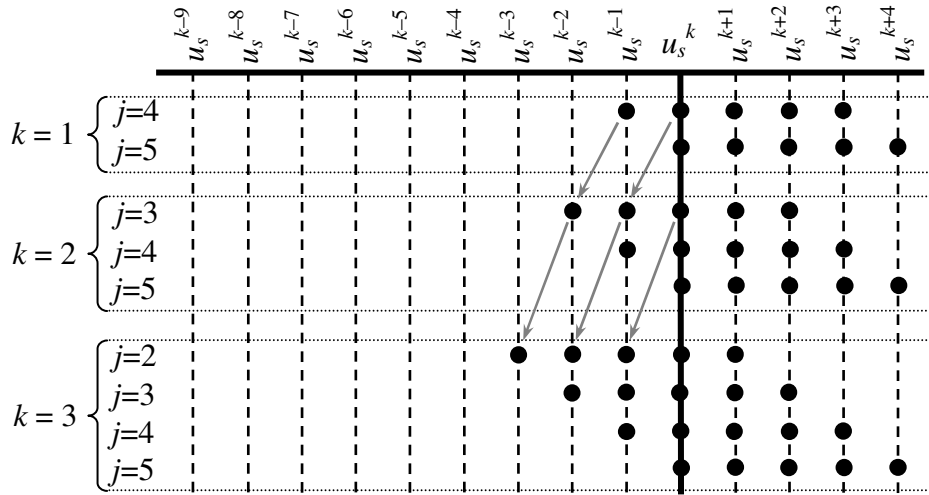


**Figure 3.6:** Illustration of the increase in step ahead predictions for  $0 < k < 4$ .

The complete inequality in (3.24) is hence reduced to include the current and future control actions along with the available historical data at sampling instant  $k$ . This is formulated in (3.27):

$$-\sum_{i=1}^j R_s u_s^{k+j-i} \leq \left( \sum_{i=j+1}^{Wh} R_s u_s^{k+j-i} - WM_{\min} \right) \quad \text{for } \begin{matrix} j = (P-k), \dots, P \\ 0 < k < P-1 \end{matrix} \quad (3.27)$$

For the case where  $H$  is chosen equal to  $h$  resulting in  $Wh = H$ , the summation on the right of the inequality will not be possible at  $j = P$  since  $P$  always equals  $H$  in this problem. For this reason the summation in question needs to be excluded from (3.27) at  $j = P$  for the special case of  $H = h$  since  $P = H$ .

*Phase 3:*  $P - 1 \leq k < N - 1$

During phase 3 the amount of historical data available will increase to  $u_s^{-(k+1)}$  after optimisation at each sampling instant  $k$ . The window size can however only increase in multiples of  $h$  which in the case of the example will be when  $u_s^{-9}$  is obtained after optimisation at  $k = 8$ . Therefore the window will remain five elements for  $k = 4, 5, 6, 7$  and 8 as illustrated in Fig. 3.7.

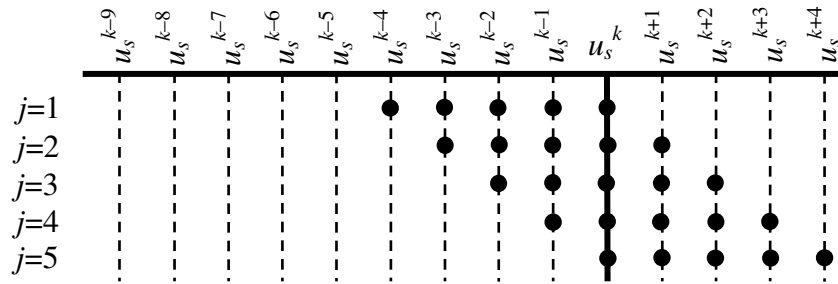


**Figure 3.7:** Illustration of  $u_s$  values required in hoist target constraint for  $4 \leq k < 9$ .

The complete inequality in (3.24) is hence written to include the current and future control actions along with the available historical data at sampling instant  $k$  over as large a window as is available. This is formulated in (3.30):

$$-\sum_{i=1}^j R_s u_s^{k+j-i} \leq \left( \sum_{i=j+1}^{W'h} R_s u_s^{k+j-i} - W'M_{\min} \right) \text{ for } \begin{matrix} j = 1, 2, \dots, P \\ P-1 \leq k < N-1 \end{matrix} \quad (3.30)$$

As in phase 2 for the case where  $H$  is chosen equal to  $h$  resulting in  $W'h = H$ , the summation on the right of the inequality will not be possible at  $j = P$  as long as  $w = 0$ . For this reason the summation in question also needs to be excluded from (3.30) at  $j = P$  for the special case of  $H = h$  as long as  $w = 0$ .

*Phase 4:*  $k \geq N-1$

From this point in time sufficient historical data is available to make use of the complete inequality of (3.24). Note that all historical data beyond  $k - (N-1)$  becomes redundant as seen from Fig. 3.3 and can therefore be discarded.

### 3.3 MPC algorithm for hoist control and scheduling

#### 3.3.1 Branch and bound

It has been stated in section 2.4.2 that the number of hoists can only be controlled as integer values. There are two common approaches to solving integer programming problems: cutting planes and the branch and bound (BnB) method [52]. A comprehensive yet simplistic description of the fundamental principles behind the BnB method is given in [53] stating the BnB to be a general search method in finding an optimal or near optimal integer solution in the optimisation of a function  $f(x)$  subject to constraints on  $x$ .

The BnB method is applied in solving various linear and mixed integer programming problems. Examples include the selection of optimal substation locations in [54], cyclic scheduling of hoist moves with time window constraints in a printed circuit board electroplating facility in [55] and linearised reactive power and voltage control in a power system in [56].

Since a linear relaxation programming problem (LR) giving real solutions are less constrained than the equivalent integer programming problem (IP) the following holds true [52]:

- In the case of a minimisation problem such as the winder scheduling problem, the optimal objective value for LR as determined by (2.15) is less than or equal to the optimal objective for the IP. This provides a lower bound on the optimal objective value.
- Any optimal solution to the overall problem must be feasible to one of the subproblems. Hence if the LR is infeasible, then so is the IP.
- The above statement implies that if an optimal solution is found to a subproblem it is a feasible solution to the overall problem, but not necessarily optimal [53].

The essence of the BnB algorithm as stated in [52] is as follows:

- i. Solve the linear relaxation problem. If the solution is integer the process ends here. Otherwise create two new subproblems by branching on a fractional variable by rounding up and rounding down.
- ii. A subproblem is not active when any of the following occurs:
  - a. You used the subproblem to branch on.
  - b. All variables in the solution are integer.
  - c. The subproblem is infeasible.
  - d. You can fathom the subproblem by a bounding argument.
- iii. Choose an active subproblem and branch on a fractional variable. Repeat until there are no active subproblems.

The application of the above principles will be shown in the MPC algorithm that will now be laid out and explained, in particular Steps 3 through 6. It must be emphasized that the manner in which the BnB principles are applied in the algorithm below does not constitute a true BnB methodology. The reason for this is that the nature of the winder scheduling

problem does not allow the exploration of active subproblems created in the past in case of an infeasible subproblem because it is not possible to go back in real-time. This point will be elaborated upon in Step 5 below.

### 3.3.2 Step 1: Initialise variables

Before starting the algorithm a number of variables needs to be initialised for this particular system. These variables are listed in Table 3.1 below.

**Table 3.1: List of variables to be initialised at  $k = 0$ .**

Variable	Units	Description
$E_s$	kWh	Surface winder energy consumption per hoist.
$E_g$	kWh	Underground winder energy consumption per hoist.
$R_s$	Ton	Surface winder fixed payload.
$R_g$	Ton	Underground winder fixed payload.
$M_{min}$	Ton	Minimum required daily hoist target.
$M_{blast}$	Ton	Planned amount of rock to be blasted each day in the stopes.
$m_{in}$	Ton	Estimated ore to be transported from stopes into the orepass system during each period equalling $M_{blast}$ over a 24-hour period.
$m_1^0$	Ton	Level of rock inside the change-over at $k = 0$ .
$m_2^0$	Ton	Level of rock inside the orepass system at $k = 0$ .
$m_{1min}, m_{1max}$	Ton	Minimum and maximum rock levels allowed inside the change-over. Lower and upper boundaries respectively.
$m_{2min}, m_{2max}$	Ton	Minimum and maximum rock levels allowed inside the orepass system. Lower and upper boundaries respectively.
$h$	Periods	Number of half hour periods per 24 hours, $h = 48$ .
$D$	Days	Number of days in the control horizon, $H = Dh = 48D$ .
$c'$	c/kWh	TOU energy cost matrix containing the cost for every half hour period between 00:00 and 23:30.
$T_{start,s}$	Time	Starting time of surface winder maintenance or testing.
$T_{ms}$	Periods	The number of half hours required for surface winder maintenance or testing.
$T_{start,g}$	Time	Starting time of underground winder maintenance or testing.
$T_{ms}$	Periods	The number of half hours required for surface winder maintenance or testing.
$N$	Periods	Model horizon for MPC control such that $2H \leq N \leq 3H$ .
$P$	Periods	Prediction horizon, $P = H$ .



### 3.3.3 Step 2: Construct and define vectors and matrices

In this part of the algorithm all the vectors and matrices required for the objective function and constraints are written or formulated at the beginning of the specific sampling instant  $k$ . The steps required are given below:

- i. Calculate  $k'$  and  $k_{tr}$  as defined in (3.5).
- ii. Construct the cost vector  $C$  as defined in (3.10).
- iii. Construct the  $f$  vector required in  $\min_u f^T \cdot u$  as defined in (3.7).
- iv. Construct the  $lb$  and  $ub$  vectors required for the hoist boundary constraints defined in (2.23).
- v. Construct the  $A$  matrix and  $b$  vector elements required in  $A \cdot u \leq b$  from the level inequality constraints according to (3.11) through (3.14).
- vi. Construct the  $A$  matrix and  $b$  vector elements required in  $A \cdot u \leq b$  from the hoist target inequality constraints according to (3.24) if historical data is available. If historical data is not available at  $k = 0$  construct according to either (3.26), (3.27) or (3.30) depending on the phase of  $k$ .
- vii. Construct the  $A_{eq}$  and  $beq$  vector elements required in  $A_{eq} \cdot u \leq beq$  according to either (3.20), (3.21) or (3.22) depending on the phase of  $k'$ .

### 3.3.4 Step 3: Minimise for a real solution

At this point an optimal real solution must be obtained for the vector  $u$  as defined in (3.7) representing the optimal hoist schedule for both surface and underground winders over the current control horizon starting at the current sampling instant  $k$ . This is achieved by the solving the minimisation problem using static linear integer programming as stated in section 2.6.1:

$$\min_u f^T \cdot u \quad (2.15)$$

$$lb \leq u \leq ub \quad (2.16)$$

$$A \cdot u \leq b \quad (2.17)$$

$$A_{eq} \cdot u = beq \quad (2.18)$$

The optimal solution to the minimisation problem puts a lower bound on the optimal objective value as described in BnB methodology of [52].

### 3.3.5 Step 4: Branch and add equality constraints

The BnB principles as described in [52] will be adapted and applied in context of the rock winder problem as follows. Using the first two elements  $u_1$  and  $u_2$  from the feasible optimal solution obtained in Step 3 for  $u$  as defined in (3.7), branch into four subproblems as illustrated in Fig. 3.8.

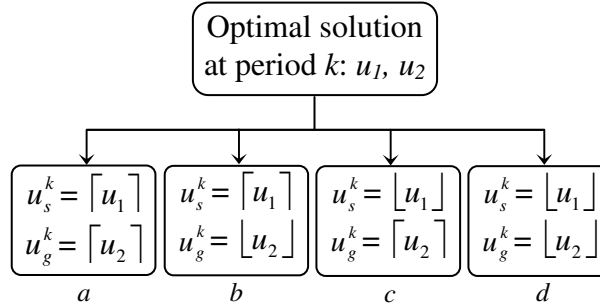


**Figure 3.8: Branching of the solution at period  $k$  into four subproblems.**

A preliminary integer solution is thereby assigned to  $u_s^k$  and  $u_g^k$  by rounding  $u_1$  and  $u_2$  respectively either up or down to the nearest integer values in each of the four subproblems  $a$  through  $d$ . For each of the four subproblems obtained create and add two equality constraints to the  $Aeq$  matrix and  $beq$  vector  $Aeq \cdot u = beq$  as defined in (3.31) using subproblem  $c$  as an example:

$$\begin{bmatrix} 1 & 0 \\ 0 & 1 \end{bmatrix} \cdot \begin{bmatrix} u_1 \\ u_2 \end{bmatrix} = \begin{bmatrix} u_s^k \\ u_g^k \end{bmatrix} = \begin{bmatrix} \lfloor u_1 \rfloor \\ \lceil u_2 \rceil \end{bmatrix} \quad (3.31)$$

### 3.3.6 Step 5: Re-minimise for a mixed integer solution

Re-minimise the problem  $\min_u f^T \cdot u$  for each of the four subproblems with their specific added equality constraints now included into  $Aeq \cdot u = beq$ . This will result in a maximum of four feasible, mixed integer, near optimal solutions for  $u$  at the beginning of sampling instant  $k$ . If no feasible solutions are found at this point the BnB methodology described in [52] would now move to any of the active subproblems created in the past to follow an alternative branch in searching for a near optimal integer solution. Physically going back in time is of course not possible in a real-time winder system and hence the MPC algorithm would theoretically need to terminate. However an alternative to termination is implemented in analytically going back in time by respectively assigning to  $u_s^k$  and  $u_g^k$  the rounded down values scheduled for  $u_s^{k+1}$  and  $u_g^{k+1}$  at the beginning of the previous sampling period,  $k - 1$ , provided that that solution was feasible. This allows the algorithm to

continue and in some cases provides a feasible solution at the very next sampling period. The methodology described above clearly indicates the deviation from the original BnB methodology as described in [52] and applied in [54, 55, 56].

### 3.3.7 Step 6: Select, set and implement only $u_s^k$ and $u_g^k$ .

If one or more feasible solutions were obtained from *Step 5*, select the values of  $u_s^k$  and  $u_g^k$  in the feasible subproblem having the lowest objective value that is not less than the optimal objective value obtained from the first minimisation in *Step 3*. Implement only these two values in period  $k$ . If no feasible solution was obtained in *Step 5* but a feasible solution was obtained in the previous sampling period  $k - 1$ , the rounded values scheduled for  $u_s^{k+1}$  and  $u_g^{k+1}$  at the beginning of the previous sampling period  $k - 1$  are assigned to  $u_s^k$  and  $u_g^k$  respectively and implemented. If even the previous sampling period  $k - 1$  could not provide a feasible solution,  $u_1$  and  $u_2$  can be both rounded down to the nearest integer and assigned to  $u_s^k$  and  $u_g^k$  respectively if the user wants to continue with the scheduling instead of terminating the algorithm.

### 3.3.8 Step 7: Update system state.

At the end of period  $k$ , obtain the following feedback information from the winder system:

- Actual number of hoists achieved by the surface winder  $\hat{u}_s^k$ , and the underground winder  $\hat{u}_g^k$ , during period  $k$ .
- The actual tons of ore transported from the stopes into the orepass system during period  $k$ ,  $\hat{m}_m^k$ .

Calculate the new initial system state values for period  $k + 1$  as indicated in (3.32):

$$\begin{aligned} m_1^{k+1} &= m_1^k + R_g \hat{u}_g^k - R_s \hat{u}_s^k \\ m_2^{k+1} &= m_2^k - R_g \hat{u}_g^k + \hat{m}_m^k \end{aligned} \quad (3.32)$$

Update the historical data vector for  $u_s$  according to Fig. 3.3 such that:

$$u_s^{k-n} = u_s^{k-(n-1)} \text{ for } n = N - 1, N - 2, \dots, 1 \quad (3.33)$$

Finally increment  $k$ :  $k = k + 1$ , and repeat from *Step 2*.

For simulation purposes a variable  $k_{max}$  can be defined to put a limit on  $k$  and hence the number of times the algorithm is to be repeated or the number of periods to simulate. Figure 3.9 provides a summary of the MPC algorithm in the form of a flow diagram.

### 3.4 Rock winder model predictive control summary

Chapter 3 gave a brief background on MPC followed by a detailed discussion on the application of the DMC MPC algorithm formulation to the SLPM of the twin rock winder system. New formulations were provided for the state variable functions, the objective cost function and all inequality and equality constraints. It was observed that the availability of historical data for  $u_s$  is a determining factor in how the constraints are written for  $k < N - 1$ . Finally an MPC algorithm that includes the BnB methodology was presented and summarised in the flow diagram of Fig. 3.9.

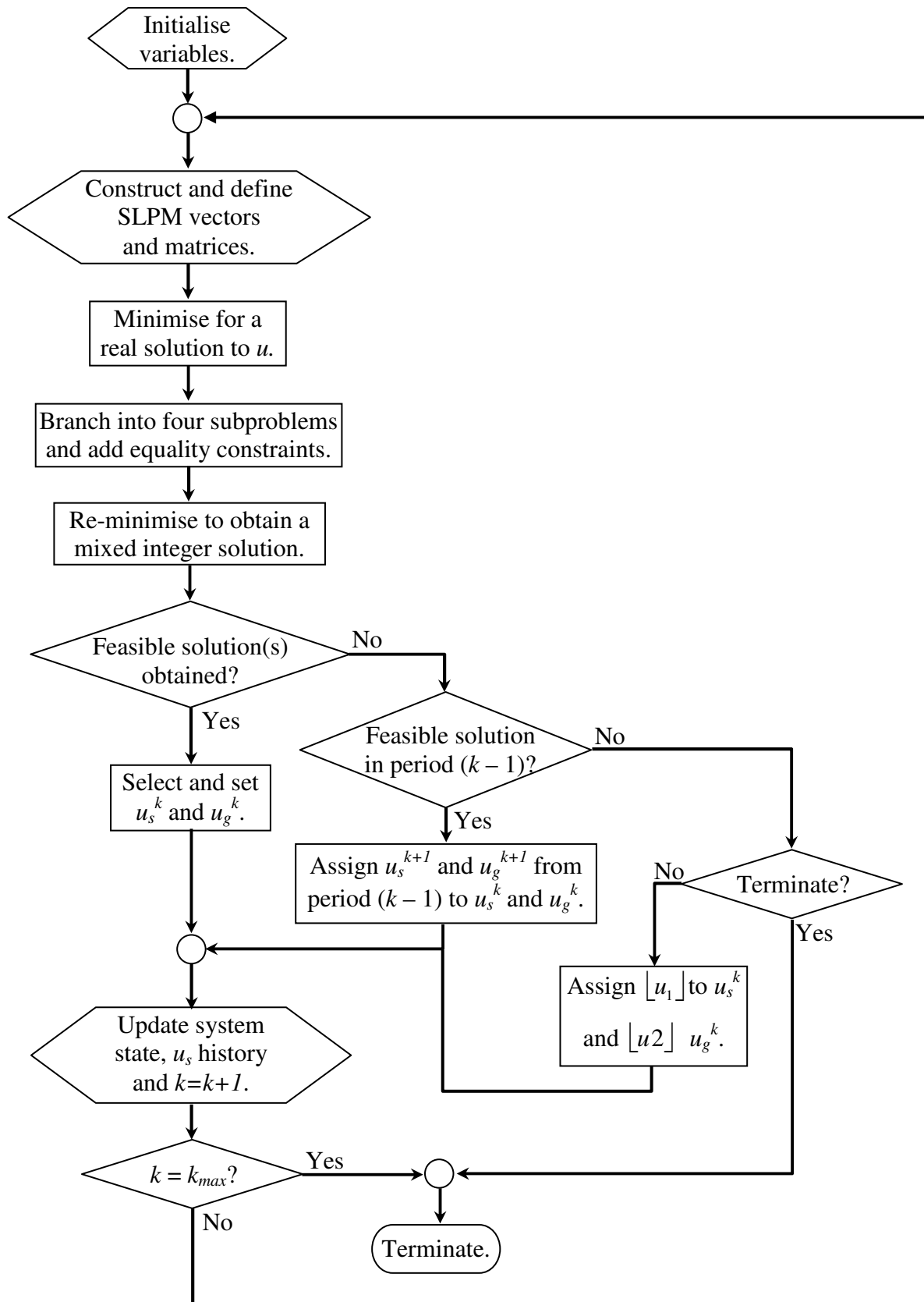


Figure 3.9: MPC algorithm flow diagram for rock winder feedback control.

## CHAPTER 4

### IMPACT SIMULATION RESULTS AND DISCUSSIONS EXCLUDING DELAYS

Chapter 4 begins with an explanation and layout of all initialisation values, methods and assumptions that includes the two aspects of setting the feed-in rate into the orepass system over a 24-hour period and the creation of a steady state history of surface rock winder hoists through and for simulation. Secondly the impact of applying or not applying MPC, having or not having historical hoist information and applying or not applying the BnB methodology is studied. The impact on costs and schedules with respect to the type of tariff applied is investigated in the third section. A fourth impact study is conducted on the effect the ratio between  $M_{min}$  and  $M_{blast}$  has on the costs, schedules and ore levels. The impact of introducing delays into the rock winder system is presented separately in Chapter 5.

#### 4.1 Initialisation and assumptions.

##### 4.1.1 Calculation of $E_s$ and $E_g$

The energy consumed by each winder per hoist is calculated using (2.4) stated below for ease of reference:

$$E_{hoist} = \frac{(1 + ff)R \times g \times h}{\eta \times 3600} \quad [kWh] \quad (2.4)$$

Both efficiencies  $\eta$  were set at 95% and both friction factors  $ff$  at 18% with gravitational acceleration set at  $9.81 \text{ m/s}^2$ . The vertical height for the surface winder is 1645 m with a fixed payload per hoist of  $R_s$  set at 23.5 ton. The vertical height of the underground winder is 939 m with  $R_g$  set at 13.5 ton. Substituting these values into (2.4) resulted in:

$$E_s = \frac{(1 + 0.18) \cdot 23.5 \text{ ton} \times 9.81 \text{ m/s}^2 \times 1645 \text{ m}}{0.95 \times 3600 \text{ kJ/kWh}} = 130.85 \text{ kWh per hoist}$$

$$E_g = \frac{(1 + 0.18) \cdot 13.5 \text{ ton} \times 9.81 \text{ m/s}^2 \times 939 \text{ m}}{0.95 \times 3600 \text{ kJ/kWh}} = 42.91 \text{ kWh per hoist}$$

### 4.1.2 Feed-in rate into orepass system

The feed-in rate of rock from the stopes via the box holes into the orepass system was calculated per period as a percentage of  $M_{blast}$ . The percentage function drawn in Fig. 4.1 was assumed to be constant for each day and built around the shift times and their respective purposes. The decrease in feed-in rate around 05:00, 14:00 and 22:00 is due to the change in shifts around those times. No feed-in occurs between 14:00 and 17:00 since that is the time that blasting occurs and no people are allowed underground. The afternoon shift's feed-in rate is lower than the morning and night shifts' since the afternoon shift's main purpose is cleaning the stopes by scraping the rock into the box holes and not transporting the rock into the orepass system.

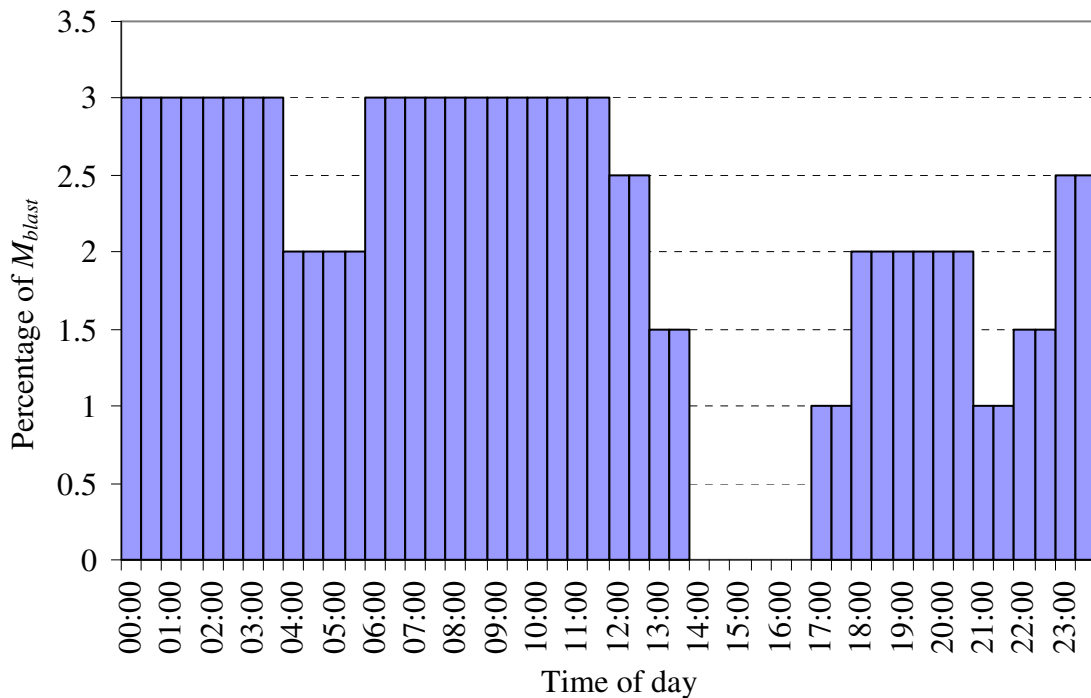


**Figure 4.1: Percentage function for feed-in rate of rock from stopes into orepass system.**

### 4.1.3 Megaflex TOU energy rates

The TOU active energy rates used in all simulations were taken from the MegaFlex rates in Addendum A according to the high-demand season. In the form of (2.7) the rates used can be written as:

$$c(t) = \begin{cases} c_p = 72.05 \text{ c/kWh} & t \in [7,10) \cup [18,20) \\ c_s = 19.04 \text{ c/kWh} & t \in [6,7) \cup [10,18) \cup [20,22) \\ c_o = 10.38 \text{ c/kWh} & t \in [0,6) \cup [22,24) \end{cases} \quad (4.1)$$

These values were then transferred to Table 2.2 and (3.8) through (3.10).

4.1.4 Initial system and control variable values

Table 4.1 below states all except three of the system and control variables along with their initial values. System variables are based on the physical parameters of the mine and on information provided by the mine’s engineer. The last five variables in Table 4.1 are the control variables determining the control and model horizon lengths and hence the aggressiveness of the control algorithm.

**Table 4.1: System and control variables to be initialised at  $k = 0$ .**

Variable	Value	Units	Description
$E_s$	130.85	KWh	Surface winder energy consumption per hoist.
$E_g$	42.91	KWh	Underground winder energy consumption per hoist.
$R_s$	23.5	Ton	Surface winder fixed payload.
$R_g$	13.5	Ton	Underground winder fixed payload.
$u_{smax}$	11	Hoists	Maximum surface winder hoists per 30 min.
$u_{gmax}$	17	Hoists	Maximum underground winder hoists per 30 min.
$M_{min}$	8 013.5	Ton	Minimum required daily hoist target, a multiple of $R_s$ .
$M_{blast}$	8 200	Ton	Planned amount of rock to be blasted each day in the stopes.
$m_{1min}$ $m_{1max}$	5000 20 000	Ton	Minimum and maximum rock levels allowed inside the change-over.
$m_{2min}$ $m_{2max}$	500 5 000	Ton	Minimum and maximum rock levels allowed inside the orepass system.
$T_{start,s}$	07:00	Time	Starting time of surface winder maintenance or testing.
$T_{ms}$	8	Periods	The number of half hours required for surface winder maintenance or testing.
$T_{start,g}$	08:00	Time	Starting time of underground winder maintenance or testing.
$T_{mg}$	4	Periods	The number of half hours required for underground winder maintenance or testing.
$h$	48	Periods	Number of half hour periods per 24 hours, $h = 48$ .
$D$	2	Days	Number of days in the control horizon, $H = Dh = 48D$ .
$H$	$2h$	Periods	Control horizon $H = Dh$
$N$	$2Dh$	Periods	Model horizon for MPC control such that $2H \leq N \leq 3H$ .
$P$	$2h$	Periods	Prediction horizon, $P = H$ .

Three variables remain to be given initial values namely that of the level of rock inside the change-over  $m_1^0$  and inside the orepass system  $m_2^0$  as well as the vector containing the historical record of the past  $(N - 1)$  measured or actual surface rock winder hoists denoted as  $u_{sm}$ .

#### 4.1.5 Obtaining values for $m_1^0$ , $m_2^0$ and $u_{sm}$

The software has been designed to start without having any historical record in order to create the history required in  $u_{sm}$  for future simulations as well as the initial values  $m_1^0$  and  $m_2^0$ . However, the algorithm does require an initial estimate of  $m_1^0$  and  $m_2^0$  that falls within the lower and upper boundaries to begin a simulation and hence arbitrary values of 1 500 ton and 11 000 ton were chosen for  $m_1^0$  and  $m_2^0$  respectively. In creating  $u_{sm}$  the simulation was allowed to run without requiring an integer solution, without introducing any delays and using the values in Table 4.1. The result obtained and illustrated in Fig. 4.2 shows the ore levels in the change-over  $m_1$  and in the orepass system  $m_2$  as broken lines to have a transient nature.

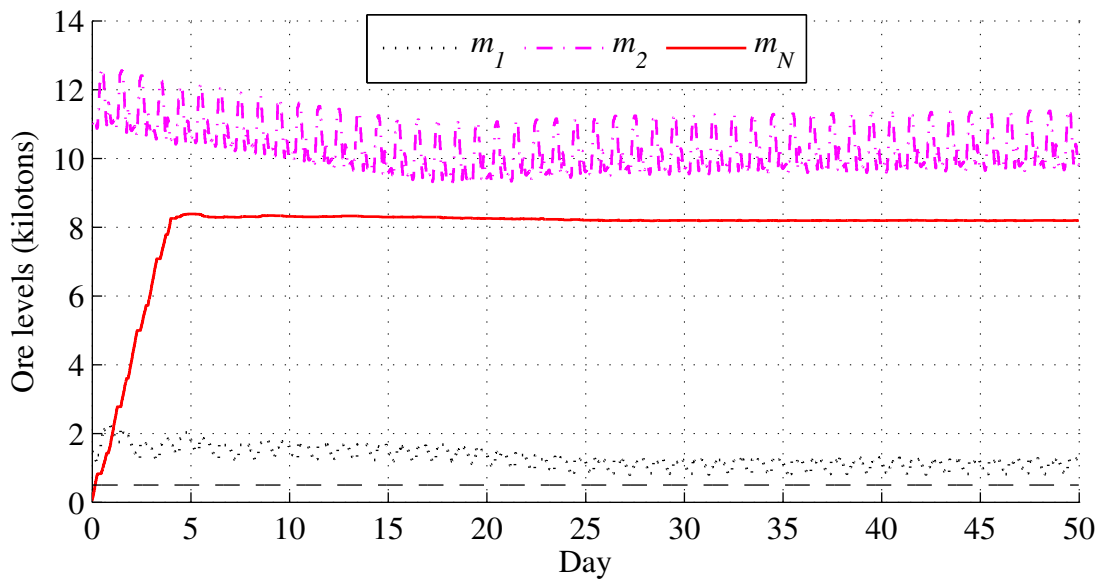


**Figure 4.2: Ore levels  $m_1$  and  $m_2$  showing a transient behaviour along with  $m_N$  approaching steady state after  $N = 4$  days.**

The solid red line represents  $m_N$ , which is defined as the average tons hoisted per 24 hours over all model horizon windows  $N$  within the simulated period in accordance with (3.24). This running average  $m_N$  is calculated at the end of each and every period as the summation of the number of hoists the surface winder completed over the past  $N$  periods multiplied by the payload  $R_s$  of which the product is then divided by  $N/h$  days. Therefore  $m_N$  at the end of any period  $k$  can be calculated using (4.2) where the summation can be visualised with the help of Fig. 3.3 for the case of  $j = 1$ .

$$m_N^k = \frac{R_s}{N/h} \sum_{i=k-(N-1)}^k u_s^i \quad (4.2)$$

The hoist schedules are not shown in Fig. 4.2 but the effect thereof in combination with the feed-in rate of rock into the orepass system can be seen in the oscillatory nature of  $m_1$  and  $m_2$ .

A few significant observations are made from Fig. 4.2 that will be of importance in the results presented later in this Chapter.

- Looking at  $m_1$  and  $m_2$  a distinct transient is observed moving towards a steady state after approximately 45 to 50 days. The final values of  $m_1$  and  $m_2$  at the end of the transient period were to be taken as the initial values for  $m_1^0$  and  $m_2^0$  for use in future simulations where  $M_{min} = 8\ 013.5$  tons and  $M_{blast} = 8\ 200$  tons. These values were  $m_1^0 = 1\ 168$  tons and  $m_2^0 = 9\ 806$  tons. Should either  $M_{min}$  or  $M_{blast}$  be changed new steady state values would have to be obtained for future simulations based on the changed  $M_{min}$  or  $M_{blast}$ .
- The level of  $m_1$  and  $m_2$  remain within the minimum and maximum constraints set in Table 4.1 at all times.
- It took four days for  $m_N$  to reach  $M_{min}$ , which equals the length of the model horizon  $N$  of four days.
- The steady state value of  $m_N$  does not equal the target  $M_{min}$ , but rather the amount of rock blasted per day  $M_{blast}$ , because what is blasted needs to be hoisted or else both orepass and change-over levels will eventually exceed their upper boundaries. This will saturate the whole ore transport system.
- For this particular scenario the change-over level came very close to its lower boundary of 500 tons providing very little room for underground winder delays or a sudden increase in surface winder hoists. Either of the above would result in the lower boundary  $m_{1min}$  constraint to be violated.

## 4.2 Impact of MPC, historical information and BnB

The steady state values obtained in Fig. 4.2 was used in this section to illustrate the impact of applying or not applying MPC in scheduling the hoists for two scenarios. In the first scenario it was assumed that no historical hoist information  $u_{sm}$  was available. In the second scenario the historical hoist information for  $u_{sm}$  obtained from Fig. 4.2 was taken into account. It is important to keep in mind that it is the number of surface hoists

achieved that determines whether or not the target of  $M_{min}$  is obtained. For the case of exploring the impact of MPC and history only real or non-integer solutions were considered. The application of BnB to obtain an integer solution is introduced and investigated later in this chapter.

#### 4.2.1 Impact of not applying MPC and not having historical hoist information

Using the initial values of Table 4.1 and that of  $m_1^0$  and  $m_2^0$  obtained in the previous section, a schedule was determined for both winders for and only at the beginning of a 2-day period having assumed that past hoist schedule information was not available. A 2-day period was required since the control horizon equaled two days. The resulting schedule in Fig. 4.3 shows an optimal scheduling solution over the two days that did not consider effects or consequences beyond the 2-day period.

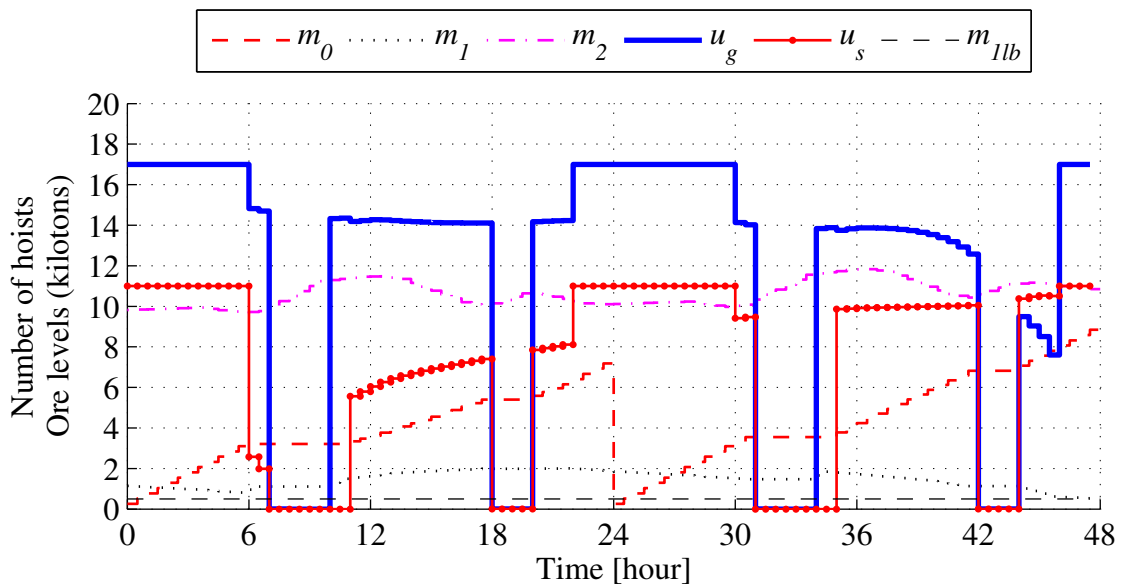


**Figure 4.3: An optimal 2-day hoisting schedule without applying MPC and not having historical hoist information.**

The solid blue line represents the underground winder hoist schedule while the solid red line with markers represents the surface winder hoist schedule. The change-over  $m_1$  and the orepass  $m_2$  levels are presented as in Fig. 4.2. The broken red line  $m_0$  represents the amount of tons hoisted to surface at a specific time of day starting at zero each day and ending at the amount of tons hoisted to surface for that particular day. The broken black line at 500 tons represents the lower boundary of  $m_{1min}$  denoted as  $m_{llb}$ .

The following observations should be noted from Fig. 4.3:

- Both winder schedules contain real or non-integer values that never exceeded their upper boundaries of  $u_{smax} = 11$  and  $u_{gmax} = 17$ .
- No hoisting was scheduled for either winder during the evening peak period between 18:00 and 20:00. Neither was hoisting scheduled during the morning peak period between 07:00 and 10:00 even though the underground winder's mandatory maintenance or testing only starts at 08:00.
- Limited hoisting was scheduled during standard periods and maximum hoisting was scheduled during off-peak periods.
- The surface winder only had hoists scheduled from 11:00 since its maintenance only ends at 11:00.
- The level of  $m_l$  was at the lower boundary of 500 tons at the end of the 2-day scheduled period.

The numerical results in Table 4.2 indicate the tons hoisted and the energy costs on days 1 and 2 along with the averages.

**Table 4.2: Numerical results for Fig. 4.3.**

	Tons hoisted	Energy cost
Day 1	7 184.35	R 9 394
Day 2	8 842.65	R 10 881
Average	8 013.50	R 10 137

Notice that the average tons hoisted over the two days equals 8 013.5 tons, which is the absolute minimum the surface winder can hoist and still achieve the hoist target of  $M_{min}$ . Not knowing how much has been hoisted in the past therefore forced the controller to schedule sufficient hoists during the two days to achieve the target of  $M_{min}$  over the 2-day control horizon  $H$ .

#### 4.2.2 Impact of not applying MPC but taking historical hoist information into account

The same experiment conducted in section 4.1.1 was repeated with the only difference having been that historical hoist information of the surface winder  $u_{sm}$  was taken into account. Again a schedule was determined for both winders for and only at the beginning of a 2-day period. However, since the historical hoist information was taken into account the horizon not only spanned the two future days in the control horizon but also the two previous days which in total formed the 4-day model horizon. Graphically this

corresponds to the case of  $j = P$  in Fig. 3.3 where the controller ensures that the tons hoisted in the past plus the tons scheduled to be hoisted in future will on average over the model horizon satisfy the  $M_{min}$  target. The following observations can be made from the resulting schedule illustrated in Fig. 4.4:

- Again no hoisting was scheduled during peak periods while limited hoisting was scheduled during standard and maximum during off-peak periods to provide a minimal energy cost schedule. A distinct decline occurs in the number of hoists scheduled for both winders during the second day's standard period between 10:00 and 22:00 compared to the scenario in Fig. 4.3.
- The level of  $m_1$  was again at its lower boundary of 500 tons at the end of the 2-day scheduled period. The schedule therefore again did not consider effects or consequences beyond the 2-day period.

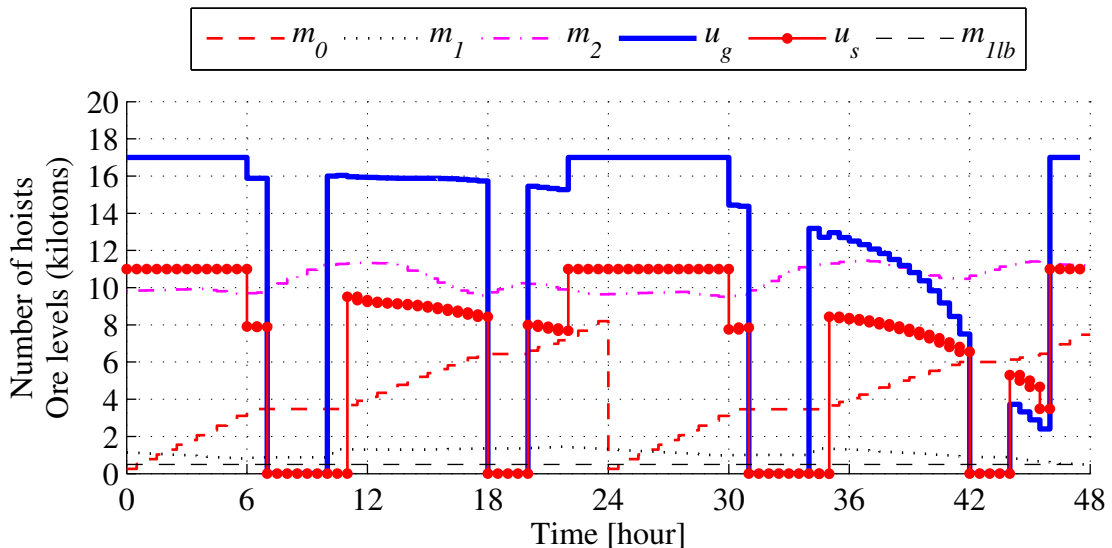


**Figure 4.4: An optimal 2-day hoisting schedule without applying MPC but taking into account historical hoist information.**

An explanation for the distinct decline in the number of scheduled surface and underground winder hoists during the second day's standard period can be found in the numerical results listed in Table 4.3. Included in Table 4.3 are the tons hoisted for the previous two days and the tons scheduled to be hoisted over the next two days. The average tons hoisted per day was now calculated over a 4-day period in contrast to the 2-day period in Table 4.2. This resulted in a much lower target required for day 2 in order to achieve an average of  $M_{min} = 8\ 013.5$  tons.

**Table 4.3: Numerical results for Fig. 4.4.**

	Tons hoisted	Energy cost
Day -2	8 181.33	-
Day -1	8 192.71	-
Day 1	8 202.24	R 10 751
Day 2	7 477.72	R 8 941
Average	8 013.50	R 9 846

Knowing and taking past hoisting history into account therefore resulted in the minimum hoists being scheduled for day 1 and much less for day 2 when compared to the scenario in Fig. 4.4 and Table 4.3. The minimal scheduling of hoists is also an optimal schedule that resulted in the lowest possible energy cost.

#### 4.2.3 Impact of applying MPC whilst not having historical hoist information

In this scenario MPC was applied to the same experiment conducted in section 4.2.1 where it was assumed that no historical information was available. This was in effect a repeat of the experiment conducted to create historical data as discussed in section 4.1.4 and illustrated in Fig. 4.2 with the only difference having been the initial values of  $m_1^0$  and  $m_2^0$ . The resulting 2-day schedule is illustrated in Fig. 4.5 in which the average tons hoisted over the previous  $N$ -periods  $m_N$  as defined in (4.2) is now also shown.

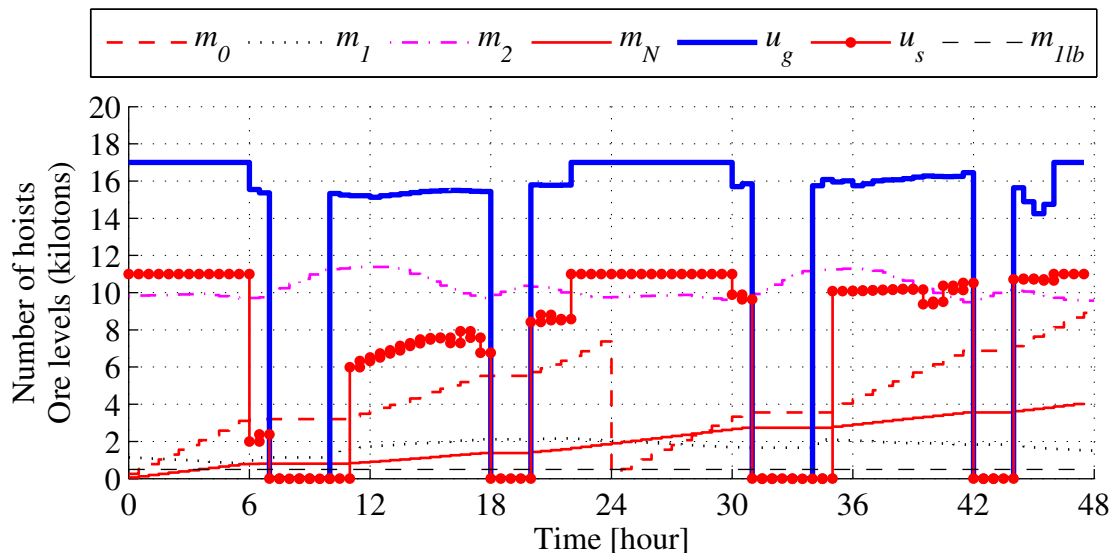


**Figure 4.5: An optimal 2-day hoisting schedule with MPC applied and not having historical hoist information.**

The above schedules and information is not the result of only a single optimisation as was the case for the two previous schedules in Fig. 4.3 and Fig. 4.4, but of 96 optimisations each carried out at the beginning of each of the 96 sampling periods within the scheduled horizon.

The following observations are to be noted from Fig 4.5:

- No hoisting was scheduled during peak periods while limited hoisting was scheduled during standard and maximum during off-peak periods to provide a minimal energy cost schedule.
- The level of  $m_l$  did not finish at the lower boundary of 500 tons at the end of the 2-day scheduled period. This is because the MPC at the start of each period took into account what would happen over the whole control horizon of two days into the future ensuring that all constraints would be adhered to. The final optimisation at the 48<sup>th</sup> period would be similar to that of Fig. 4.4.
- No decrease in the number of hoists scheduled occurred at the end of the two days as in Fig. 4.4 because of having applied MPC.
- The  $m_N$  average was calculated over the entire 4-day model horizon and hence started at zero and slowly increased towards reaching steady state after approximately four days as in Fig. 4.2.

The numerical results provided in Table 4.4 indicate that the average tons hoisted over the two days is higher than  $M_{min}$  as it increases towards a steady state value of approximately  $M_{blast}$  as shown in Fig. 4.2.

**Table 4.4: Numerical results for Fig. 4.5.**

	Tons hoisted	Energy cost
Day 1	7 373.99	R 9 809
Day 2	8 918.72	R 11 518
Average of 2 days	8 146.35	R 10 664
$m_N$ at the end of day 2	4 073.18	-

The resulting MPC hoist schedule therefore not only provided a minimal energy cost by hoisting just  $M_{min}$  tons, but an optimal energy cost and schedule that would ensure that all constraints are adhered to during the two scheduled days and also in future.

#### 4.2.4 Impact of applying MPC and taking historical hoist information into account

Finally MPC was applied while taking history into account resulting in the schedule illustrated in Fig. 4.6. In essence the two days depicted in Fig. 4.6 is a continuation from the 50<sup>th</sup> day in Fig. 4.2. In other words, days 1 and 2 in Fig. 4.6 are days 51 and 52 for Fig. 4.2. The following can be observed from Fig. 4.6:

- The  $m_N$  average continued at its steady state value of almost  $M_{blast} = 8\ 200$  tons.
- As in the previous three scenarios no hoisting was scheduled during peak periods while limited hoisting was scheduled during standard and maximum during off-peak periods to provide a minimal energy cost schedule.
- The level of  $m_l$  came very close to the minimum 500 ton level and in particular between 03:00 and 10:00 in the mornings. This was also noted in Fig. 4.2.

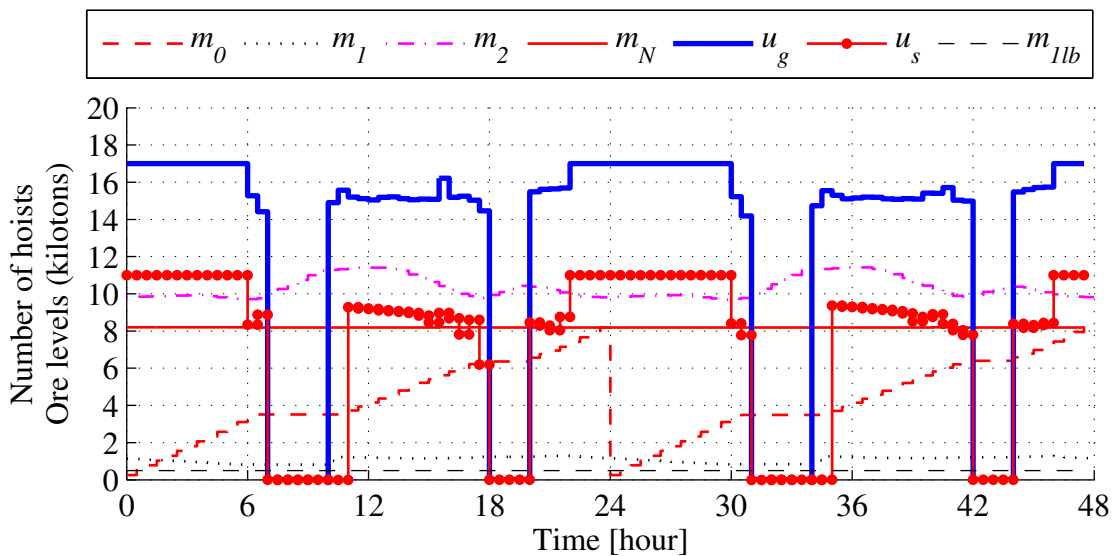


**Figure 4.6: An optimal 2-day hoisting schedule with MPC applied and taking into account historical hoist information.**

From the numerical results in Table 4.5 it is evident that  $m_N$  moves ever closer to  $M_{blast}$  with time and that the average energy cost for the two days are the same as for the scenario in which history was not taken into account in Table 4.4.

**Table 4.5: Numerical results for Fig. 4.6.**

	Tons hoisted	Energy cost
Day -2	8 181.33	-
Day -1	8 192.71	-
Day 1	8 183.62	R 10 628
Day 2	8 211.91	R 10 660
Average	8 192.39	R 10 664
$m_N$ at the end of day 2	8 193.20	-

#### 4.2.5 Impact of applying BnB

The schedules presented up to this point all consisted of real or non-integer values. As mentioned earlier it is not possible to for instance control the number of hoists to be 7.38 hoists during a 30min period. For the controller to implement the scheduled hoist values, they need to be integer. Applying the branch and bound methodology presented in section 3.3 to the scenario and conditions from which Fig. 4.6 was obtained, resulted in the schedule presented in Fig. 4.7.

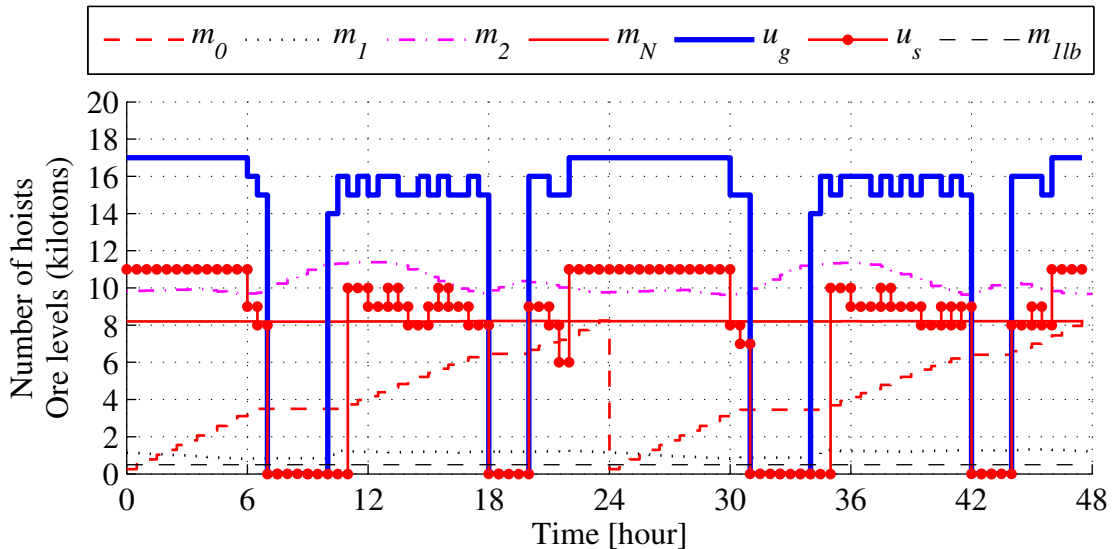


**Figure 4.7: A near optimal 2-day hoisting schedule with MPC and BnB applied while taking into account historical hoist information.**

From Fig. 4.7 the following is observed when compared to the real optimal solution in Fig. 4.6:

- All scheduled hoist values are now integer values. As a consequence it can be noted from Table 4.6 that even though the tons hoisted for the two historical days, which were based on an optimal real solution, contain values that are not multiples of  $R_s$ , the two scheduled days' tons hoisted divided by  $R_s$  results in integer multiples of  $R_s$ .
- The hoist schedule and ore level patterns remained essentially the same as in the optimal solution of Fig. 4.6.
- The underground winder schedule alternated seemingly unnecessarily between 16 and 15 hoists per period during standard energy cost periods. One would have liked to see the 16's and 15's grouped together which in this scenario should still have resulted in a feasible solution. This might however not be the case in other

scenarios. Fortunately an automated control system will have no objections against alternating between 15 and 16 hoists per period, as might manual human operators.

Comparing the numerical results for Fig. 4.7 in Table 4.6 to the results in Table 4.5 reveals an increase in both tons hoisted and energy cost. This is consistent to what was stated in section 3.3.1 in that the optimal objective energy cost value for the non-integer solution must be less than or equal to the near-optimal objective energy cost value for the integer solution. Indeed the average energy cost for the optimal solution in Table 4.5 is less than the energy cost for the near-optimal integer solution in Table 4.6 below.

**Table 4.6: Numerical results for Fig. 4.7.**

	Tons hoisted	Energy cost
Day -2	8 181.33	-
Day -1	8 192.71	-
Day 1	8 248.50	R 10 731
Day 2	8 225.00	R 10 722
Average	8 211.89	R 10 727
$m_N$ at the end of day 2	8 212.70	-

Two very important and related observations need to be noted:

- The difference of approximately 19 tons between  $m_N$  in Tables 4.5 and 4.6 is less than a single hoist capacity of 23.5 tons.
- The increase in the average energy cost or objective value from R 10 664 to R 10 727 is a mere 0.6%.

The solution obtained in applying BnB can therefore be taken as a near optimal integer solution, a solution that is very close to the optimal real solution.

#### 4.2.6 MPC, historical information and BnB impact summary

From the observations made in the past five scenarios the impact of MPC, history and BnB can briefly be summarised as follows:

- Having taken historical hoisting information into account expanded the horizon from the 2-day control horizon  $H$  to a 4-day model horizon  $N$  thereby providing a more optimal scheduling solution.
- Having applied MPC increased the average tons hoisted to beyond the  $M_{min}$  required towards  $M_{blast}$ . This however ensured sustainable hoisting in future by

making sure that constraints are adhered to not only during the two scheduled days, but also for two days into the future as from the end of the scheduled period.

- In all scenarios the optimal solution ensured that no hoisting was scheduled during peak periods while limited hoisting was scheduled during standard and maximum during off-peak periods.
- The levels of  $m_1$  and  $m_2$  were controlled within their lower and upper boundaries at all times.
- Having applied BnB resulted in a near optimal integer solution.

### 4.3 Tariff impact on winder schedules

This section studies three aspects with regards to the impact of tariffs on the winder schedule. First a comparison is made between a schedule based on a TOU and a flat rate tariff. Secondly the effect of increasing  $M_{blast}$  sufficiently enough to enforce hoisting during peak periods is investigated. Finally  $M_{blast}$  is increased to near the system's maximum hoisting capacity to explore the impact of the TOU tariff on the winder schedules and storage capacity levels.

#### 4.3.1 TOU versus flat rate

The objective of the comparative study in this scenario is to determine what the energy cost based on the TOU active energy cost of (4.1) would be if the scheduling of both winders were done based on a flat rate tariff thereby essentially ignoring the TOU tariff structure. The flat rate tariff was calculated as the weighted average of the TOU tariff in (4.1) which resulted in 27.197 c/kWh. Before substituting the TOU tariff with the calculated flat rate tariff in the control algorithm and repeating a simulation similar to that presented in section 4.2.5, history for  $u_{sm}$  had to be created based on the flat rate tariff. The new flat rate history of  $u_{sm}$  was then used in the simulation in which both MPC and BnB was applied and that resulted in the schedules and levels illustrated in Fig. 4.8.

From Fig. 4.8 the following observations are made in comparison with Fig. 4.7:

- First and foremost to be noted is that hoisting was scheduled and distributed almost evenly across all periods of the day except during the mandatory maintenance and testing times.

- Maximum hoisting capacity  $u_{smax}$  or  $u_{gmax}$  was never utilised since it was not required at the hoist target level of 8 013.5 tons.
- The change-over level  $m_1$  remained extremely close to the lower boundary of 500 tons which would result in an immediate violation of the lower boundary level constraint in the case of a delay in the underground winder system.
- The average orepass level  $m_2$  had also decreased considerably being much closer to its lower boundary of 7 000 tons.

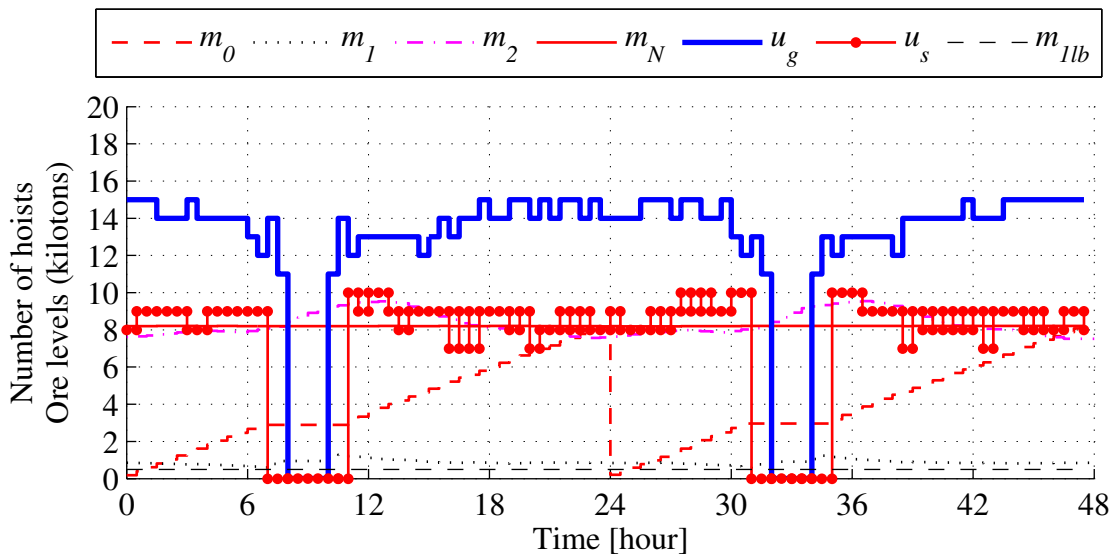


**Figure 4.8:** A near optimal hoist schedule based on a weighted average flat rate tariff with both MPC and BnB applied and  $u_{sm}$  taken into account.

Comparing the numerical results in Table 4.7 below to that of Table 4.6 revealed the following:

- The  $m_N$  average decreased by a mere 3.6 tons.
- The tons hoisted each day for the flat rate tariff were very close and similar to that of the TOU tariff.
- Applying the flat rate schedule on the TOU tariff resulted in an energy cost increase of 44.5% from R 10 727 to R 15 504 on the average daily energy cost for the two scheduled days.
- If the weighted flat rate tariff were to be implemented it would result in an increase of 82.2% on the average daily energy cost increasing from R 10 727 to R 19 544.

**Table 4.7: Numerical results for Fig. 4.8.**

	Tons hoisted	Energy cost on TOU	Energy cost on average flat rate
Day -2	8 204.71	-	-
Day -1	8 197.45	-	-
Day 1	8 154.50	R 15 493	R 19 420
Day 2	8 272.00	R 15 514	R 19 668
Average	8 207.17	R 15 504	R 19 544
$m_N$ at the end of day 2	8 209.10	-	-

From the numerical results it was calculated that scheduling the hoists according to the TOU tariff resulted in an energy cost saving of  $(R\ 15\ 504 - R\ 10\ 727)/R\ 15\ 504 = 30.8\%$ .

#### 4.3.2 Effect of a high $M_{blast}$ on the hoisting schedule

Until now all schedules shown had no hoisting during peak periods as all constraints could be adhered to without having to hoist during peak periods. In this scenario it is shown that hoisting is scheduled during peak periods if  $M_{blast}$  is increased sufficiently enough even while keeping  $M_{min}$  at 8 013.5 tons. First it had to be determined by how much  $M_{blast}$  could be increased without saturating the system?

Theoretically the maximum tons each winder can hoist per day if no delays occur can be calculated using (4.3) below:

$$\begin{aligned} S_{\max} &= (48 - T_{ms}) \cdot u_{s\max} \cdot R_s = (48 - 8) \cdot 11 \cdot 23.5 = 10\ 340 \text{ tons per day} \\ UG_{\max} &= (48 - T_{mg}) \cdot u_{g\max} \cdot R_g = (48 - 4) \cdot 17 \cdot 13.5 = 10\ 098 \text{ tons per day} \end{aligned} \quad (4.3)$$

The surface winder can therefore hoist a maximum of 10 340 tons per day and the underground winder 10 098 tons per day thereby setting the combined system's maximum at the lower limit of 10 098 tons. For the purposes of this section  $M_{blast}$  was set to 9 000 tons before simulating over a long enough period to reach a near steady state for the new  $M_{blast}$  value. From the near steady state solution  $u_{sm}$ ,  $m_1^0$  and  $m_2^0$  was extracted for use in this experimental simulation in which both MPC and BnB was applied. From the result in Fig. 4.9 the following important observations are noted:

- The underground winder had maximum hoists scheduled during both standard and off-peak periods and also had a few hoists scheduled during peak periods to ensure that the orepass level  $m_1$  was kept below the 20 000 ton upper boundary.
- The surface winder very nearly had maximum hoists scheduled during all standard and off-peak periods to ensure sufficient storage in the change-over for the large amount of tons that needed to be hoisted by the underground winder from the orepass system.
- Standard periods were scheduled to their maximum before any hoists were scheduled during peak periods.
- The orepass storage capacity was utilised to its maximum level of 20 000 tons around 12:00 each day and therefore left no available storage capacity for underground winder delays.
- The change over level  $m_2$  had now increased to around 4000 tons nearing the upper boundary of 5000 tons.

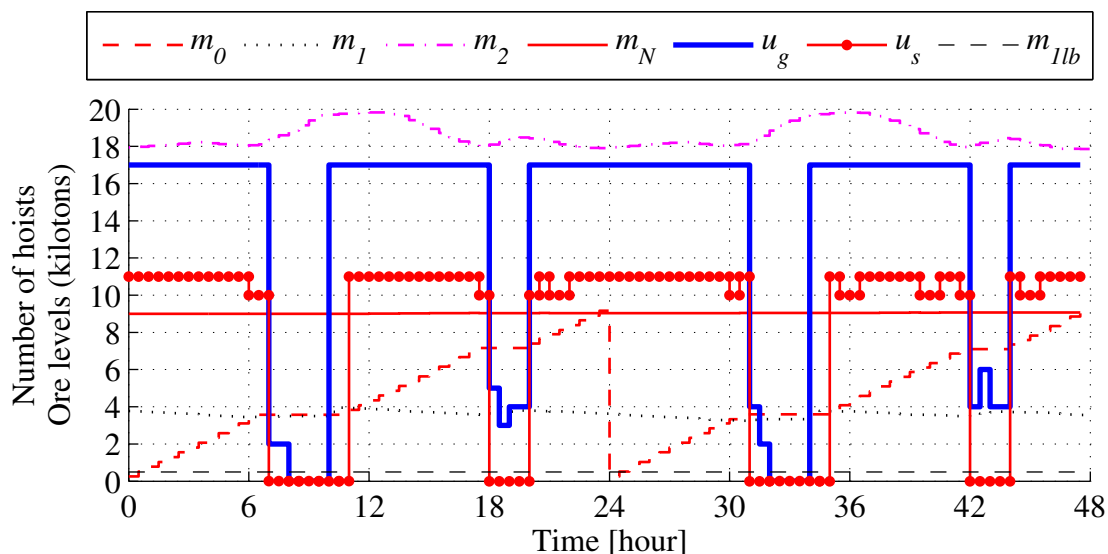


**Figure 4.9: A near optimal solution with  $M_{min} = 8013.5$  tons and  $M_{blast} = 9000$  tons.**

From the numerical results in Table 4.8 it should be noted that the optimal real solution resulted in a steady state  $m_N$  average of exactly  $M_{blast} = 9000$  tons as seen in Fig. 4.9 as well as in the tons hoisted on days  $-1$  and  $-2$ . Upon introduction of the BnB, resulting in a near optimal solution, the daily hoist level increased slightly as expected thereby causing a slight increase in  $m_N$  as well.

**Table 4.8: Numerical results for Fig. 4.9.**

	Tons hoisted	Energy cost on TOU
Day -2	9 000	-
Day -1	9 000	-
Day 1	9 165	R 12 607
Day 2	9 118	R 12 681
Average	9 071	R 12 644
$m_N$ at the end of day 2	9 067.5	-

Calculating the average energy cost per ton (c/ton) hoisted on days 1 and 2 from Table 4.8 and comparing the results to that of a lower  $M_{blast}$  value of 8 200 tons in Table 4.6 resulted in 138.31 c/ton for  $M_{blast} = 9\ 000$  tons versus 130.23 c/ton for  $M_{blast} = 8\ 200$  tons. For this scenario an increase of 10.4% in tons hoisted per day on days 1 and 2 was therefore achieved in exchange for a 6.2% increase in energy cost per ton hoisted on days 1 and 2. Since the cost increase was less than the increase in tons hoisted the increase of  $M_{blast}$  to 9 000 tons seem a viable option if only energy cost was to be taken into account and assuming that no delays would occur that would saturate the system.

#### 4.3.3 Effect of a high $M_{min}$ and $M_{blast}$ on the hoisting schedule

In this the third and final scenario in studying the tariff impact on the hoisting schedule,  $M_{blast}$  was increased to 10 000 tons which is very near to the system's upper boundary of 10 096 tons per day as calculated in (4.3).  $M_{min}$  was also increased and set to 9 611.5 tons to explore the effect of both an extremely high target and production rate in combination with the TOU tariff on the hoisting schedule. Again the system first had to be simulated for a few days until a near steady state could be achieved from which  $u_{sm}$ ,  $m_1^0$  and  $m_2^0$  could be extracted for use in this experimental simulation over two days. The following important observations should be noted from the result illustrated in Fig. 4.10:

- Both winders were scheduled to hoist at maximum for almost all periods of the day, excluding of course mandatory maintenance and testing periods.
- Both orepass and change-over levels reached their upper boundaries.
- The winder system was essentially saturated and would not have been able to handle any delays.

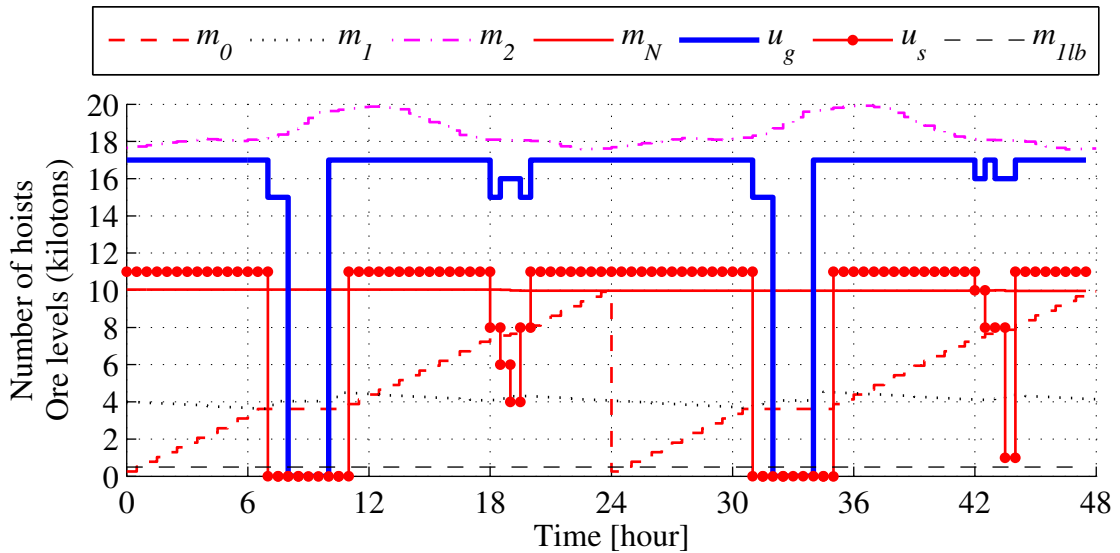


**Figure 4.10: A near optimal solution with  $M_{min} = 9\ 611.5$  tons and  $M_{blast} = 10\ 000$  tons.**

From the numerical results in Table 4.9 the average energy cost per ton hoisted on day 1 and 2 is 176.53 c/ton. Compared to the case in Table 4.6 this is an increase of 35.55% in energy cost per ton hoisted that exceeds the 20.5% increase in tons hoisted. The  $m_N$  average of 9 962 tons is but 134 tons short from the systems maximum hoisting capacity leaving a mere 10 underground hoists per day in reserve for making up lost time due to possible delays.

**Table 4.9: Numerical results for Fig. 4.10.**

	Tons hoisted	Energy cost
Day 1	9 917	R 17 433
Day 2	9 940	R 17 620
$m_N$ at the end of day 2	9 962	-

#### 4.3.4 Tariff impact summary

From the three scenarios studied in section 4.3 the impact of the TOU tariff on the schedules can be summarised as follows:

- Scheduling the winder hoists based on the TOU tariff structure resulted in significant energy cost savings compared to scheduling the hoists as if on a flat rate tariff.
- A high enough increase in production or  $M_{blast}$  resulted in an increase in hoists scheduled during standard periods until all standard periods were maximised and only then were hoists to be scheduled during peak periods.

- Assuming no delays would occur and having increased production or  $M_{blast}$  to near the systems maximum hoisting capacity resulted in all periods being forced to maximum hoisting capacity to prevent the system from saturating.
- The underground winder being the limiting hoist capacity factor needed to start hoisting during peak periods before the surface winder did.
- At  $M_{blast} = 9\ 000$  tons, which was still well below the systems theoretical maximum ability, the orepass level already reached its upper boundary even with hoists having been scheduled during peak periods.
- The percentage increase in energy cost per ton hoisted at some point surpassed the percentage increase in tons hoisted.

#### 4.4 Impact of $M_{blast}$ ratio to $M_{min}$

##### 4.4.1 Motivation for ratio impact study

The focus in this section is on an impact study of the ratio or difference between the underground production  $M_{blast}$  and the required minimum hoist target  $M_{min}$ . It has been noted in the previous sections that the number of hoists are controlled not only with respect to  $M_{min}$ , but primarily with respect and proportional to  $M_{blast}$  in that  $m_N$  in steady state increased towards  $M_{blast}$ . The reason for this was that if  $m_N$  were to be less than  $M_{blast}$  the system would eventually saturate because of the orepass system and change-over levels reaching their upper boundaries. If  $m_N$  were to be greater than  $M_{blast}$  the system would eventually run empty because of the orepass system and change-over levels reaching their lower boundaries forcing the winders to a stand still even during the low cost off-peak periods.

It is also important to take note of the orepass and change-over levels because of the buffer role they play in providing flexibility in the scheduling of the winders when delays occur. If the levels are too low the system cannot increase the hoists to compensate or make up for hoists lost due to delays that occurred in the past. If the levels are too high the system will not be able to increase the number of hoists sufficiently enough to prevent the system from saturating. This section of Chapter 4 will study three scenarios that are all initialised based on the history and set points obtained from Fig. 4.2. In all three scenarios only the optimal

real solutions will be studied instead of the near-optimal integer solutions. The three scenarios to be studied are:

- a)  $M_{blast}$  equal to  $M_{min}$  at the target set in Table 4.1 of 8 013.5 tons.
- b)  $M_{blast}$  equal to the level set in Table 4.1 of 8 200 tons with  $M_{min}$  decreased to approximately 7 700 tons giving a 500-ton difference between the production and hoist targets.
- c)  $M_{blast}$  still equal to 8 200 tons with a further decrease in  $M_{min}$  to 7 200 tons resulting in a 1 000 ton difference.

The winder schedules are excluded from the graphical analyses in this section because of the long periods over which the simulations were done, to prevent cluttering of the graphs and also because the focus of this study were on the ore levels and not the schedules.

#### 4.4.2 $M_{blast}$ equal to $M_{min}$ at 8 013.5 tons

Having run the simulation over a period of 60 days resulted in the change-over  $m_1$ , orepass  $m_2$  and  $m_N$  level transients in Fig. 4.11.

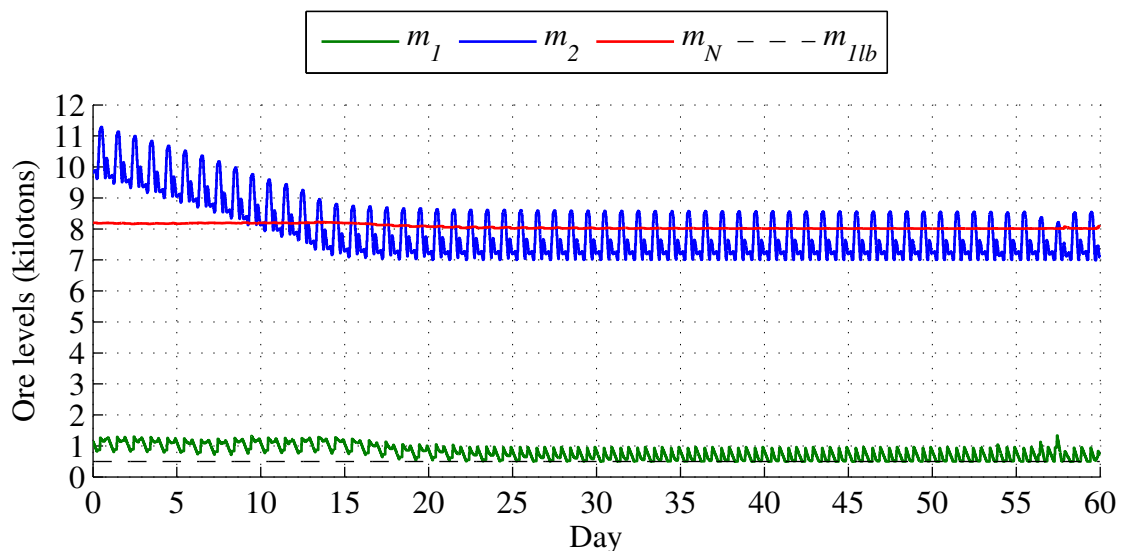


**Figure 4.11: Ore level transient analysis for  $M_{blast}$  and  $M_{min}$  equal to 8 013.5 tons over 60 days.**

The following can be observed from Fig. 4.11:

- The system would seem to reach a steady state after approximately 20 days.
- Both orepass and change-over levels reached their lower boundaries in steady state.
- The  $m_N$  average stabilised at its minimum allowable level of 8 013.5 tons.

During the simulation numerous infeasible solutions were however encountered during the last number of days of which some are encircled in green on Fig. 4.12. A closer inspection of the graphical and numerical data and hoist schedules revealed the cause of the infeasible solutions. The following is noted:

- Both surface and underground winders exceeded their maximum hoist levels of respectively 11 and 17 hoists per period on days 58 and 59. Physically the winders can of course not exceed these boundaries and hence the control algorithm needs to ensure that the solution provided does not exceed these boundaries. This problem is however discussed in more detail in Chapter 5 dealing with the impact of enforcing delays into the system.
- The  $m_N$  average dropped below the target of 8 013.5 tons on days 58 and 59.
- The orepass level dropped below the lower boundary of 7 000 tons at around day 59.7.
- The change-over level dropped below its lower boundary of 500 tons on days 53, 54, 57 and 58.

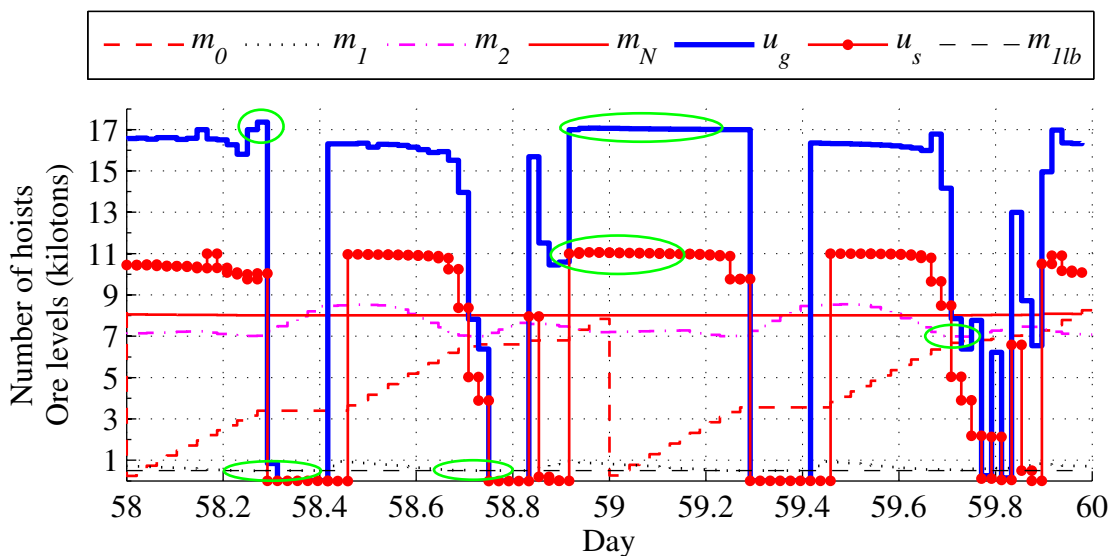


**Figure 4.12: Indication of some of the days for infeasible solutions on the last two days.**

The above-mentioned observations led to the conclusion that setting the target of  $M_{min}$  equal to the production rate  $M_{blast}$  eventually leads to an infeasible solution even in the absence of any delays. Introducing delays would only further complicate the situation since both orepass and change-over levels operate at their lower boundaries leaving no surplus ore to absorb the effects of delays.

#### 4.4.3 $M_{min}$ equal to 7 700 tons and $M_{blast}$ equal to 8 200 tons

Having increased the difference between  $M_{min}$  and  $M_{blast}$  to 500 tons at the levels of 7 700 and 8 200 tons respectively, resulted in the level transients illustrated in Fig. 4.13 from which the following is observed:

- The orepass level settled between 16 and 18 kilotons and the change-over level between 2.1 and 2.7 kilotons thereby providing a buffer capacity for absorbing the effects of possible delays.
- Only a 2 000 ton storage capacity was available in the orepass system to serve as a buffer for delays.
- The  $m_N$  average settled at just below  $M_{blast} = 8 200$  tons.
- Steady state was only achieved after a very long period of approximately 85 days due to the relative small difference between  $M_{min}$  and  $M_{blast}$ .
- No infeasible solutions occurred.

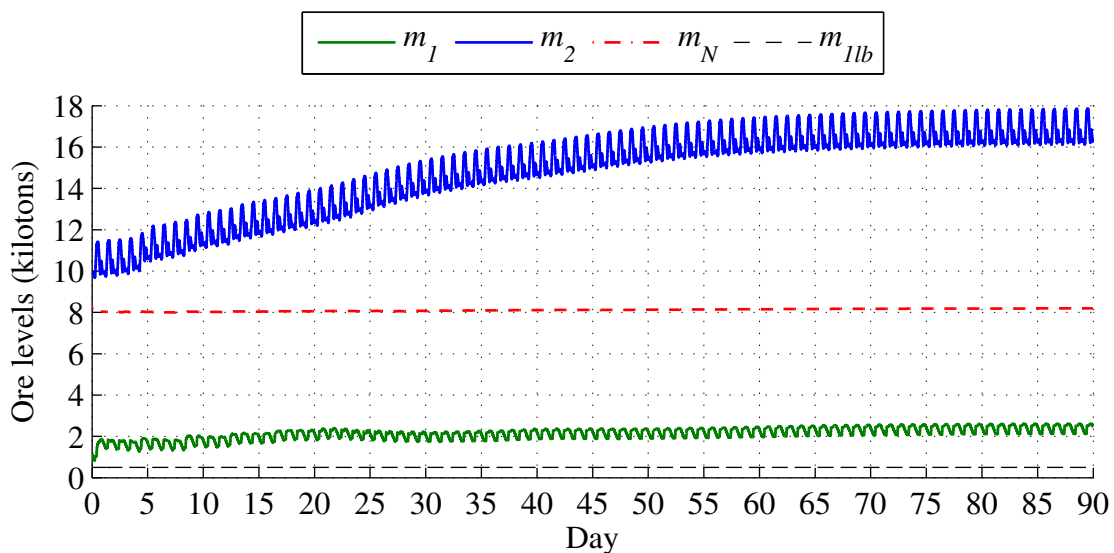


**Figure 4.13: Ore level transient analysis for  $M_{blast} = 8 200$  tons and  $M_{min} = 7 700$  tons over 90 days.**

A difference between  $M_{min}$  and  $M_{blast}$  therefore provided a buffer capacity in both orepass and change-over for absorbing the effects of possible delays. It would however seem that even a relative small difference of 500 tons brought the orepass level close to its upper boundary of 20 000 tons leaving little leverage to decrease the underground winder schedule. From the result in Fig. 4.2 where  $M_{blast}$  also equaled 8 200 tons but  $M_{min}$  was approximately only 200 tons less at 8 013.5 tons, it was noted that both orepass and change-over levels settled at lower values. It can therefore be concluded that increasing

the difference between  $M_{min}$  and  $M_{blast}$  also increases the values at which the ore levels settle in steady state.

#### 4.4.4 $M_{min}$ equal to 7 200 tons and $M_{blast}$ equal to 8 200 tons

As a final study the difference between  $M_{min}$  and  $M_{blast}$  was increased by a further 500 tons to 1 000 tons while keeping  $M_{blast}$  at 8 200 tons. Even though the simulation was also completed over 90 days, only the first 40 days are illustrated in Fig. 4.14 because steady state was already achieved after the 25<sup>th</sup> day. From Fig. 4.14 the following is noted:

- The orepass steady state level increased, settling between 17 500 and 19 300 tons thus leaving a mere 700 ton storage buffer before reaching its upper boundary at 20 000 tons.
- The change-over steady state level also increased settling between 2 800 and 3 300 tons.
- The  $m_N$  average again settled at just below  $M_{blast} = 8 200$  tons.
- As mentioned steady state was reached after only 25 days compared to the 85 days for the scenario presented in Fig. 4.13.

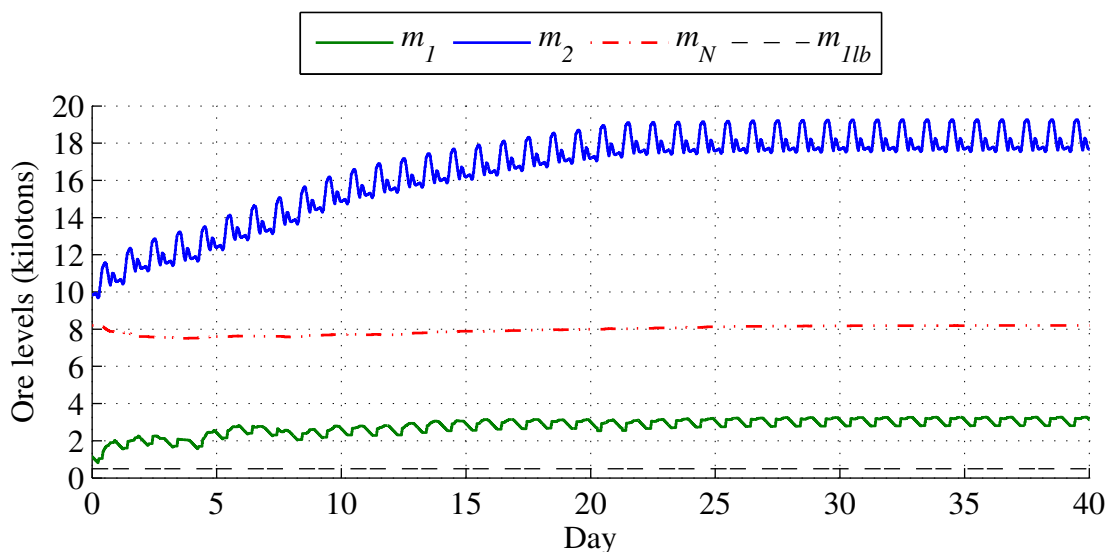


**Figure 4.14: Ore level transient analysis over 40 days for  $M_{blast} = 8 200$  tons and  $M_{min} = 7 200$  tons.**

This study supports the conclusion made in the previous scenario that an increase in difference between  $M_{min}$  and  $M_{blast}$  increases the values at which the ore levels settle in steady state. However making the difference too high caused the orepass level to come too close to its upper boundary.

#### 4.4.5 $M_{min}$ to $M_{blast}$ difference impact summary

The observations made in the three scenarios studied in this section can be summarised as follows:

- Setting  $M_{min}$  equal to  $M_{blast}$  not only provided no surplus ore for absorbing changes in winder schedules due to delays, but eventually also resulted in infeasible solutions even in the absence of any delays.
- Increasing the difference between  $M_{min}$  and  $M_{blast}$  increased the values at which the ore levels settled in steady state.
- To high a difference however led to the orepass level approaching its upper boundary thereby leaving little flexibility for rescheduling the hoists should there be a decrease in underground winder hoists.
- It was not only high values of  $M_{blast}$  that resulted in possible system saturation as noted in section 4.3, but also a to high a difference between  $M_{min}$  and  $M_{blast}$ .

## CHAPTER 5

# DELAY IMPACT SIMULATION RESULTS AND DISCUSSIONS

In this final study on the impact that the introduction of delays have on the hoist schedule and ore levels, the true worth of applying MPC will be studied and revealed. First a very elementary illustration is given to show how the occurrence of delays changed the future schedule over a fixed 24-hour window when MPC was applied. Secondly a brief analysis on how and how much delay was applied to the system in simulations is presented. Next the impact of applying an artificial 5-day delay schedule over a 5-day scheduling period is studied for two scenarios:

- a)  $M_{blast}$  and  $M_{min}$  equal to 8 200 and 8 013.5 tons respectively.
- b)  $M_{blast}$  remaining at 8 200 tons with  $M_{min}$  decreased to approximately 7 200 tons.

The reason for having chosen a 5-day period is that the model horizon was still set at four days and hence a 5-day schedule ensured that the schedule of the fifth day was entirely based on historical information containing the effects of the delays. The two-scenario study is followed by a cause and effect analysis of the level boundary constraint violations encountered in the two scenarios. Finally a summarising comparative study between the impacts studied in Chapters 4 and 5 is presented

### 5.1 Elementary delay impact illustration

This section provides an elementary illustration of the impact delays have on the outcome of the hoist schedules when applying MPC. The illustration is based on the graphical MPC illustration of Fig. 3.1 and starts in Fig. 5.1a where an initial hoist schedule at the beginning of a 24-hour period is shown. For the first three hours the hoists are implemented as scheduled without any delays being enforced. Then in Fig. 5.1b a 1-hour delay was enforced for both winders at 03:00. Notice how the hoists scheduled for the remaining 20 hours changed compared to what was initially scheduled in Fig. 5.1a. The most significant change is seen in the increase of the surface winder's schedule between 11:00 and 18:00. In Fig. 5.1c another 1-hour delay was enforced for both winders at 15:00

again resulting in a different hoist schedule for the remaining 8 hours when compared to what was scheduled in Fig. 5.1b.

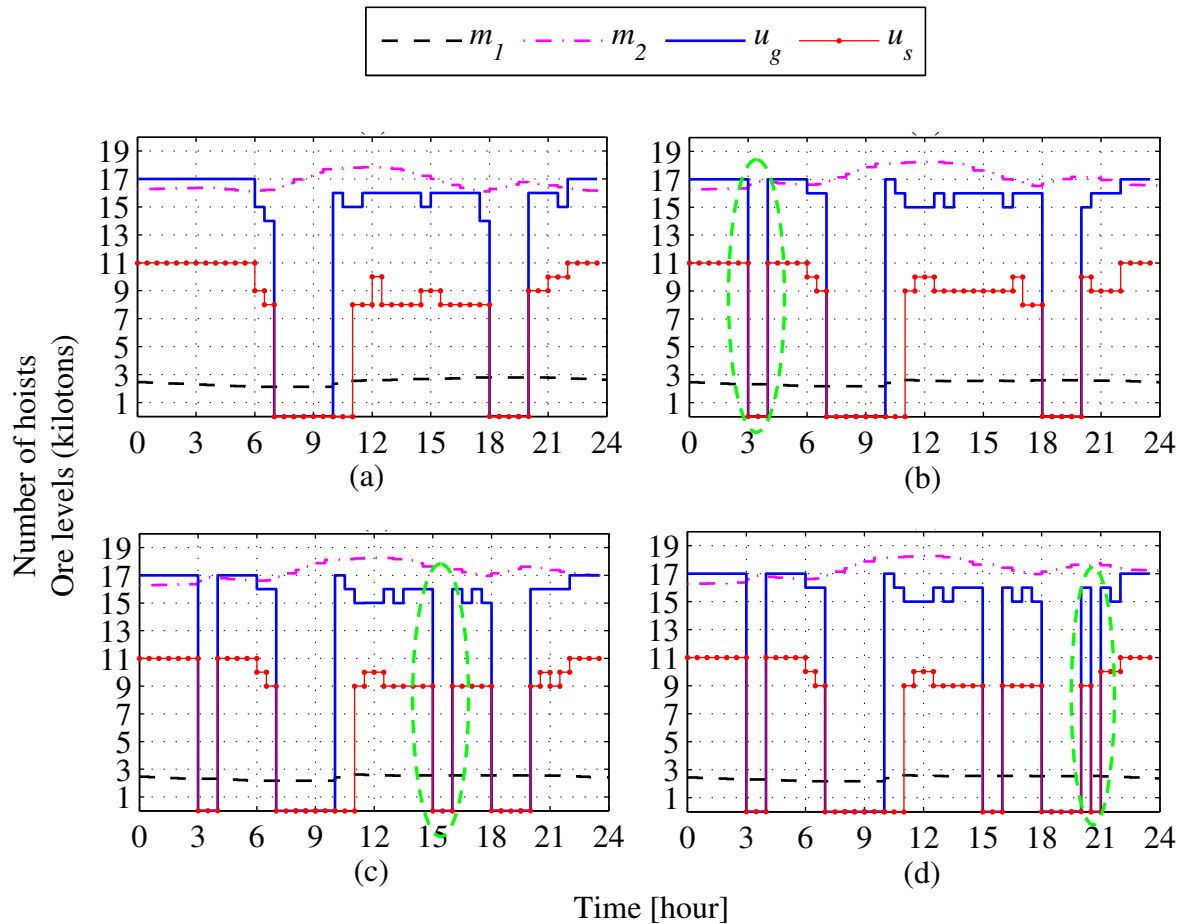


**Figure 5.1: Elementary illustration of the effect that delays have on the hoist schedules when using MPC.**

Finally in Fig. 5.1d a 30-minute delay was enforced for both winders at 20:30 resulting in a slight alteration of the hoist schedule for the remaining 3 hours during which no further delays were enforced. The hoist schedule at the end of the 24-hour period in Fig. 5.1d clearly differs significantly from the original schedule in Fig. 5.1a.

From Fig. 5.1 it is clear that each time delays were introduced the future hoisting schedule was altered to provide an optimal hoist schedule solution while adhering to all the constraints. Even though a fixed 24-hour window was used, it must be remembered that the control horizon in this illustration was two days and hence the schedule was not only altered for the hours remaining inside the 24-hour window visible in Fig. 5.1, but for the whole control horizon spanning over 48 hours beginning at the current sampling period.

## 5.2 How and how much delay can be introduced

The various types of delays encountered by and recorded for the rock winder system was discussed in section 1.4 and is illustrated here in Fig. 5.2 for ease of reference.

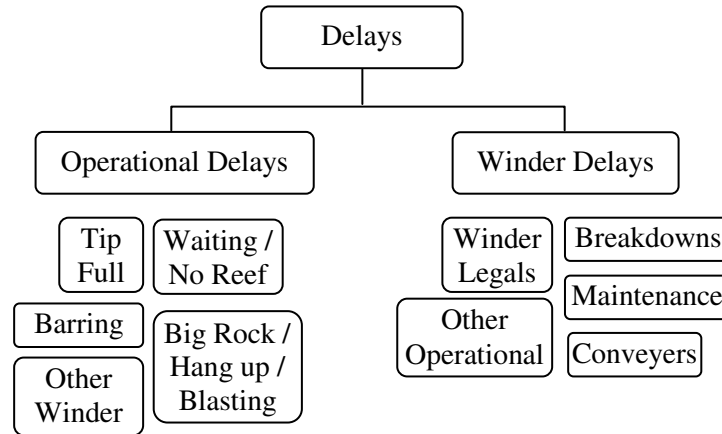


**Figure 5.2: Recorded rock winder system delays.**

From the above delays the following were excluded in determining how much delay should be introduced in the simulations:

- Winder legals and maintenance since these are accounted for in the control.
- Waiting / No Reef since these primarily resulted from an absence of a scheduling algorithm.

The remaining delays all occur outside the control of the algorithm as part of the day-to-day operation of the winders and its peripheral feeding and transport systems. Daily hoist reports were available for March and June to November of 2005 resulting in 138 weekdays of usable data from which the total minutes delay for each day and for each winder could be calculated. Important to note is that the daily hoist reports provided no information on the number of times delays occurred, the duration of individual delays and when during the day delays occurred. The reports did not state if the values provided represents a single delay event or the sum of a number of individual delay events that occurred during that particular day.

From the screened data the box plot in Fig. 5.3 was generated indicating the median values and the outliers that were to be excluded in further calculations. Excluding the outliers from the data the averages calculated are as follows:

- Surface winder average = 151.5 minutes per day equating to 56 hoists per day that could not be done due to system delays.
- Underground winder average = 205.8 minutes per day equating to 117 hoists per day that could not be done due to system delays.

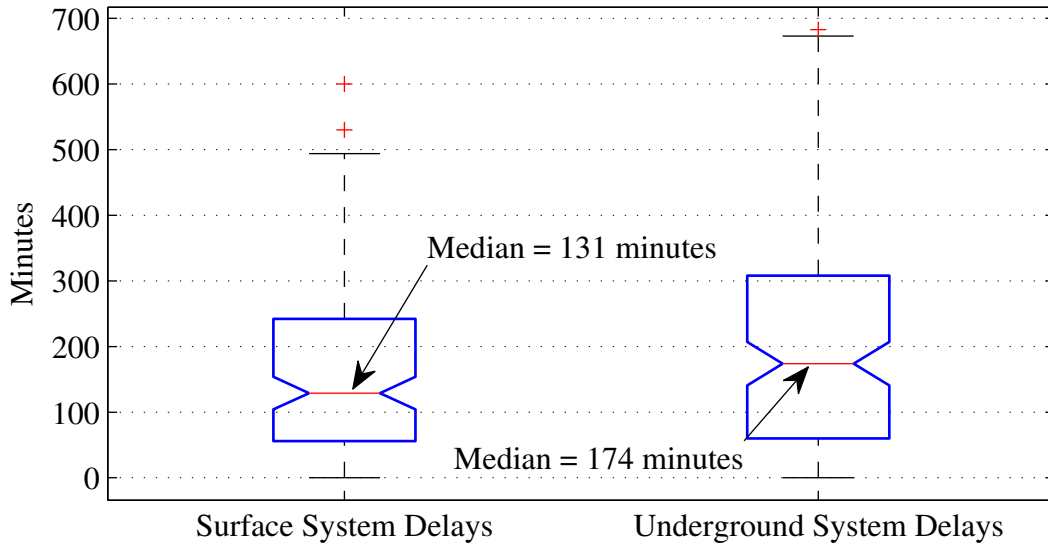


**Figure 5.3: Box plot of winder system delays within the 138 available working days of data.**

Two delay matrices were created, one for each winder, in which the period number and associated number of hoists to subtract from the scheduled amount were randomly generated over a period of five days. The tabled results are presented in Addendum D in which it will be noted that the total duration of delays chosen for each day was less than the calculated average. The delays were enforced in the simulation algorithm by first subtracting from period  $k$ 's scheduled hoist value the corresponding period's delay value in the delay matrix before implementing the difference at the beginning of period  $k$ . If the delay value was zero, it implied that no delays occurred during that period. If the delay value was for example 3, it meant that 3 hoists less than originally scheduled could actually be completed during that period. If the delay value exceeded the scheduled value it was assumed that no hoists could be completed during that particular period.

### 5.3 $M_{blast}$ equal to 8 200 tons and $M_{min}$ equal to 8 013.5 tons

As a first experiment the delays were introduced to the steady state scenario presented in both Fig. 4.2 and Fig. 4.6 over a period of 5 days. In order to evaluate the full impact of

the delays over the 5 days the algorithm had to be adjusted so as to ignore infeasible solutions and continue with the scheduling process until all days were completed. The resulting simulated schedule representing the measured historical information for 5 days is presented in Fig. 5.4.

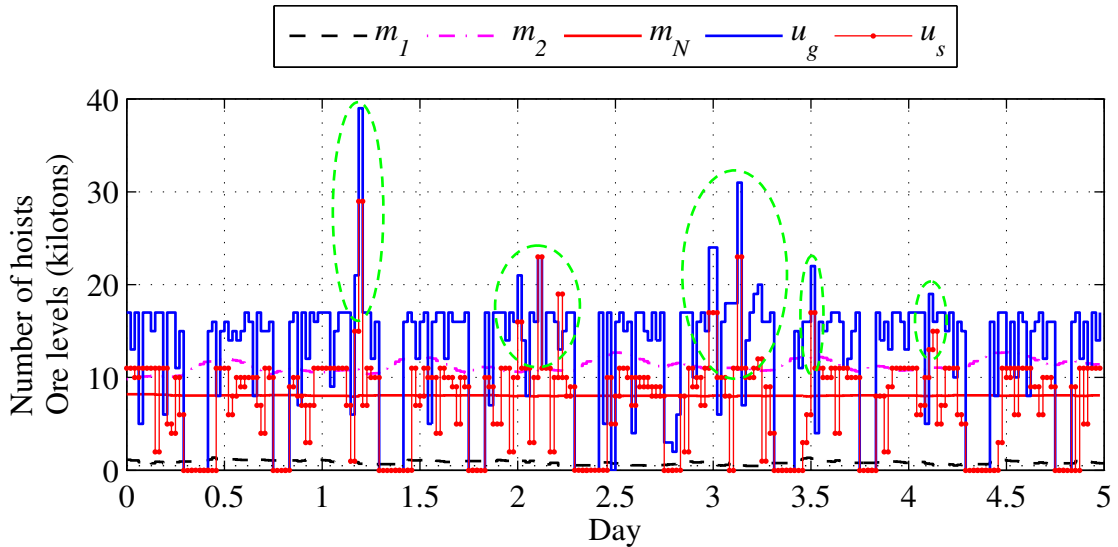


**Figure 5.4: Simulated historical winder schedules and ore levels with delays introduced at  $M_{blast} = 8\ 200$  tons and  $M_{min} = 8\ 013.5$  tons.**

Clearly both surface and underground winders' upper boundary constraints were violated a number of times indicated where encircled in green. The controller's response was either to slow or the delays to frequent to bring  $m_N$  back to  $M_{blast}$  fast enough to absorb new delays and thereby cause  $m_N$  to drop below  $M_{min}$  and resulted in infeasible solutions. Because the solution was infeasible the algorithm used to solve the linear programming problem ignored the upper boundary of the hoist constraints and assigned high enough values to  $u_s^k$  and  $u_g^k$  in order to increase  $m_N$  above  $M_{min}$ . As mentioned in section 4.4.2 it is physically not possible for the winders to exceed  $u_{smax}$  or  $u_{gmax}$ . Hence the scheduling algorithm was adapted to ensure that infeasible solution never result in  $u_s$  and  $u_g$  exceeding their respective upper boundaries of 11 and 17 hoists per half hour. In other simulations that also resulted in infeasible solutions the hoist schedules showed that hoists were scheduled during the maintenance and testing periods and hence the adapted algorithm also had to ensure that no hoists were scheduled during these periods in case of an infeasible solution.

The infeasible solutions had another significant consequence. If the whole problem did not have a feasible solution then neither would and could any of the four subproblems created for determining a near optimal integer solution. This meant that in the case of an infeasible solution, the BnB method could not be applied and in its stead if either  $u_s^k$  and  $u_g^k$  were to be less than 11 or 17 respectively, the real values were rounded down to the nearest integer and assigned to  $u_s^k$  and  $u_g^k$ .

Repeating the experiment in Fig. 5.4 with the adapted algorithm resulted in the schedules and levels presented in Fig. 5.5. Added to the graph is the lower boundary for the change-over at 500 tons and  $M_{min}$  at 8 013.5 tons indicated by the thin green lines at the respective levels. These two boundaries serve as a reference to determine when either of the target or level constraints is violated.

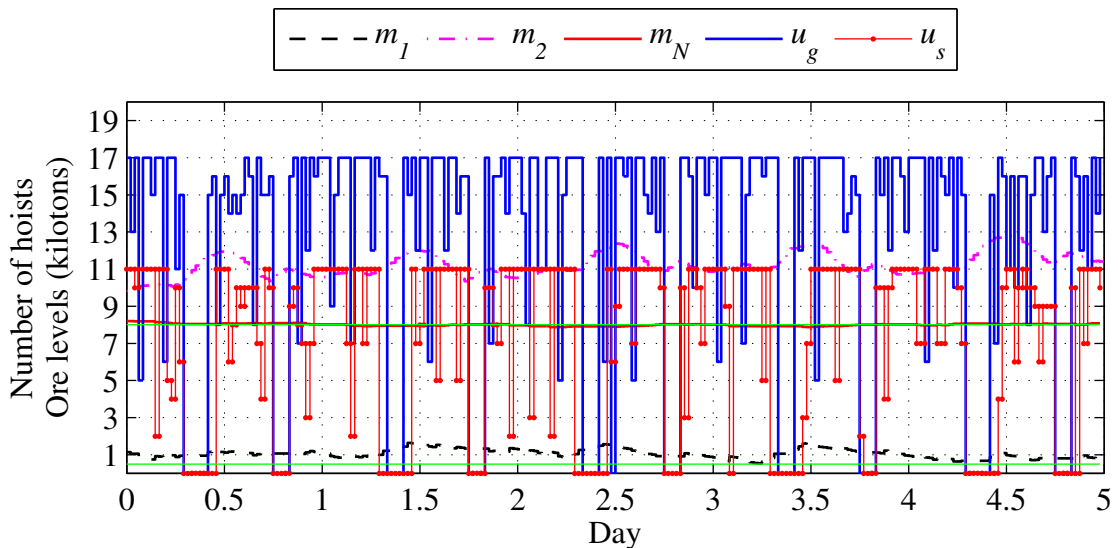


**Figure 5.5: Repeated simulation of Fig. 5.4 where  $M_{blast} = 8\ 200$  tons and  $M_{min} = 8\ 013.5$  tons but with hoist boundaries enforced.**

Two significant observations are noted from Fig. 5.5:

- The  $m_N$  average seems to oscillate around the hoist target of  $M_{min}$  thereby effectively violating the target constraint numerous times. Important however is that the level was maintained around the target.
- The controller scheduled underground winder hoists during the morning peak periods of the second, third and fourth days and also for the surface winder during

the evening peak period on the fourth day in order to adhere to the target constraint by trying to keep  $m_N$  above  $M_{min}$ .

- The orepass level  $m_2$  slowly but continuously rose over the 5-day period. The question arises as to what would happen if the orepass level continued to rise up to its upper boundary of 20 000 tons? This question shall be addressed in section 4.5.5.

A closer look at the level of  $m_N$  with respect to the level of  $M_{min}$  in Fig. 5.6 more clearly revealed that a violation of the target constraint occurs at numerous instances where  $m_N$  dropped below the  $M_{min}$  level of 8 013.5 tons. Significant to note however is the fact that the extent of the violations became much less after four days as the model horizon at that time only contained days in which delays occurred. The controller therefore began to absorb and incorporate the effect of past delays into its future scheduling thereby controlling the average tons hoisted to surface closer to the target of  $M_{min}$ .

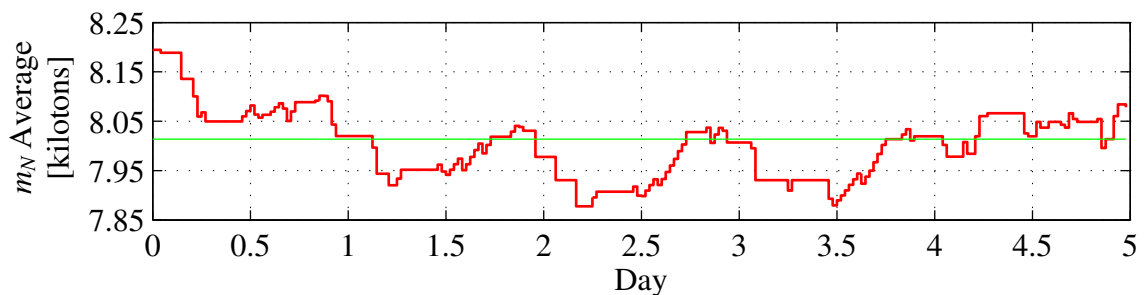


**Figure 5.6: Indication of the times at which  $m_N$  from Fig. 5.4 is less than the target constraint of 8 013.5 tons.**

A final and very important observation made during the evaluation of this experiment was that the occurrence of infeasible solutions and the enforcement of hoists to remain within their boundaries and constraints did not result in all future solutions to be infeasible. In time solutions at future sampling instants proved to be feasible again despite the periodic infeasible solutions of the past.

#### 5.4 $M_{blast}$ equal to 8 200 tons and $M_{min}$ equal to 7 200 tons

In this section the delays were again enforced over a 5-day period but the initial values was based on the historical data obtained from Fig. 4.14 in which the target was reduced to

7 200 tons. The reason for having chosen the history in Fig. 4.14 was that the steady state orepass level  $m_2$  was already very close to its upper boundary of 20 000 tons and hence the effect of the delays on the orepass level could be investigated. The result of the simulation is presented in Fig. 5.7 with a thin green line drawn at 20 000 tons to indicate the orepass level upper boundary.

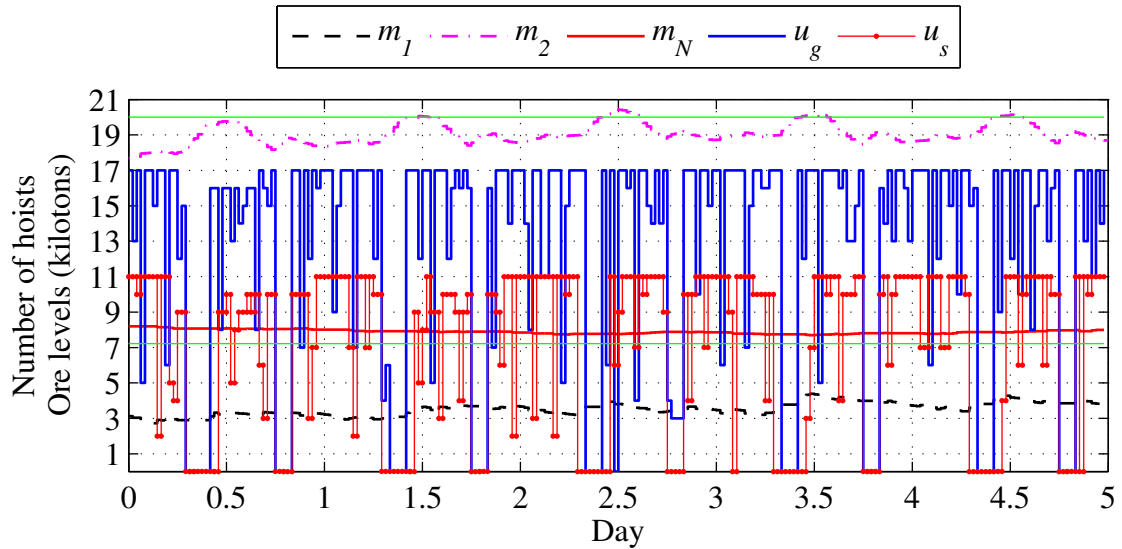


**Figure 5.7: Simulated historical winder schedules and ore levels with delays introduced at  $M_{blast} = 8\,200$  tons and  $M_{min} = 7\,214.5$  tons.**

The following observations are noted from Fig. 5.7:

- The orepass level  $m_2$  constraint was already violated on day 1.5 seen where the  $m_2$  level indicator passes the thin green line at 20 000 tons. The orepass level did however seem to decrease as the model horizon moved into the fifth day when comparing the peak value of  $m_2$  at day 4.5 to the peaks on days 2.5 and 3.5.
- The controller scheduled underground winder hoists during the morning peak periods of all the days except the first and also during the evening peak period on the third day as a result of the MPC wanting to decrease the orepass level to below its upper boundary.
- The  $m_N$  average and change-over level  $m_1$  never dropped to below their respective boundaries of  $M_{min}$  and  $m_{1min}$ .
- With the orepass level having been controlled at its upper boundary, the change-over level  $m_1$  seemed to slowly increase towards its upper boundary. Again the question arises as to what would happen if the level continued to rise to its upper boundary? The answer to this question shall be addressed in the following section.

## 5.5 Cause and effect of level boundary constraint violations

From Fig. 5.5 and Fig. 5.7 it would seem that the change-over level was kept low as long as the orepass system had storage capacity available. Once the orepass system saturated at its upper boundary the underground winder's scheduled hoists were increased in order to control the orepass level at its upper boundary level. This in turn caused the change-over level to begin rising as the excess ore fed into the orepass system needed to be hoisted to surface via the change-over. The question that needs to be answered at this point is what will happen if and when the change-over reaches its upper boundary?

The answer to this question is provided in Fig. 5.8 in which more delays closer to the averages calculated in section 4.5.2 were enforced over a much longer period of 90 days. The 5-day delay pattern in Addendum E was repeated every 5 days to form the 90-day delay matrices. The transient in Fig. 5.8 of the system can be divided into three stages as indicated on Fig. 5.8. While evaluating the transients within the different stages it must be remembered that the objective of the controller is to adhere to all constraints with the objective to do so at minimum energy cost.

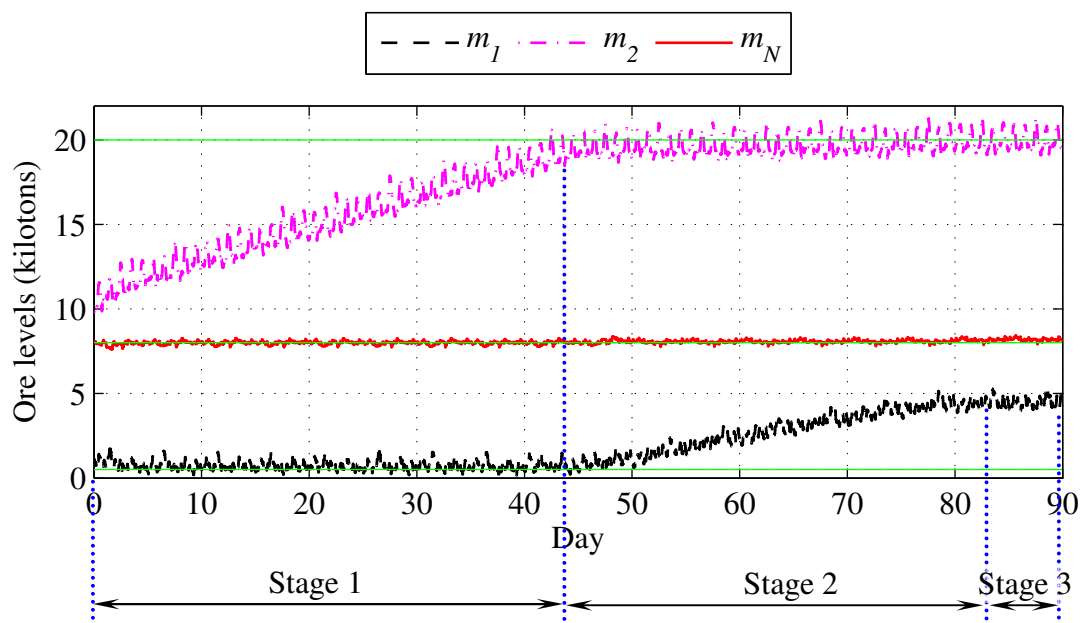


**Figure 5.8: Cause and effect of level boundary constraint violations with  $M_{min} = 8\ 013.5$  tons and  $M_{blast} = 8\ 200$  tons with  $H = h$ .**

Stage 1: The change-over level was kept at minimum while  $m_N$  was controlled around  $M_{min}$ . The orepass level increased because the mining production

flow rate exceeded the underground winder hoist rate that was being kept as low as possible in order to achieve a minimum energy cost.

- Stage 2: The orepass level reached its upper boundary forcing the underground winder to increase its hoist rate to match the production inflow rate. This in turn caused a slight increase in the surface winder hoist rate to cope with the additional inflow of ore as seen by the slight increase in the level of  $m_N$ . The increase was however not enough to prevent the change-over level from increasing because the surface winder hoist rate was still kept at minimum for a minimum energy cost while satisfying the hoist target constraint  $M_{min}$ .
- Stage 3: The change-over level reached a steady state level which in this scenario was at its upper boundary. This forced another slight increase in the surface winder's hoist rate, again seen in the slight increase of the level of  $m_N$ , in order to match the production inflow rate thereby controlling the change-over level to below its upper boundary most of the time.

In a second scenario studied the target and production was set well below the winders' hoist rates even with delays taken into account. The effect of the delays on the hoist schedules and ore levels as illustrated in Fig. 5.9 were again as in Fig. 5.8.

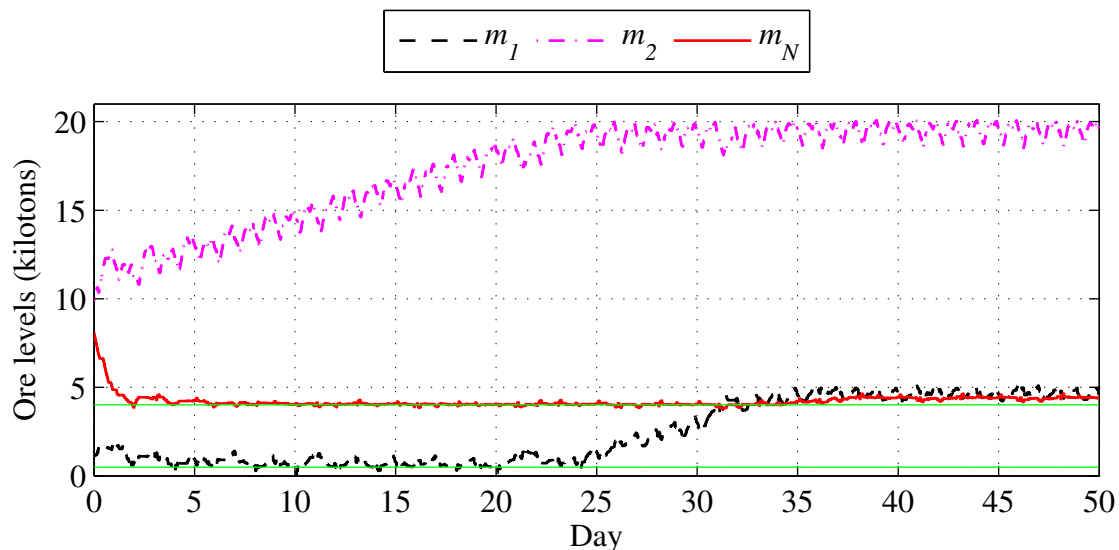


**Figure 5.9: Effect of level boundary constraint violations for  $M_{min} = 4\,000$  tons and  $M_{blast} = 4\,400$  tons with  $H = h$ .**

A noticeable difference because of the lower production rate  $M_{blast}$  is that both orepass and change-over levels remained below their upper boundaries in Fig. 5.9 as opposed to both levels having exceeded their boundaries from time to time in Fig. 5.8. A very important observation was however made on inspection of the winder schedules for Fig. 5.9 though not shown here. It was observed that both winders only hoisted at approximately half their maximum allowed hoist rates during standard periods because of the low hoist target required. This led to both orepass system and change-over levels being controlled at their upper boundaries.

From a third and final scenario study illustrated in Fig. 5.10 in which  $M_{min} = 7\ 200$  and  $M_{blast} = 7\ 600$  it can be seen that the orepass level was again eventually controlled around its upper boundary but the change-over ended up being controlled well below its upper boundary. The exact reason for what might be interpreted as a discrepancy in the level at which the change-over was being controlled in Fig. 5.10 compared to the previous two scenarios is unclear but will be a combination of factors which include the values of and difference between  $M_{min}$  and  $M_{blast}$  and also the formulation of the objective energy cost function along with the system constraints. Fig. 5.10 does however show that it cannot be assumed that all scenarios will end in the change-over level being controlled at its upper boundary.

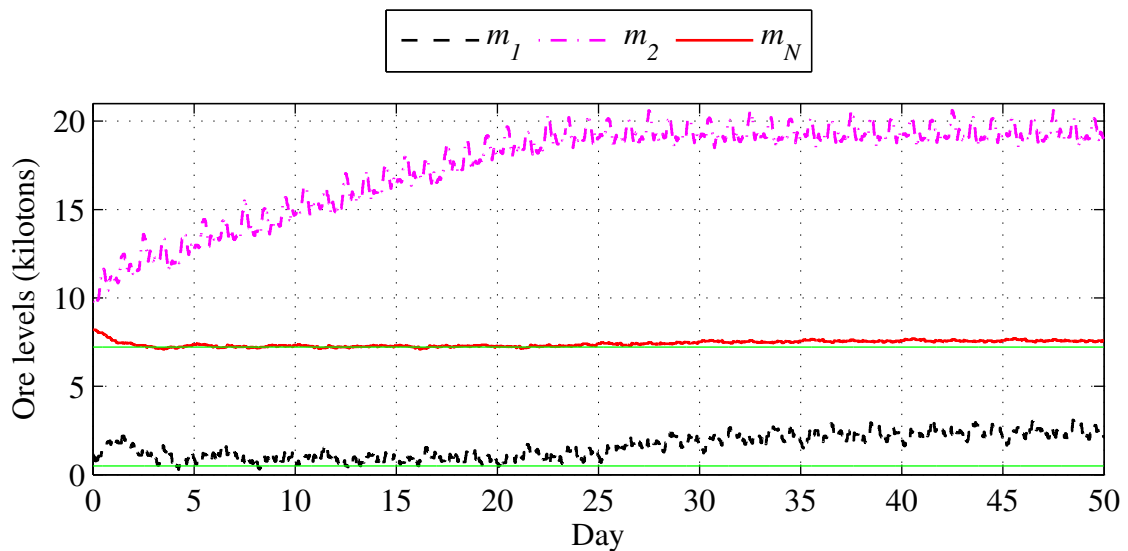


**Figure 5.10: Effect of level boundary constraint violations for  $M_{min} = 7\ 200$  tons and  $M_{blast} = 7\ 600$  tons with  $H = 2h$ .**

## 5.6 Level and energy cost comparison for various impact factors

As a summarising comparison between the different impact factors studied in this and the previous chapter, seven case studies described in Table 5.1 were completed for the case of  $M_{min} = 7\,200$  tons and  $M_{blast} = 7\,600$  tons over a period of six days following on each case's particular steady state period. The history and initial condition values for the first two cases in which no delays were enforced are different to those of the remaining 5 cases. The initialisation values for cases 3 through 7 were based on the steady state achieved with case 3 as illustrated in Fig. 5.10. Hence the six days of cases 3 through 7 is a continuation from day 50 in Fig. 5.10 based on the case description given in Table 5.1. The comparative results and averages taken over the last 3 of the 6 days are also included in Table 5.1.

**Table 5.1: Comparative results for the various impact factors on the ore levels and energy costs.**

Case	Case description	$m_N$ level [tons]	Average daily tons hoisted	Average daily energy cost.	Average daily winder hoist delays [hoists]	
					Surface	U/G
1	Optimal solution without BnB and without delays.	7 598.4	7 598	R 9 649	0	0
2	Near optimal solution with BnB but without delays.	7 596.4	7 598	R 9 647	0	0
3	Optimal solution with MPC and delays applied but without BnB.	7 644.4	7 609	R 10 739	48.3	101.3
4	Near optimal solution with MPC, delays and BnB applied.	7 655.1	7 598	R 10 707	48.7	100.7
5	Near optimal solution with control horizon of $H = h$ .	7 590.5	7 622	R 10 717	48.2	101.0
6	Manually controlled based on 'hoist what you can when you can' approach.	8 783	8 703	R 16 927	-	-
7	Repeat of case 6 with no hoisting during peak periods if possible within constraints.	7 608	7 661	R 10 532	-	-

When comparing cases 1 and 2 it is again apparent that the near optimal solution provides almost the exact same results as the optimal solution. Unexpected however is the almost negligible lower cost of the near optimal solution in case 2 which is suppose to be slightly higher than the optimal solution. This could however be due to the fact the average cost was calculated over the last three days of which the first still contained control decisions based on real optimal solutions in the past.

A comparison of cases 3 and 4 in which delays were introduced again shows the almost identical results for the optimal and near optimal solutions, but again the near-optimal solution resulted in a lower average energy cost than the optimal solution. In addition to the 3-day average effect, it must also be remembered that algorithm was adapted such that in the case of infeasible solutions the optimal real solution's scheduled values were taken and rounded down which would account for the lower energy cost.

The significance and effectiveness of the optimal hoist scheduling algorithm is revealed when comparing the results of cases 1 and 2 to that of cases 3 and 4. Despite the high number of hoists that were delayed in cases 3 and 4, the  $m_N$  average and the average tons hoisted per day remained at or above the inflow of ore into the system  $M_{blast}$ . Even more significant is the relatively small increase in energy cost of just over R 1 000 incurred despite the high number of hoists that were delayed. This again supports the cost effectiveness of the scheduling algorithm.

In case 5 the control horizon was reduced from  $H = 2h$  to  $H = h$  thus decreasing the aggressiveness of the controller. Though the effect cannot be seen in a difference of the numerical results in Table. 5.1 when compared to cases 3 and 4, the effect is visible when comparing  $m_N$  in Fig. 5.10 for  $H = 2h$  to that of Fig. 5.9 and Fig. 5.8 having  $H = h$ . The only noticeable effect of setting  $H = h$  is that it resulted in a less stable or constant  $m_N$  level. Having  $H = h$  also drastically reduced the computation time required.

Regarding cases 6 and 7 the following notes. The 'hoist what you can when you can' approach meant that the manual operator did not take into account any future information such as the inflow rate into the orepass system and hence there was no feedback or predictive control involved. The operator purely looked at the orepass and change-over

levels at a given point in time and if they were above their lower boundaries the operator hoisted irrespective of the time of day. The result for case 6 is illustrated in Fig. 5.11 in which it is observed that the change-over level quickly dropped to its lower boundary and that the ore-pass level would also have reached its lower boundary after another 5 to 6 days.

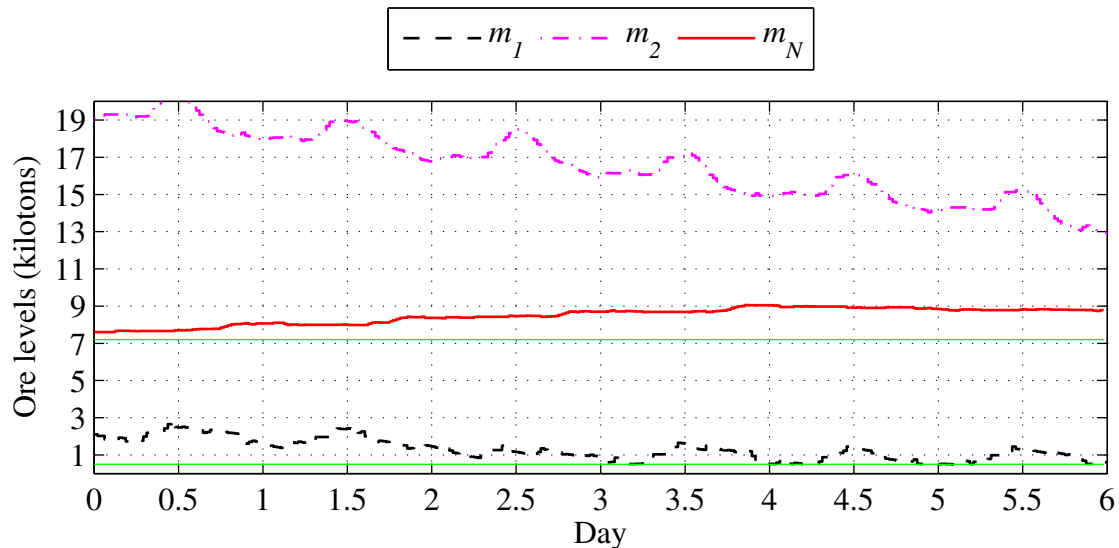


**Figure 5.11: Six day ore level result for the case 6 operating on the bases of hoisting ‘what you can when you can’.**

At the point where the orepass level would have reached its lower boundary the underground winder hoist rate would have drastically decreased as would have the level of  $m_N$  even after having reached 2 000 tons above the required target at the end of day 4. The hoist ‘what you can when you can’ approach would therefore eventually have reached the point where both winders could not hoist during off-peak periods due to an empty system and where both winders would have to hoist during peak periods to ensure that the hoist target constraint was met.

In case 7 the operator was instructed not to hoist during peak periods unless the ore levels exceeded their upper boundaries. Again the operator did not take into account future information and only looked at the here and now levels of the orepass and change-over. The 6-day result illustrated in Fig. 5.12 shows that the orepass level exceeded its upper boundary even more than before when compared to Fig. 5.10. The change-over level again quickly reached its lower boundary which resulted in more surface winder hoisting having to be done during standard periods that could have been done during off-peak periods due

to the change-over continuously running empty while having to maintain the required hoist target  $M_{min}$ .

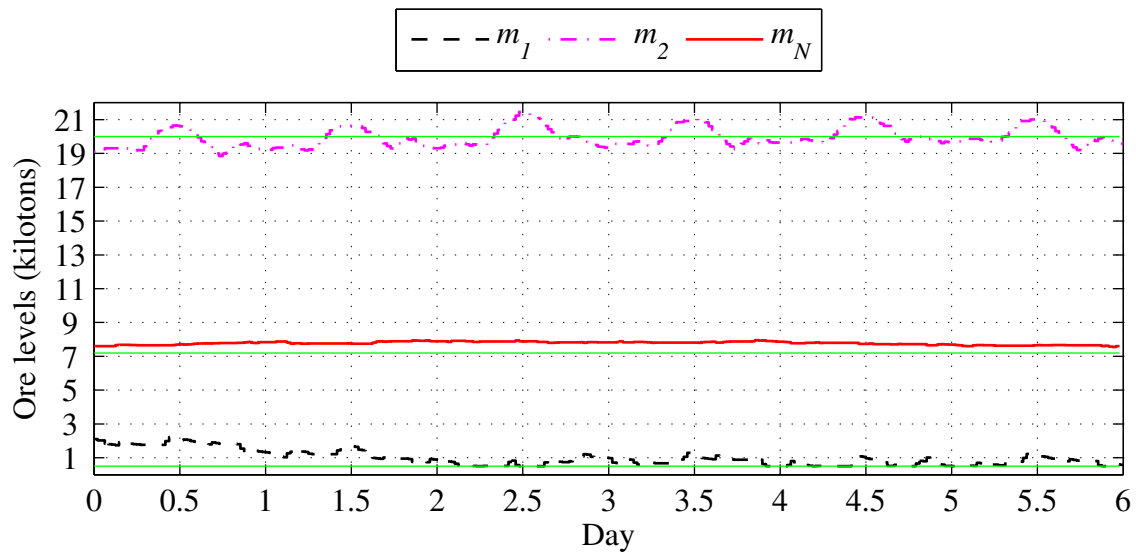


**Figure 5.12: Six day ore level result for the case 6 with no hoisting during peak periods unless the ore levels exceeded their upper boundaries.**

## 5.7 Summary of the delay impact study

Having delays in the winder system effectively decreased the system's rate at which it could hoist the ore and thereby forced more hoists to be scheduled during the more expensive periods. A near steady state was eventually reached which was determined by the following factors:  $M_{blast}$  to  $M_{min}$  ratio, orepass feed-in rate, hoist rates, average relative delay ratios. Average relative delay ration means the average delays of a specific winder relative to that specific winder's maximum hoist rate capability.

Initially the introduction of delays caused the violation of the boundary constraints, which led to the linear programming software giving infeasible results with regards to the number of hoists being scheduled. The scheduling algorithm had to be adapted in order to contain the hoists scheduled within their lower and upper boundaries in the case of an infeasible solution.

The effect of the delays on the winder schedules and ore levels can be summarised as follows:

- If the production  $M_{blast}$  exceeds the underground winder's effective hoist rate during less expensive periods, the orepass system will eventually saturate and be controlled around its upper boundary by hoisting during more expensive periods.
- If the surface winder's effective hoist rate exceeds the underground winder's effective hoist rate, the change-over will run empty and will be controlled at its lower boundary.
- If the production  $M_{blast}$  exceeds the underground winder's effective hoist rate, which in turn exceeds the surface winder's effective hoist rate, both orepass and change-over will saturate and be controlled around their upper boundaries. This is however only possible if hoisting during peak periods is sufficient to compensate for the number of delays incurred. If this is indeed the case  $m_N$  will increase until the system reaches steady state.
- If the production  $M_{blast}$  exceeds the underground winder's effective hoist rate but not the surface winder's effective hoist rate, the orepass system will eventually be controlled at its upper boundary but the change-over level will stabilise before reaching its upper boundary.
- If either of the winders' effective hoist rate during less expensive periods are less than the production rate, the orepass system will saturate and be controlled around its upper boundary.
- Should the effective hoist rate of the rock winder system be lower than the production inflow into the orepasses due to excessively high delays, the scheduling algorithm will not be able to compensate due to physical constraints and not because of controller limitations. This will be indicated in the schedule in that the orepass level will not be controlled around its upper boundary but instead it will keep on increasing beyond  $m_{2max}$ .

The controller will never be able to ensure that all constraints are adhered to all the time, which will cause the orepass and change-over levels to be controlled around their upper or lower boundaries instead of staying within their boundaries. This can primarily be attributed to the following two factors:

- i. The high number and frequency of delays compared to the slow transient response of the controller. As mentioned earlier no information is available from the daily hoist reports on the actual duration and frequency of individual delays and hence the delays introduced are random by nature.

- ii. The high feed-in rate of the rock into the orepass system during the morning peak period when the winders are forced to stand still for testing and maintenance. A practical solution would be to alter the feed-in rate so as to decrease the rate during the morning peak period and compensating for the decrease during the night shift's standard and off-peak periods. This process can however not be automated and hence cannot necessarily be sustained and controlled effectively due to the feed-in process being entirely dependant on human labour.

To compensate for the fluctuation of the ore levels around their upper or lower boundaries, the lower boundary set point  $m_{min}$  such that  $m_{min}$  is slightly and sufficiently higher than the true plug-hole or minimum desired level. Similarly the upper boundary set point  $m_{max}$  much be chosen such that it is slightly and sufficiently less than the true maximum storage capacity. The upper and lower level boundaries should therefore be seen as control set points rather than boundaries.

Ultimately, despite the occurrence of infeasible solutions at various sampling instants, the MPC control algorithm was still able to create a steady state solution in all scenarios studied. The algorithm ensured that the hoist target was achieved while controlling all levels within or around their boundaries for a sustainable and continuous hoist schedule.

## CHAPTER 6

### CONCLUSIONS AND RECOMMENDATIONS

#### 6.1 Conclusions

The primary objective of this dissertation was the development of a near optimal half hourly hoist scheduling program for a deep level mine twin rock winder system in order to achieve a set hoist target at minimum energy cost based on a TOU tariff whilst operating within various physical and operational constraints. The challenge was to achieve the objective in an unpredictable mining environment in which delays occur without knowing when or for how long. The scheduling therefore had to be done in real-time [10], in this case half hourly, to compensate for any delays that might have occurred during the past half hour. To this extent an MPC based algorithm was proposed and implemented to provide a manner of feedback for a closed-loop control or scheduling algorithm.

The primary objective was achieved through the following secondary objectives based on the two steps identified in literature [11, 28, 29, 30, 31, 32, 33, 34] when assessing DSM opportunities or programs as mentioned in section 2.1. The first step was the development of an accurate and adequate model of rock winder system. The second step involved applying the developed load model in methods and strategies of evaluating and selecting between different DSM or LM control strategies. The two secondary objectives were achieved through:

- The formulation of a physically based SLPM of the winder system in Chapter 2 was based on the physical models developed in [11, 12, 28, 35, 36, 37]. The primary difference in this dissertation is that the winder problem did not allow for binary integer programming that was used in most of the model formulations mentioned. The developed model consists of a discrete dynamic model of the winder system based on the theory in [39], various types of system constraints and an energy cost objective function similar to those stated and developed in [28, 35, 36, 37].
- The formulation of a closed-loop MPC based scheduling algorithm in Chapter 3 based on the MPC theory of [41, 51]. The algorithm includes solving the static linear programming model; compensating for infeasible solutions and incorporating

MILP and an adapted BnB methodology from [52, 54] to provide a near optimal integer schedule solution.

- The testing and evaluation of the scheduling algorithm in Chapters 4 and 5 in accordance with the second step in assessing DSM opportunities: application of the developed model. The evaluation was done through an extensive set of simulated impact studies on the cost, schedules and ore levels. The most significant impact study was on the introduction of delays into the rock winder system.

From the evaluations on the simulated impact study results, the following important conclusions were and can be made:

- The SLPM of the rock winder fulfilled both objectives for load models to be used in DSM evaluations as mentioned in section 2.1 and set out in [30]. First the winder model provided sufficient information to evaluate the benefits obtained through DSM through comparisons of the energy costs, ore levels and hoist production outputs. Secondly the model allowed for the impact evaluation of numerous control strategies and parameter setpoints.
- In practice where delays are inevitable, orepass and change-over level boundary constraints should rather be seen as control levels instead of boundaries because the controller will never be able to ensure that the all level boundary constraints are adhered to all the time.
- Application of the BnB principle resulted in near optimal integer solutions on condition that a feasible optimal solution could be determined at the particular sampling instant. However, an infeasible solution for the current sampling period did not necessarily result in an infeasible solution at the beginning of the next sampling period.
- The energy cost objective function proved to be very effective in ensuring minimal hoisting during expensive peak periods and maximum hoisting during low energy cost off-peak periods. One of the experiments showed the scheduling according to a TOU tariff instead of a flat rate tariff resulting in an energy cost reduction or saving of almost 31%.
- The scheduling algorithm cannot compensate for cases where the effective hoist rates of the winders are so far below the feed-in rate or mining production rate that the time left for hoisting is not enough to hoist  $M_{blast}$  tons to surface. In such cases

the system will inevitably saturate and steps will have to be taken to reduce the number or duration of delays in order to increase the winder system's availability.

- The MPC based scheduling algorithm was able to successfully generate schedules that resulted in steady state solutions in all scenarios studied, including where delays were enforced. The algorithm ensured that the hoist target was achieved while controlling all levels within or around their boundaries for a sustainable and continuous hoist schedule.

## 6.2 Recommendations for further study

The work done in this dissertation can be continued or improved on through any of the following:

- Studying the impact of delays by alternating between days with delays above and below the average daily delay time.
- Inclusion of demand cost into the objective function since NAC is applicable even during off-peak periods.
- Application of other more robust MPC algorithms or linear programming solvers that might prevent or reduce the occurrence of infeasible solutions.
- Developing a more complex, non-linear model by including control over winder speed, acceleration and payloads.
- Expansion of the system model by including other high energy consuming loads such as conveyors and crushers into the system model.

## REFERENCES

- [1] IEA, IEA World Energy Outlook 2008, Executive Summary, p. 4.
- [2] H. Nilsson, “The many faces of demand-side management,” *Power Engineering Journal*, vol. 8, no. 5, pp. 207 – 210, 1994.
- [3] S.J. Redford, “The rationale for demand side management,” *Power Engineering Journal*, vol. 8, no. 5, pp. 211-217, 1994.
- [4] Eskom, Eskom Energy Efficiency and Demand Side Management Programme Overview, 2008.
- [5] G.T. Bellarmine, “Load management techniques,” in *Proceedings of the IEEE Southeastcon 2000*, 7-9 April 2000, pp. 139-145.
- [6] Z.J.Paracha, P Doulai, “Load management, techniques and methods in electric power system,” in *Proceedings of the International Conference on Energy Management and Power Delivery*, 3-5 March 1998, vol. 1, pp. 213 – 217.
- [7] Eskom, Eskom Demand Side Management, <http://www.eskomdsm.co.za>. Last accessed on 22 July 2009.
- [8] DME, Department Minerals and Energy, Republic of South Africa, Digest of South African Energy Statistics, 2006.
- [9] Eskom, Eskom Western Cape Newspaper Insert, April 2006, p28, <http://www.eskom.co.za/content/newspaper%20insert-content~2.doc>. Last accessed 28 October 2009.
- [10] R. Pelzer, E.H. Mathews, D.F. le Roux, M. Kleingeld, “A new approach to ensure successful implementation of sustainable demand side management (DSM) in South African mines,” *Energy*, vol. 33, pp. 1254-1263, 2008.
- [11] G.J. Delport, “Integrated electricity end-use planning in deep level mines,” Doctoral thesis, University of Pretoria, 1994.
- [12] J.C. Vosloo, “Control of an underground rock winder system to reduce electricity costs on RSA gold mines,” Master’s thesis, North West University, South Africa, 2006.
- [13] P.H. Bosman, “The control of rock winders for maximum demand management on deep South African mines,” Master’s thesis, North West University, South Africa, 2006.
- [14] C.W. Gellings, “The concept of demand-side management for electric utilities,” *Proceedings of the IEEE*, vol. 73, no. 10, pp 1468-1470, October 1985.

- [15] J.Y. Boivin, "Demand side management – the role of the power utility," *Pattern Recognition*, vol. 28, no. 10, pp. 1493-1497, 1995.
- [16] S. Ashok, R. Banerjee, "Load-management applications for the industrial sector," *Applied Energy*, vol. 66, no. 2, pp. 105-111, 2000.
- [17] G. Strbac, "Demand side management: Benefits and challenges," *Energy Policy*, vol. 36, no. 12, pp. 4419-4426, 2008.
- [18] R. Freeman, "Managing energy. Reducing peak load and managing risk with demand response and demand side management," *reFocus*, vol. 6, no. 5, pp. 53-55, 2005.
- [19] E.L. Vine, "International DSM and DSM program evaluation: an INDEEP assessment," *Energy*, vol. 21, no. 10, pp. 983-996, 1996.
- [20] Eskom, Eskom Retail Tariff Restructuring Plan, Non-local-authority Tariffs 2008/9.
- [21] AngloGold Ashanti, AngloGold Ashanti Virtual Mine Tour, <http://www.anglogold.co.za/subwebs/VirtualTour/menu.asp>, Last accessed on 22 July 2009.
- [22] P.D.T O'Connor, *Practical Reliability Engineering*, 4<sup>th</sup> ed. Chichester: Wiley, 2002.
- [23] V. Knyazkin, C.A. Cañizares, L.H. Söder, "On the parameter estimation and modelling of aggregate power system loads," *IEEE Transactions on Power Systems*, vol. 19, no. 2, pp. 1023-1031, 2004.
- [24] S. Jebaraj, S. Iniyar, "A review of energy models," *Renewable and Sustainable Energy Reviews*, vol. 10, no. 4, pp. 281-311, 2006.
- [25] R.B. Hiremath, S. Shikha, N.H. Ravindranath, "Decentralized energy planning; modelling and application - a review," *Renewable and Sustainable Energy Reviews*, vol. 11, no. 5, pp. 729-752, 2007.
- [26] Yinhong Li, Hsiao-Dong Chiang, Byoung-Kon Choi, Yung-Tien Chen, Der-Hua Huang, Mark G. Lauby, "Load models for modelling dynamic behaviours of reactive loads: Evaluation and comparison," *Journal of Electrical Power & Energy Systems*, vol. 30, no. 9, pp. 497-503, 2008.
- [27] D.P. Stojanović, L.M. Korunović, J.V. Milanović, "Dynamic load modelling based on measurements in medium voltage distribution network," *Electric Power Systems Research*, vol. 78, no. 2, pp. 228-238, 2008.

- [28] S. Ashok, R. Banerjee, “An optimisation mode for industrial load management,” *IEEE Transactions on Power Systems*, vol. 16, no. 4, pp. 879-884, 2001.
- [29] J.C. van Tonder, I.E. Lane, “A load model to support demand management decisions on domestic storage water heater control strategy,” *IEEE Transactions on Power Systems*, vol. 11, no. 4, pp. 1844-1849, 1996.
- [30] C. Alvarez, R.P. Malhamé, A. Gabaldon, “A class of models for load management application and evaluation revisited,” *IEEE Transactions on Power Systems*, vol. 7, no. 4, pp. 1435-1443, 1992.
- [31] S. Rahman, Rinaldy, “An efficient load model for analyzing demand side management impacts,” *IEEE Transactions on Power Systems*, vol. 8, no. 3, pp. 1219-1226, 1993.
- [32] S. Rahman, J. Pan, A.R. Osareh, “A simplified technique for screening utility DSM options for their capacity and operational benefits,” *Energy*, vol. 21, no. 5, pp. 401-406, 1996.
- [33] H. Jorge, C.H. Antunes, A.G. Martins, “A multiple objective decision support model for the selection of remote load control strategies,” *IEEE Transactions on Power Systems*, vol. 15, no. 2, pp. 865-872, 2000.
- [34] A. Gomes, C.H. Antunes, A.G. Martins, “A multiple objective evolutionary approach for the design and selection of load control strategies,” *IEEE Transactions on Power Systems*, vol. 19, no. 2, pp. 1173-1180, 2004.
- [35] S. Ashok, R. Banerjee, “Optimal cool storage capacity for load management,” *Energy*, vol.28, no. 2, pp. 115-126, 2003.
- [36] S. Ashok, “Peak-load management in steel plants,” *Applied Energy*, vol. 83, no. 5, pp. 413-424, 2006.
- [37] A. Middelberg, J. Zhang, X. Xia, “An optimal control model for load shifting – With application in the energy management of a colliery,” *Applied Energy*, vol. 86, pp. 1266-1273, 2009.
- [38] W. Badenhorst, J. Zhang, X. Xia, “A near optimal hoist scheduling for deep level mine rock winders,” in *Proceedings of the IFAC Symposium on Power Plants and Power Systems Control, 5-8 July 2009, Tampere, Finland*.
- [39] D.P. Bertsekas, *Dynamic Programming and Optimal Control*, 2<sup>nd</sup> ed., Athena Scientific, Belmont, Massachusetts, 2001.

- [40] D.Q. Mayne, J.B. Rawlings C.V. Rao, P.O.M. Scokaert, “Constrained model predictive control: Stability and optimality,” *Automatica*, vol. 36, no. 6, pp. 789-814, 2000.
- [41] C.E. Garcia, D.M. Prett, M. Morari, “Model predictive control theory and practice – A survey,” *Automatica*, vol. 25, no. 3, pp. 335-348, 1989.
- [42] G. De Nicolao, L. Magni, R. Scattolini, “Stability and robustness of nonlinear receding horizon control,” *Allgower F, Zheng A (eds) Nonlinear Model Predictive Control, Progress in Systems and Control Theory*. Birkhauser Verlag, pp. 3-22, 2000.
- [43] E.F. Camacho, C. Bordons, *Model Predictive Control*, 2<sup>nd</sup> ed., Berlin, Springer, 2004.
- [44] E. Gallestey, A. Stothert, M. Antoine, S. Morten, “Model predictive control and the optimization of power plant load while considering lifetime consumption,” *IEEE Transactions on Power Systems*, vol. 15, no. 1, pp. 186-181, 2002.
- [45] M. Zima, G. Anderson, “Model predictive control of electric power systems under emergency conditions,” *Real-Time Stability in Power Systems: Techniques for Early Detection of the Risk of Blackouts*, New York, Springer, pp. 273-292, 2006.
- [46] B. Otomega, A. Marinakis, M. Glavic, T. van Cutsem, “Model predictive control to alleviate thermal overloads,” *IEEE Transactions on Power Systems*, vol. 22, no. 3, pp. 1284-1385, 2007.
- [47] G. Ferrari-Trecate, E. Gallestey, P. Letizia, M. Spedicato, M. Morari, M. Antoine, “Modelling and control of co-generation power plants: a hybrid system approach,” *IEEE Transactions on Control Systems Technology*, vol. 12, no. 5, pp. 694-705, 2004.
- [48] A.J. van Staden, J. Zhang, X. Xia, “A model predictive control strategy for load shifting in a water pumping scheme with maximum demand charges,” in *Proceedings of the IEEE PowerTech Conference, 28 June - 2 July, 2009, Bucharest, Romania*.
- [49] X. Xia, J. Zhang, A. Elaiw, “A model predictive control approach to dynamic economic dispatch problem,” in *Proceedings of the IEEE PowerTech Conference, 28 June - 2 July, 2009, Bucharest, Romania*.
- [50] A.I. Propoi, “Use of LP methods for synthesizing sampled-data automatic systems,” *Autumn Remote Control*, vol. 24, p. 837, 1963.

- [51] D.E. Seborg, T.F. Edgar, D.A. Mellichamp, *Process Dynamics and Control*, 2<sup>nd</sup> ed., New York, John Wiley & Sons, 2006.
- [52] M.A. Trick, “A Tutorial on Integer Programming,” 1998, Carnegie Mellon University, Graduate School of Industrial Administration, Pittsburgh, USA, <http://mat.gsia.cmu.edu/orclass/integer/integer.html>. Last accessed on 20 October 2009.
- [53] P. Gray, W. Hart, L. Painton, C. Phillips, M. Trhan, J. Wagner, “A survey of global optimization methods,” 1997, Sandia National Laboratories, <http://www.cs.sandia.gov/opt/survey/main.html>. Last accessed on 20 October 2009.
- [54] G.L. Thompson, D.L. Wall, “A branch and bound model for choosing optimal substation locations,” *IEEE Transactions on Power Apparatus and Systems*, vol. PAS-100, no. 5, pp. 2683-2688, 1981.
- [55] H. Chen, C. Chu, J. Proth, “Cyclic scheduling of a hoist with time window constraints,” *IEEE Transactions on Robotics and Automation*, vol. 14, no. 1, pp. 144-152, 1998.
- [56] D.H. Kim, J.H. Lee, S.H. Hong, S.R. Kim, “A mixed-integer programming approach for the linearized reactive power and voltage control – comparison with gradient projection approach,” in *Proceedings of the International Conference on Energy Management and Power Delivery*, 3-5 March 1998, vol. 1, pp. 67-72.

## ADDENDUM A: ESKOM MEGAFLEX CHARGES



TOU electricity tariff for urban<sub>p</sub> customers with an NMD > 1 MVA that are able to shift load

This tariff is characterised by:

- Seasonally and time differentiated c/kWh active energy charges
- Three time-of-use periods namely; peak, standard and off-peak
- A R/kVA network access charge applicable during all time periods, differentiated voltage and transmission zone
- A R/kVA network demand charge applicable during peak and standard periods
- A R/day service and administration charge based on the size of supply
- A c/kWh contribution to cross-subsidies to the rural and Homelight tariffs

### Capital costs

A connection charge will be payable in addition to the tariff for new connections or additional capacity.

### Connection fee

Refer to Appendix E (Table 1).

**The rates listed below are for non-local-authority supplies. The rates for local-authority supplies are listed at the end of this book.**

### Service charge

Charged per account and is based on the sum of the monthly utilised capacity of all premises linked to an account.

**≥ 1 MVA** R71,10 + VAT = **R81,06/day**

**Key customers** R556,20 + VAT = **R634,07/day**

### Administration charge

Based on, and payable for, the monthly utilised capacity of each premise linked to an account.

**≥ 1 MVA** R41,00 + VAT = **R46,74/day**

**Key customers** R42,50 + VAT = **R48,45/day**

### Network demand charge

R8,10 + VAT = **R9,24/kVA** payable for each kVA of the chargeable demand supplied during peak and standard periods per premise per month.

### Network access charge

R7,15 + VAT = **R8,16/kVA** payable each month and is based on the annual utilised capacity of each premise. This charge is applicable during all time periods.

### Active energy charge

#### High-demand season (June – August)

63,20c + VAT = **72,05c/kWh**

16,70c + VAT = **19,04c/kWh**

9,10c + VAT = **10,38c/kWh**

Peak

Standard

Off-peak

#### Low-demand season (September – May)

18,00c + VAT = **20,52c/kWh**

11,20c + VAT = **12,77c/kWh**

7,90c + VAT = **9,10c/kWh**

### Reactive energy charge

3,30c + VAT = **3,65c/kVARh** supplied in excess of 30% (0,96 PF) of kWh recorded during peak and standard periods. The excess reactive energy is determined per 30-minute integrating period and accumulated for the month and will only be applicable during the high-demand season.

### Voltage surcharge

Calculated as a percentage of network demand, network access and active energy charges.

<u>Supply voltage</u>	<u>Surcharge</u>
> 132 kV	0,00%
≥ 66 kV and ≤ 132 kV	7,63%
≥ 500 V and < 66 kV	10,07%
< 500 V	17,30%

### Transmission surcharge

Calculated as a percentage of the network demand, network access, active energy and reactive energy charges after the voltage surcharge has been levied. The surcharge rate depends on the distance from a central point in Johannesburg.

≤ 300 km	0%
> 300 km and ≤ 600 km	1%
> 600 km and ≤ 900 km	2%
> 900 km	3%

### Electrification and rural subsidy

1,84c + VAT = **2,10c/kWh** applied to the total active energy consumption (not subject to the voltage and/or transmission surcharge).



## ADDENDUM B: DAILY HOIST REPORT

<b>Reef Call</b>	<b>8269</b>	<b>Waste Call</b>	<b>0</b>	<b>Date:</b>	<b>26-Nov-04</b>	<b>Shift:</b>	<b>4</b>
<b>Winder</b>	<b>Ore</b>	<b>Skips</b>	<b>Tons</b>	<b>Prog. Skips</b>	<b>Prog. Tons</b>	<b>Prog.Target</b>	<b>Variance</b>
<b>Blair</b>	<b>Reef</b>	<b>269</b>	<b>6,322</b>	<b>1,191</b>	<b>27,989</b>	<b>33,076</b>	<b>-5,088</b>
23.5	<b>Waste</b>	<b>0</b>	<b>0</b>	<b>0</b>	<b>0</b>	<b>0</b>	
<b>Siemens</b>	<b>Reef</b>	<b>448</b>	<b>6,160</b>	<b>1,833</b>	<b>25,204</b>	<b>33,076</b>	<b>-7,872</b>
13.75	<b>Waste</b>	<b>0</b>	<b>0</b>	<b>0</b>	<b>0</b>	<b>0</b>	
		<b>CCTV Tons Trammed</b>	<b>5697</b>	<b>Prog. CCTV Tons</b>	<b>29043</b>	<b>Variance Hoist vs Tram</b>	<b>-1055</b>
	<b>R1 Weightometer</b>		<b>0</b>		<b>22923</b>	<b>Prog. Variance</b>	<b>-5066</b>
	<b>R3 Weightometer</b>		<b>0</b>		<b>21400</b>		<b>6589</b>

Tons in System										
Ore	Reef 1	Reef 3	Reef 4	Waste	Silos					
Capacity/Actual	2025	0	5150	0	12670	3000	29400	26800	No 1	2440
64 - 68					1570	0	2850	2000	No 2	7200
68 - 70					1750	0	3800	3600	Surface Stock Pile	
70 - 73			3650	0	4400	0	9500	8000	Scan Waste	0
73 - 76			1500	0	4950	3000	9500	9500	Reef	0
76 - 78	2025	0	990	0			2250	2200		
78 - 79	1500	0					1500	1500		
<b>Change over</b>	<b>Reef</b>	<b>Waste</b>								
Capacity	4000	4000								
52 Level	0	1000								
<b>Total Reef</b>	<b>3000</b>	<b>Total Waste</b>	<b>27800</b>							

Delays on Rock Hoisting System					
MR Winder Delays	Down Time	Siemens Winder Delays	Down Time		
Winder Legals		Winder Legals			
Maintenance	# Exam	Maintenance	# Exam	287	246
Power control		Power control			
Breakdowns		Breakdowns			
Conveyors 52 Level		Conveyors 76 Level			
Conveyors Surface		Conveyors 78 Level			
Other		Other	Daily		9
Operational	Orepasses / Tips	Down Time	Operational	Orepasses / Tips	Down Time
Tip Full			Tip Full		
Waiting / No Reef			Waiting / No Reef		
Barring	Barring	11	Barring	Barring	47
Big Rock/Hangup/Blasting			Big Rock/Hangup/Blasting	Blasting 76 / 79	219
Change over Empty	C / O Empty	383	System Empty	79 empty	31
Other	Belt stopped	18	Other	Rock in flask 79	40
Surface/52 level Conveyors		0	76 / 78 / 79 level Conveyors		0
Engineering Hoisting Delays		287	Engineering Hoisting Delays		255
Operational Delays		412	Operational Delays		337
<b>Total Delays (Hours)</b>		<b>11.7</b>	<b>Total Delays (Hours)</b>		<b>9.9</b>

# ADDENDUM C: ROCK WINDER DUTY CYCLE MODEL

## ELECTRICALLY COUPLED VERTICAL SHAFT WINDER DUTY CYCLE CALCULATION INPUT DATA

<u>WINDER:</u>	CONFIDENTIAL
<u>DUTY:</u>	NORMAL ROCK DUTY
<u>DATE:</u>	25-02-04

### 1. Shaft Particulars:

1.1	Winding depth (top station to bottom station)	1645 m
1.2	Distance from top station to headsheaves	20 m
1.3	Horizontal distance from drum to headsheaves	60 m
1.4	Vertical distance from drum to headsheaves	50 m

### 2. Suspended Masses:

2.1	Mass of ascending conveyance	11690 kg
2.2	Payload in ascending conveyance	24500 kg
2.3	Mass of descending conveyance	11690 kg
2.4	Payload in descending conveyance	0 kg
2.5	Total shaft friction allowance (usually 18% of payload)	4410 kg

### 3. Winding Cycle:

3.1	Rated mean rope speed	15.24 m/s
3.2	Mean rope speed for this duty	15.24 m/s
3.3	Linear acceleration rate	0.7 m/s <sup>2</sup>
3.4	Linear retardation rate	0.7 m/s <sup>2</sup>
3.5	Creep out speed	0.5 m/s
3.6	Creep out time	5 s
3.7	Creep in speed	0.5 m/s
3.8	Creep in time	5 s
3.9	Decking time (excluding creep time)	12 s

### 4. Speed Reference Shaping:

4.1	S-curve time between standstill and creep speed	0.000 s
4.2	S-curve time from creep out speed to acceleration	0.000 s
4.3	S-curve time from acceleration to full speed	0.000 s
4.4	S-curve time from full speed to retardation	0.000 s
4.5	S-curve time from retardation to creep in speed	0.000 s

### 5. Winding Ropes:

5.1	Number of ropes per drum	2
5.2	Nominal rope diameter	44 mm
5.3	Rope pitch factor (usually 1,04)	1.05
5.4	Unit mass of each rope	8.243 kg/m
5.5	Breaking force of each rope	1510 kN
5.6	Number of dead turns (usually 10)	12
5.7	Number of inactive turns per layer (usually 0,5)	0.5

### 6. Mechanical Parts:

6.1	Drum diameter at rope tread	4.270 m
6.2	Width of each drum compartment	1.600 m
6.3	Inertia of drums and shaft (and gear wheel)	514400 kg m <sup>2</sup>
6.4	Inertia of each headsheave	20000 kg m <sup>2</sup>
6.5	Number of motors driving each drum	1
6.6	Inertia of each motor and coupling (and pinion)	35000 kg m <sup>2</sup>
6.7	Rated motor speed (zero for direct coupled)	0 RPM
6.8	Gear efficiency (100% for direct coupled)	100 %

### 7. Productivity Data:

7.1	Production hours per day	20 h/d
7.2	Production days per month	25 d/m

CALCULATION RESULTS

WINDER:	CONFIDENTIAL
DUTY:	NORMAL ROCK DUTY
DATE:	25-02-04

1. Safety Factors:

1.1	Rope factor of safety	4.837
1.2	Rope capacity factor	8.506

2. Rope Layering:

2.1	Number of rope layers	4
2.2	Maximum number of active rope turns per layer	34
2.3	Number of rope turns on outer layer	28.140
2.4	Total number of active rope turns	118.140
2.5	Inner layer coil diameter at rope centres	4.314 m
2.6	Mean coil diameter at rope centres	4.432 m
2.7	Outer layer coil diameter at rope centres	4.539 m

3. Speeds:

3.1	Rated drum speed	65.670 RPM
3.2	Rated motor speed	65.670 RPM
3.3	Maximum drum speed for this duty	65.670 RPM
3.4	Maximum motor speed for this duty	65.670 RPM
3.5	Gear ratio	1.000 : 1
3.6	Maximum rope speed on inner rope layer	14.834 m/s
3.7	Maximum rope speed on outer rope layer	15.606 m/s

4. Duty Cycle Times:

4.1	Acceleration to creep speed	0.714 s
4.2	Creep out	5.000 s
4.3	Acceleration to full speed	21.057 s
4.4	Full speed	85.840 s
4.5	Retardation to creep speed	21.057 s
4.6	Creep in	5.000 s
4.7	Retardation to standstill	0.714 s
4.8	Decking / loading	12.000 s
4.9	Total cycle time	151.383 s

5. Duty Cycle Drum Turns:

5.1	Creep out	0.192
5.2	Acceleration to full speed	11.902
5.3	Full speed	93.952
5.4	Retardation to creep speed	11.902
5.5	Creep in	0.192
5.6	Total drum turns per wind	118.140

6. Winder Productivity:

6.1	Production per hour, running continuously	582.6 t
6.2	Production per 20 hour day	11653 t
6.3	Production per 25 day month	291314 t
6.4	Production per 12 month year	3495770 t

## ADDENDUM D: PERIODS AND NUMBER OF HOISTS DELAYED

TIME				
DAY ONE				
00:00	1	11	17	Period
00:30	2	54	70	Surf BMR 56 hoists
01:00	3			UG Siemens 117 hoists
01:30	4	1	12	
02:00	5			
02:30	6		2	
03:00	7			
03:30	8	9		
04:00	9		11	
04:30	10			
05:00	11	6		
05:30	12	7	4	
06:00	13			
06:30	14			
07:00	15			
07:30	16			
08:00	17			
08:30	18			
09:00	19			
09:30	20			
10:00	21	4		
10:30	22		7	
11:00	23			
11:30	24	2	2	
12:00	25	4		
12:30	26		1	
13:00	27			
13:30	28			
14:00	29			
14:30	30			
15:00	31			
15:30	32	3	8	
16:00	33	6		
16:30	34		1	
17:00	35			
17:30	36			
18:00	37			
18:30	38			
19:00	39			
19:30	40			
20:00	41			
20:30	42		10	
21:00	43			
21:30	44	8	5	
22:00	45	4		
22:30	46		1	
23:00	47			
23:30	48			
DAY TWO				
	49	11	17	Period
	50	50	60	Surf BMR 56 hoists
	51		8	UG Siemens 117 hoists
	52		2	
	53			
	54			
	55	4		
	56	9	10	
	57			
	58			
	59	4		
	60		5	
	61			
	62			
	63			
	64			
	65			
	66			
	67			
	68			
	69			
	70			
	71			
	72	4	5	
	73			
	74	3		
	75		11	
	76			
	77	6		
	78		5	
	79			
	80			
	81			
	82	5	1	
	83			
	84			
	85			
	86			
	87			
	88			
	89			
	90	2	10	
	91			
	92	4		
	93		3	
	94			
	95	9		
	96			
DAY THREE				
	97	11	17	Period
	98	39	96	Surf BMR 56 hoists
	99		9	UG Siemens 117 hoists
	100	8		
	101			
	102		6	
	103			
	104		6	
	105	9		
	106			
	107		12	
	108		2	
	109			
	110			
	111			
	112			
	113			
	114			
	115			
	116			
	117			
	118		11	
	119			
	120	5	17	
	121			
	122	2		
	123		1	
	124			
	125	4	12	
	126			
	127			
	128		2	
	129		3	
	130			
	131		3	
	132			
	133			
	134			
	135			
	136			
	137	7		
	138			
	139	7		
	140		7	
	141			
	142	4		
	143		2	
	144			
DAY FOUR				
	145	11	17	Period
	146	42	59	Surf BMR 56 hoists
	147		11	UG Siemens 117 hoists
	148	2		
	149	11		
	150			
	151			
	152		10	
	153		2	
	154			
	155			
	156			
	157	6	1	
	158			
	159			
	160			
	161			
	162			
	163			
	164			
	165		5	
	166			
	167	8		
	168		4	
	169			
	170		12	
	171			
	172			
	173			
	174			
	175	6		
	176			
	177		4	
	178		3	
	179			
	180		1	
	181			
	182			
	183			
	184			
	185			
	186		2	
	187	5		
	188		3	
	189			
	190		1	
	191			
	192		4	
DAY FIVE				
	193	11	17	Period
	194	43	72	Surf BMR 56 hoists
	195		4	UG Siemens 117 hoists
	196	4		
	197		11	
	198			
	199		5	
	200	4		
	201	4		
	202		2	
	203			
	204		7	
	205			
	206			
	207			
	208			
	209			
	210			
	211			
	212			
	213		8	
	214			
	215	7		
	216			
	217		5	
	218			
	219	5	7	
	220			
	221		8	
	222			
	223		2	
	224			
	225	4		
	226		4	
	227			
	228			
	229			
	230			
	231			
	232			
	233			
	234	11		
	235		4	
	236			
	237		6	
	238			
	239		3	
	240			

## ADDENDUM E: HIGH NUMBER OF HOISTS DELAYED OVER 5 DAYS

TIME			
DAY ONE			
00:00	Max	11	17
00:30	Tot	52	99
01:00	Period	2	4
01:30	Surf BMR	3	1
02:00	UG Siemens	4	12
02:30		5	
03:00		6	
03:30		7	
04:00		8	9
04:30		9	
05:00		10	11
05:30		11	6
06:00		12	
06:30		13	3
07:00		14	4
07:30		15	
08:00		16	2
08:30		17	
09:00		18	
09:30		19	
10:00		20	
10:30		21	4
11:00		22	7
11:30		23	
12:00		24	
12:30		25	
13:00		26	4
13:30		27	2
14:00		28	
14:30		29	2
15:00		30	1
15:30		31	
16:00		32	8
16:30		33	3
17:00		34	6
17:30		35	1
18:00		36	
18:30		37	3
19:00		38	3
19:30		39	2
20:00		40	
20:30		41	
21:00		42	17
21:30		43	17
22:00		44	
22:30		45	8
23:00		46	4
23:30		47	5
		48	1
DAY TWO			
	Max	11	17
	Tot	59	100
	Period	49	
	Surf BMR	50	8
	UG Siemens	51	8
		52	2
		53	
		54	
		55	11
		56	10
		57	
		58	
		59	4
		60	
		61	
		62	5
		63	
		64	4
		65	
		66	
		67	
		68	
		69	
		70	
		71	
		72	4
		73	5
		74	3
		75	
		76	11
		77	
		78	4
		79	17
		80	
		81	17
		82	
		83	5
		84	1
		85	
		86	3
		87	
		88	2
		89	
		90	4
		91	10
		92	
		93	2
		94	
		95	3
		96	
DAY THREE			
	Max	11	17
	Tot	56	121
	Period	97	
	Surf BMR	98	3
	UG Siemens	99	9
		100	
		101	7
		102	
		103	6
		104	6
		105	
		106	5
		107	
		108	12
		109	2
		110	
		111	
		112	3
		113	
		114	
		115	
		116	
		117	
		118	11
		119	11
		120	17
		121	5
		122	17
		123	
		124	1
		125	
		126	4
		127	12
		128	11
		129	2
		130	3
		131	
		132	3
		133	
		134	5
		135	
		136	2
		137	
		138	
		139	7
		140	
		141	7
		142	
		143	4
		144	2
DAY FOUR			
	Max	11	17
	Tot	53	111
	Period	145	
	Surf BMR	146	17
	UG Siemens	147	
		148	5
		149	17
		150	
		151	11
		152	
		153	10
		154	
		155	7
		156	
		157	6
		158	1
		159	
		160	1
		161	
		162	
		163	
		164	
		165	
		166	5
		167	11
		168	
		169	
		170	2
		171	17
		172	
		173	
		174	
		175	11
		176	
		177	4
		178	4
		179	3
		180	1
		181	
		182	2
		183	
		184	4
		185	
		186	3
		187	
		188	2
		189	
		190	5
		191	17
		192	17
DAY FIVE			
	Max	11	17
	Tot	53	115
	Period	193	
	Surf BMR	194	
	UG Siemens	195	4
		196	11
		197	
		198	11
		199	
		200	5
		201	4
		202	
		203	2
		204	
		205	7
		206	
		207	
		208	7
		209	
		210	
		211	
		212	
		213	
		214	8
		215	
		216	11
		217	
		218	5
		219	
		220	7
		221	
		222	8
		223	
		224	17
		225	
		226	4
		227	4
		228	
		229	1
		230	
		231	2
		232	
		233	1
		234	
		235	11
		236	
		237	17
		238	
		239	6
		240	